



**University of Benghazi
Faculty of Medicine**

**Molecular Genetics of Chronic Granulomatous Disease in
Libyan Patients in Benghazi**

By:

Muna Hamed Othman Elramli

Supervised by:

Asso Professor. Ahmed Elajily Zaid

Co-Supervisor:

Professor. Idris Matoug Alamari

***A Thesis Submitted in partial Fulfillment for the Requirements of
the Degree of Master in Biochemistry***

**Department of Biochemistry, Faculty of Medicine
University of Benghazi**

2015

DEDICATION

*TO MY PARENTS
AND MY FAMILY
WITH LOVE*

ACKNOWLEDGMENT

I am honored to remember the people whom without their help the completion of my project and thesis would not have been possible, while at the same time ask forgiveness of anybody that was not acknowledged for providing assistance to me no matter how small.

It is a great pleasure to thank those who provided me with assistance, cooperation and support that have made the completion of this thesis possible.

Being in the beginning of my research career, I am grateful and indebted to my supervisor **Associate Professor Ahmed Zaid**, for his guidance and encouragements and in providing help to bring this project from planning, working and writing to revising and editing.

My gratitude to my supervisor **Professor Idris Matoog**, for his guidance, encouragement and continuous support throughout the project.

My thanks and appreciation is extended to **Dr. Farag ElShaari**, He has been generous with his time setting up an example in dedication. His support was without limits throughout the project.

I am also grateful to the Head of Nurse in Immunology Department **Mrs. Fatma Elsheiki** and **Mrs. Sabra Elbarghati**, for their help in collecting blood sample from patient.

I am grateful to the Researcher Assistant in Biochemistry Department, University of Tripoli **Mr. Lamin Mohammed** for his technical help.

I am thankful to **Mr. Salah Bohajar** , Senior Technician in faculty of Public Health for his technical help.

I am grateful to my friends **Dr. Bushra Algharaf** and **Dr. Eman Elagori** for providing me with the control samples.

I would like to thank to all staff in the department of Biochemistry for their encouragement and support.

I am grateful to Faculty of Medicine, University Of Benghazi for providing me with laboratory facilities to carry out my experiments.

I am grateful to the staff of the Immunology Department, Pediatric Hospital of Benghazi for providing me with Data and information about the patients recruited for my experiments.

I am grateful to Biotechnology Center (Benghazi Branch) for providing me with laboratory facilities to carry out the experiments.

I am grateful to the Biochemistry Department of the Faculty of Medicine, the University of Tripoli for providing me with laboratory facilities to carry out part of my experiments.

I am deeply grateful to all my friends for their support.

Special thanks with love to my family. I am indebted to them for their support, patience and devotion.

CONTENTS

List of figures	iii
List of tables	v
Abbreviations	vi
Abstract	viii
Chapter 1: Introduction	1
1. Review of Literature	3
1.1 Over view on Chronic Granulomatous Disease.....	3
1.1.1 Nicotinamide adenine dinucleotide phosphate (NADPH) oxidase complex.....	3
a. Phosphorylation and oxidase assembly.....	3
b. NADPH Oxidase Inhibitors.....	4
c. Nox family protein acting as the catalytic subunit.....	4
d. Defective NADPH Oxidase Complex.....	5
1.1.2 Reduced Superoxide Anions and their role in killing of Micro-organisms.....	6
1.1.3 Mutations in Genes of NADPH Oxidase Complex.....	7
a. <i>CYBB</i> Gene.....	7
b. <i>NCF1</i> and pseudogenes.....	9
c. <i>CYBA</i> Gene.....	11
d. <i>NCF2</i> Gene.....	11
1.1.4 Diagnosis of CGD.....	12
1.1.5 Correlation between genetic defect and clinical course.....	13
1.1.6 Clinical features, infections, treatment and drugs toxicity in CGD patients.....	13
1.1.7 Hematopoietic cell transplantation for patients with CGD.....	16
1.1.8 Gene therapy of CGD.....	17
1.1.9 Inflammatory complications and autoimmunity in patients with CGD.....	18
1.2 Aim of study.....	21
Chapter 2: Material and Methods	22
2.1. Patients and samples.....	22
2.1.1. Patients.....	22
2.1.2. Blood sampling.....	32
2.2. Extraction of DNA.....	32
2.3. Measuring of DNA purity and concentration.....	33
2.4. Agarose gel electrophoretic analysis of extracted DNA.....	34
2.5. PCR (polymerase chain reaction).....	37
2.6. DNA Sequencing.....	41
2.7. Real time PCR (High Resolution Melting).....	42
2.8. Blast Alignment.....	45

Chapter 3: Results	47
1.3 The biochemical data.....	47
2.3 Measuring DNA purity and concentration.....	48
3.3 Size of DNA bands after PCR.....	48
4.3 Purification of PCR product.....	49
5.3 High Resolution melting analysis Real Time PCR (HRM Real Time PCR).....	49
6.3 Chromatogram and sequences of patients and controls samples.....	49
7.3 Blast Alignment.....	50
Chapter 4: Discussion	112
Chapter 5: Conclusion	120
Chapter 6: References	121

LIST OF FIGURES

Figure (1.1): Topology of NOX proteins in phagocytes and nonphagocytes.....	5
Figure (1.2): Sequential reduction of O ₂ to H ₂ O ₂ then to H ₂ O.....	6
Figure (1.3): Schematic representation of a phagocyte engulfing a microbe into a phagocyte vacuole.....	7
Figure (1.4): A. Crossing over between NCF1 gene and one of its pseudogenes, B. Crossing over within NCF1 gene and one of its pseudogenes.....	10
Figure (2.1): Family Pedigree of patient No. 1.....	22
Figure (2.2): Family Pedigree of patient No. 2.....	23
Figure (2.3): Family Pedigree of patient No. 3.....	24
Figure (2.4): Family Pedigree of patient No. 4.....	24
Figure (2.5): Family Pedigree of patient No. 5.....	25
Figure (2.6): Family Pedigree of patient No. 6.....	26
Figure (2.7): Family Pedigree of patient No. 7.....	26
Figure (2.8): Family Pedigree of patient No. 8.....	27
Figure (2.9): Family Pedigree of patient No. 9.....	28
Figure (2.10): Family Pedigree of patient No. 10.....	28
Figure (2.11): Family Pedigree of patient No. 11.....	29
Figure (2.12): Family Pedigree of patient No. 12.....	30
Figure (2.13): Family Pedigree of patient No. 13.....	30
Figure (2.14): Family Pedigree of patient No. 14.....	31
Figure (3.1): Photograph showing the bands that reflect the measured DNA purity and concentration by gel electrophoresis.....	55
Figure (3.2): DNA bands on the gel following PCR for NCF1 gene using primers (F: 2LB2, R: 2RB2).....	56
Figure (3.3): DNA bands on the gel following PCR for NCF1 gene using primers (F: il-3'f, R: 2RB2).....	56
Figure (3.4): DNA bands of NCF1 gene following PCR using the primers (F: 2LB2, R: 2RB2), and after product purification.....	57
Figure (3.5): DNA bands of NCF1 gene after purification of PCR samples of primers (F: il-3'f, R: 2RB2).....	57
Figures (3.6): The high resolution melting analysis of real time-PCR products of primers (F:il-3'f – R: 2RB2).....	58
Figures (3.7): The high resolution melting analysis of real time-PCR products of primers (F: 2LB2 – R: 2RB2).....	58
Figures for chromatogram of patients and control sample.....	59
Figures for sequencing and alignment of patients and controls samples by sequencer program	75

Figures for Blast alignment of patient's DNA sequence (*CYBB* Gene) with Gene Bank sequence.....80

Figures for Blast alignment of patient's DNA sequence (*CYBB* Gene) with control sample sequence.....96

LIST OF TABLES

Table (2.1): amount of NaAC added to the DNA samples stored in ethanol.....	36
Table (2.2): <i>NCF1</i> gene PCR Primers.....	37
Table (2.3): <i>CYBB</i> gene PCR Primers.....	37
Table (2.4): The Forward and reverse primers 100µM stock solutions for <i>NCF1</i> exon.....	38
Table (2.5): Reaction setup using HotStarTaq Master Mix for PCR.....	39
Table (2.6): Optimized cycling conditions for PCR.....	39
Table (2.7): Reagents measurements in the sequencing reaction.....	42
Table (2.8): <i>NCF1</i> Real Time-PCR Primers.....	43
Table (2.9): The Forward and reverse primers 100µM stock solutions for <i>NCF1</i> exon.....	43
Table (2.10): preparation of reaction mixture for RT-PCR.....	44
Table (2.11): the real-time cycler program.....	45
Table (3.1): The biochemical data for patients recruited for this study.....	51
Table (3.2): The biochemical data for patients recruited for this study.....	52
Table (3.3): The biochemical data for patients recruited for this study.....	53
Table (3.4): The biochemical data for patients recruited for this study.....	54
Table (3.5): The optical density of DNA samples extracted from patients' blood.....	55

Abbreviations

AR-CGD	Autosomal Recessive
ATG	Anti Thymocyte Globulin
ATP	Adenosine Triphosphate
bp	base pair
CGD	Chronic Granulomatous Disease
CRP	C- Reactive Protein
cyt <i>b558'</i>	Flavocytochrome <i>b558</i>
DHR	Dihydrorhodamine
ESR	Erythrocyte Sedimentation Rate
FAD	Flavin Adenine Dinucleotide
G6PD	Glucose-6-Phosphate Dehydrogenase
gp91phox	Glycoprotein 91 phagocyte oxidase
GvHD	Graft versus Host Disease
H ₂ O ₂	Hydrogen Peroxide
HB	Hemoglobin
HOCl	Hypochlorous Acid
HRM	High Resolution Melting
HSCs	Hematopoietic Stem Cells
IFN- γ	Interferon- γ
IgA	Immunoglobulin A
IgE	Immunoglobulin E
IgG	Immunoglobulin G
IgM	Immunoglobulin M
LOO \cdot	Lipid Peroxy Radical
MPO	Myeloperoxidase

NADPH	Nicotinamide Adenine Dinucleotide Phosphate
NBT	Nitroblue Tetrazolium
$\cdot\text{NO}$	Nitricoxide
$\text{O}_2^{\cdot-}$	Superoxide
$\cdot\text{OH}$	Hydroxyl Radical
P22phox	Protein 22 phagocyte oxidase
PCR	Polymerase Chain Reaction
PLT	Platelet
PRR	Proline-Rich Region
PT	Patients
RBC	Red Blood Cell
RLU	Relative Luminescence Unit
ROS	Reactive Oxygen Species
RT-PCR	Real Time- PCR
SD	Standard deviation
SH3	Src Homology 3
SNPs	Single Nucleotide Polymorphisms
SSCP	Single Strand Conformation Polymorphism
TNF	Tumor Necrosis Factor
TPR	Tetratricopeptide Repeat
WBC	White Blood Cell
X-CGD	X-linked CGD
ΔGT	GT deletion
$\Psi\text{-NCF1}$	Pseudo- <i>NCF1</i> Gene

Abstract

Introduction: Chronic granulomatous disease (CGD) is a rare inherited primary immune deficiency disease with prevalence of 1 in 250,000 worldwide. It is caused by mutations in the genes that encode the NADPH oxidase enzyme components responsible for the production of super oxide and other free radicals. These mutations lead to the absence or decrease of the microbicidal activity of the phagocytic cells.

CGD is inherited in two patterns, X-linked pattern caused by mutations in the *CYBB* gene which encodes the gp91^{phox} and an autosomal recessive pattern due to mutations in *NCF1*, *NCF2* and *CYBA* genes that encodes p47^{phox}, p67^{phox} and p22^{phox}, respectively.

Patients and Methods: In the present study we investigated the genetic defects of *CYBB* and *NCF1* genes that have high incidence in different regions around the world. Fourteen Libyan patients admitted to the Immunology Department of the Pediatric Hospital of Benghazi, where some of them were clinically diagnosed as CGD patients, and others were confirmed cases by using the NBT test. Mutation analysis of the *CYBB* gene performed by amplification of five exons (2, 3, 5, 7, 10) using Polymerase Chain Reaction (PCR) followed by sequencing, while the *NCF1* gene components were screened using Real Time PCR (RT-PCR). All the results were confirmed using Blast Alignment tool of the NCBI.

Results: Depending on consanguinity type of patients' parents and the pedigree analysis results, and the family history of CGD, Libyan patients most likely have the inherited autosomal recessive trait.

Following DNA amplification, sequencing and blast alignment of the five exons (2, 3, 5, 7, 10) of *CYBB* gene and screening of *NCF1* gene by High Resolution Melting (HRM-RTPCR), no mutations were detected in both genes (It is worthy to note that in our study the *CYBB* and *NCF1* genes that have the highest incidence worldwide showed no abnormalities in the sequenced hot spot of our patients' DNA). Furthermore, based on the DHR assay test of patient No. 3 we detected mutation in the *CYBA* gene, which could prove to be the hot spot for mutations in Libyan patients.

Conclusion and Recommendation: Detection of CGD causing mutation is a big task, in this study, Libyan patients in Benghazi region where the family-specific mutations are not known makes it even more difficult. Therefore, we employed different methods in addition to pedigree analysis. Completion of this study requires further analysis. For instance, partial or complete gene deletions can be recognized by MLPA or array CGH analysis of genomic DNA, and in addition to RTPCR and sequencing we may require the use of allele-specific markers for detection of more subtle mutations.

This study is the first one in Benghazi and Libya to study the molecular basis of chronic granulomatous disease to consider the genetic aspect.

Introduction

Chronic granulomatous disease (CGD) was first described in 1954 (Janeway et al., 1954) and confirmed in 1957 (Berendes et al., 1957). CGD is an inherited immunodeficiency syndrome with an incidence of approximately 1 in 250,000 newborns (Holland, 2010). It has a mortality of about 2% per year (Gallin & Zarembler, 2007).

The disease primarily affects males as most mutations are X linked. Rates are almost identical across ethnic and racial groups. However, in cultures in which consanguineous marriage is common, the autosomal recessive forms of CGD are more common than X-linked forms, and overall incidence rates may be higher (Suliaman et al, 2009).

CGD may present at any time from infancy to late adulthood, but the majority of patients are diagnosed as toddlers and children before the age of five years. In several study series, the median age at diagnosis was 2.5 to 3 years of age (Jones et al, 2008; Soler-Palacín et al, 2007). A growing number of patients are diagnosed in later childhood or adulthood. This is in part due to recognition of milder cases of autosomal recessive CGD, as well as delayed diagnosis in some patients. Diagnosis may be delayed because of potent antimicrobials that inadvertently treat many CGD-associated infections, postponing diagnosis until more severe infections indicate CGD as the underlying cause. X-linked CGD tends to have an earlier onset and be more severe than p47phox deficiency (Winkelstein et al, 2000).

Patients with this disorder usually have recurrent infection due to the decreased capacity of their immune system, hence being unable to eliminate pathogenic microorganisms (Holland, 2010). CGD results from defects in the reduced nicotinamide adenine dinucleotide phosphate (NADPH) oxidase complex, resulting in an inability to produce the superoxide anion necessary for normal killing of bacterial and fungal microorganisms, where this defect predisposes to granulomatous complications.

Mutations in at least 5 different genes involved in the assembly and activation of the NADPH oxidase can lead to CGD (Segal et al., 1998; Kang et al., 2011). The gene encoding the enzymatic center of the NADPH oxidase, gp91phox, is on the X-chromosome and accounts for about two thirds of the cases. Autosomal forms occur from mutations in p47phox, p67phox, p22phox, or p40phox, with the latter being the most recently described (Matute et al., 2009; Kang et al., 2011). Different unequal cross-over events between NCF1 and its pseudogenes are one cause of autosomal p47phox-deficient chronic granulomatous disease (Hayrapetyan A et al., 2013). Specific mutations affect the severity of disease through the amount of residual NADPH oxidase activity (Kuhns et al., 2010).

Management of CGD patients requires minimizing exposure to microorganism by avoiding environmental risk factors such as mulch, rotting plants and animal manure. Prophylaxis with interferon- γ and itraconazole can reduce the incidence of fungal infections in CGD. Once infection occurs, aggressive treatment with surgical debridement and antifungal agents can be curative in some but not all patients (Gallin & Zarembler, 2007).

Several therapeutic approaches to correcting the underlying defects in CGD have been attempted and perhaps promise a more normal life to CGD patients. Bone marrow transplants have shown some remarkable success but are accompanied by their own

significant risks (Horwitz et al, 2001). Gene therapy, where a normal copy of the defective gene is introduced to correct the mutation, has been fraught with challenges but remains the focus of significant effort (Malech, 1999).

CGD is a disease that is rapidly changing in its diagnosis, management, science, and outlook. It spans the frontiers of basic science, medicine, genetics, infectious diseases, transplantation, and gene therapy (Holland, 2010).

1. Review Of Literature

1.1. Over View On Chronic Granulomatous Disease:

1.1.1 Nicotinamide Adenine Dinucleotide Phosphate (NADPH) Oxidase Complex:

The phagocyte NADPH oxidase, an enzyme system responsible for superoxide generation in phagocytes of the innate immune system, comprises a small transmembrane electron transport system. Activation of this enzyme complex results in the oxidation of NADPH on the cytoplasmic surface and the generation of superoxide on the outer surface of the membrane. The phagocyte oxidase is the first identified and best studied member of the NOX family of NADPH oxidases (Nauseef, 2008). The phagocyte NADPH oxidase plays a key role in host defenses against microbial pathogens by generating superoxide anions (O_2^-) and other Reactive Oxygen Species (ROS) (Babior, 1984). The active NADPH oxidase is a multicomponent enzyme system located in the plasma membrane of activated cells (Chanock et al., 1994).

The NADPH oxidase consists of six hetero-subunits, which associate in a stimulus-dependent manner to form the active enzyme complex and produce O_2^- . This activity has to be spatially and temporally restricted to the closed phagosome in order to prevent destruction of host tissue (Babior, 1999).

Two NADPH oxidase subunits, gp91phox and p22phox, are integral membrane proteins. They form a heterodimeric flavocytochrome *b558* ('cyt *b558*') that constitutes the catalytic core of the enzyme, but exists in a dormant state in the absence of the other subunits. These play mostly regulatory roles, and are located in the cytosol during the resting state. They include the multi domain proteins p67phox, p47phox and p40phox, as well as the small GTPase Rac, which is a member of the Rho family of small GTPases (Groemping Y. and Rittinger K., 2005).

Activation of NADPH oxidase in phagocytes is triggered by serine phosphorylation and translocation of the cytosolic subunits to the cell membrane, followed by engagement with the membrane-bound components (Babior, 1999). Activated NADPH oxidase in phagocytes produces large quantities of superoxide, in the order of 10 nmol/min/10⁶ cells (Babior et al., 1973; Inanami et al., 1998).

a. Phosphorylation And Oxidase Assembly:

Phosphorylation has long been recognized as one of the key events in NADPH oxidase activation, and most oxidase components (apart from Rac and gp91phox) have been shown to become phosphorylated to various degrees during the activation process. In the case of p47phox, it is well established that multiple phosphorylation events are required to relieve auto-inhibition and allow translocation to the membrane. Their association with the flavocytochrome occurs by virtue of an interaction between the tandem SH3 (Src homology 3) domains and a PRR (proline-rich region) in the C-terminal cytoplasmic tail of p22phox. Neither p40phox nor p67phox is able to translocate in the absence of p47phox, as evidenced by the cytoplasmic location of p40–p67phox in stimulated cells from CGD patients that lack a functional p47phox (Dusi et al., 1996).

The phosphorylation of p47phox is extensive, and 11 phosphorylation sites have been mapped including serine residues (El Benna et al., 1994; Inanami et al., 1998; Dang et al., 2001; Chen et al., 2003).

The cytoplasmic regulatory proteins p40phox and p67phox are also known to become phosphorylated; however, the physiological role of these events is less clear (Dusi & Rossi, 1993; Someya et al., 1999).

Activation of the NADPH oxidase requires conformational changes in the cytoplasmic complex to allow the assembly of the heterohexameric enzyme at the membrane. Docking of the p47– p67–p40phox complex to the membrane bound cytochrome b558 is supported by an interaction between the tandem SH3 domains of p47phox and the cytoplasmic tail of p22phox (Leto et al., 1994; Sumimoto et al., 1994; de Mendez et al., 1997; Shiose & Sumimoto, 2000).

Once at the membrane, additional contacts between p47phox and the cytochrome take place, which are believed to either help position p67phox correctly or possibly induce a conformational change within the cytochrome. These interactions have been mapped to the first cytoplasmic loop of gp91phox (DeLeo et al., 1995, A; DeLeo et al., 1995, B), and to two regions in the cytoplasmic domain of gp91phox: to amino acids 450–457 adjacent to the NADPH-binding site and to the extreme C-terminus of the molecule (DeLeo et al., 1995,1; Leusen et al., 1994, B; Kleinberg et al., 1990) .

Another studies support that oxidase assembly, and specifically association with p67phox, induce a conformational change in the cytochrome (Paquet et al., 2000).

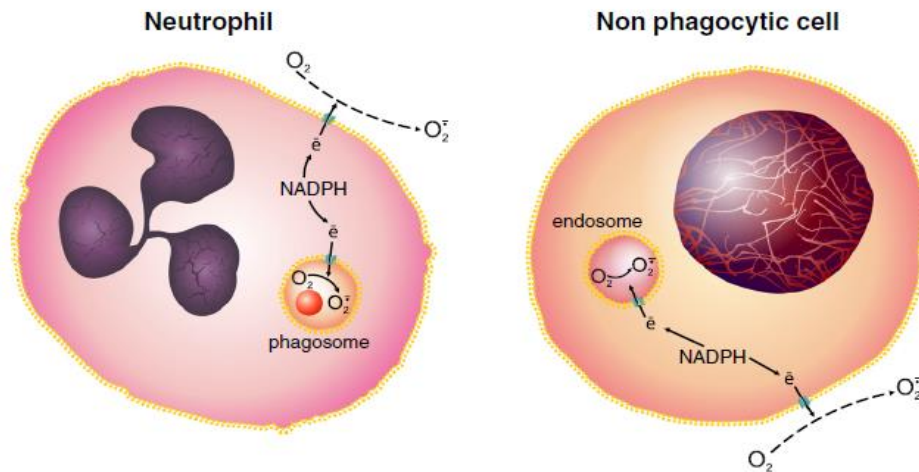
In addition to that, no evidence has been found for a direct interaction between p40phox and the cytochrome (Groemping Y. and Rittinger K., 2005).

b. NADPH Oxidase Inhibitors:

A number of NADPH oxidase inhibitors have been described. Endogenous biological molecules which inhibit NADPH oxidase activity or its activation are nitric oxide (Clancy et al., 1992; Fujii et al., 1997), steroids (Laufs et al., 2003), adrenaline (O'Dowd et al., 2004), IL-10 (Elbim et al., 2001), and IL-4(Zhou et al., 1995). Numerous exogenous pharmacological inhibitors are known, the most used being diphenylene iodonium, which inhibits electron transport by gp91phox (Hancock & Jones, 1987). Apocynin, a methoxy-substituted catechol, is a natural molecule which inhibits NADPH oxidase (Stolk et al., 1994). Other molecules, such as phenylarsine oxide (Le Cabec et al., 1995), 4-(2-amino ethyl)-benzenesulfonyl fluoride (Diatchuk et al., 1997), and N- α -tosyl phenylalanine chloromethyl ketone (Gillibert et al., 2005), inhibit NADPH oxidase by inhibiting complex assembly.

c. Nox Family Protein Acting as The Catalytic Subunit:

NOX proteins transport electrons from NADPH on the cytoplasmic face of plasma, endosomal, or phagosomal membranes to O₂ at the extracellular space or in the lumen of the endosome or phagosome, respectively (Fig. 1.1). Consequently, for O₂•⁻ or H₂O₂ produced by NOX proteins to engage detectors present in the cytoplasm, the oxidant must move from its site of origin, across a membrane, and into the cytoplasm. As a charged species, O₂•⁻ would require passage through an anion channel to reach the cytoplasm (Lynch & Fridovich, 1978; Roos et al., 1984).



Adopted from: Nauseef WM. (2014)

Figure (1.1): Topology of NOX proteins in phagocytes and nonphagocytes.

The phagocyte NADPH oxidase, illustrates many structural and functional features that are shared by other NOX proteins. However, important differences exist in composition, subcellular distribution, and activity of non-phagocyte oxidases that likely reflect their cell- or tissue specific functions. Essentially all the O_2 consumed and oxidants generated by stimulated neutrophils reflect the activity of the NADPH oxidase (NOX₂). The membrane component is flavocytochrome b₅₅₈, a heterodimeric membrane protein composed of gp91phox and p22phox, and serves as an electron transferase with O_2 as the electron acceptor. Structural stability, heme acquisition, and transport from the endoplasmic reticulum to target membranes require heterodimer formation (Biberstine-Kinkade et al., 2001; Yu et al., 1998). Gp91phox, containing one molecule of flavin adenine dinucleotide (FAD) (Cross et al., 1982) and two molecules of heme, serves as the catalytic center of the phagocyte oxidase. Two electrons from NADPH are transferred to FAD, followed by two sequential single-electron reductions of two inequivalent heme groups to O_2 to form two molecules of $O_2\bullet^-$ (Cross & Segal, 2004).

Like the phagocyte oxidase, all NOX proteins are flavoproteins that operate as electron transferases, transporting electrons derived from cytoplasmic NADPH across a membrane to the electron acceptor oxygen. However, with regard to both structural composition and organization, dependence on cofactors, and function, the non-phagocyte NOX proteins exhibit notable exceptions to the human neutrophil paradigm (Nauseef WM., 2014).

d. Defective NADPH Oxidase Complex:

CGD is an inherited deficiency of NADPH oxidase (Kuhns et al., 2010). Where the NADPH oxidase is not fully functional in CGD patients, and the production of superoxide and other reactive intermediates is impaired in their phagocytic cells, leading to infections and other complications (Halliwell & Gutteridge, 2007).

Mutation of Ser379 in p47phox to alanine prevents membrane translocation and leads to a complete loss of NADPH oxidase activity, a behavior that is similar to a mutant in which

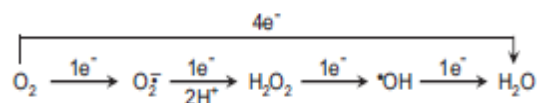
all serine residues that become phosphorylated have been replaced by alanine residues (Faust et al., 1995). Similarly, substitution of alanine for Ser359 or Ser370 dramatically reduces phosphorylation of other residues, impairs protein translocation to the membrane and severely reduces $O_2^{\cdot-}$ production (Johnson et al., 1998).

Patients with severe Glucose-6-phosphate dehydrogenase (G6PD) deficiency which catalyses the production of reducing equivalents in the form of NADPH in the hexose monophosphate shunt, may demonstrate low NADPH oxidase activity because of impaired substrate supply and suffer recurrent infections, mimicking the phenotype of CGD (Luzzatto & Battistuzzi, 1985; Roos et al., 1999).

1.1.2. Reduced Superoxide Anions and Their Role in Killing of Micro-organisms:

A free radical is an atom or molecule with a single unpaired electron, examples: Nitricoxide ($\cdot NO$), superoxide ($O_2^{\cdot-}$), hydroxyl radical ($\cdot OH$), lipid peroxy –radical ($LOO\cdot$). Molecular oxygen reacts rapidly with most other radicals, forming other free radicals that are more reactive and cause selective oxidation of lipid, protein, or DNA molecules (Halliwell & Gutteridge, 2007)

Molecular oxygen is vital for survival of all aerobic organisms. During aerobic metabolism in normal cells, 30–32 molecules of adenosine triphosphate (ATP) are generated from one molecule of oxygen. During this process, oxygen is reduced into water (4 electron reduction), (Fig. 1.2).



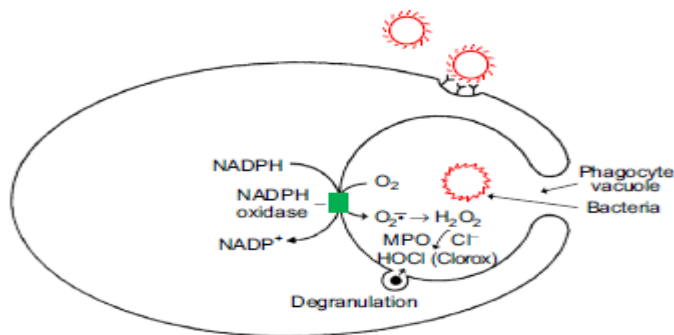
Adopted from: kalyanaraman B. (2013)

Figure (1.2): Sequential reduction of O_2 to H_2O_2 then to H_2O .

Although $O_2^{\cdot-}$ is weakly microbicidal, oxidants generated from $O_2^{\cdot-}$ are strongly microbicidal (Babior, 2004). Superoxide rapidly reacts with another molecule of superoxide to form hydrogen peroxide. Another important reaction in biology is between superoxide with nitricoxide to form a very potent oxidant and reactive nitrogen species, peroxyntirite with half-life few seconds (Beckman et al., 1990). Hydrogen peroxide (H_2O_2) is relatively stable (half-life, months) when protected against light and trace metal contamination. H_2O_2 is rapidly destroyed by antioxidant enzymes catalase, glutathione peroxidase.

During the phagocytic process (Fig. 1.3), the phagocyte finds a bacteria coated by the complement where marked as foreign body (Halliwell & Gutteridge, 2007). The phagocyte plasma membrane surrounds the bacteria and engulfs the microprobe into a phagocytic vacuole. Enzymes (NADPH oxidase) are selectively activated in the wall of vacuole, generating $O_2^{\cdot-}$ and H_2O_2 in the vacuolar lumen. Although $O_2^{\cdot-}$ production is essential for bacterial cell killing, $O_2^{\cdot-}$ alone is not responsible for bacterial killing. H_2O_2 in the presence of released iron could form hydroxyl radical, a potent antimicrobial oxidant ($\cdot OH$), (Grant et al., 2012).

The enzyme, myeloperoxidase (MPO), is released inside the phagocytic vacuole from granules and comprises 2–5% of total neutrophil protein. MPO is a heme-containing peroxidase that will oxidize halide anion (chloride, bromide, and iodide anions) in the presence of H_2O_2 , forming the corresponding hypohalous acid. In the case of chloride anion, hypochlorous acid (HOCl) or Clorox (bleach) is formed. HOCl kills many bacteria and fungi in vitro. HOCl is very reactive and causes oxidation and chlorination of biological molecules. Although HOCl plays a role in bacterial killing by phagocytes, O_2^- is more important than MPO in the overall bacterial killing during respiratory burst (Weiss, 1989).



Adopted from: kalyanaraman B. (2013)

Figure (1.3): Schematic representation of a phagocyte engulfing a microbe into a phagocyte vacuole.

1.1.3 Mutations In Genes Of NADPH Oxidase Complex:

CGD is classified by mutations in specific subunits of the NADPH oxidase enzyme. A defect in membrane gp91phox, which is encoded by the *CYBB* gene on the X chromosome, leads to X-linked recessive chronic granulomatous disease (X-CGD; approximately 70% of patients worldwide), (Roos et al., 2007; Kuhns et al., 2010). A defect in any one of the other 4 components of the NADPH oxidase (ie, p22phox, p47phox, p67phox, and p40phox encoded by the autosomal *CYBA*, *NCF1*, *NCF2*, and *NCF4* genes, respectively) leads to autosomal recessive (AR) CGD (AR-CGD), (Roos et al., 2007; Van den Berg et al., 2010). The majority of patients with X-linked recessive CGD (X-CGD) are given a diagnosis before the age of 2 years, whereas patients with p47phox deficiency might have their condition undiagnosed until adulthood (Roos et al., 2007; Kuhns et al., 2010; Van den Berg et al., 2009).

a. *CYBB* Gene:

X-CGD caused by mutation in *CYBB* gene (GenBank Accession Nos. 469757- 469769). This gene is located on chromosome Xp21.1, spans 30 kb and contains 13 exons. *CYBB* encodes gp91-phox, the β-subunit of cytochrome b558 (also known as cytochrome b245), a key transmembrane protein in the phagocyte NADPH oxidase system.

Over 300 *CYBB* mutations have been registered in an internationally maintained X-CGD database (X-CGD base). Most mutations are distributed throughout the 13 exons or at

exon/intron boundaries and almost 200 of these mutations are unique. Although less than 1% of the mutations reported in the X-CGD base has been found in the promoter/enhancer region and nearly 10% are splice mutations, (Winkelstein et al., 2000; Cross et al., 2000, A).

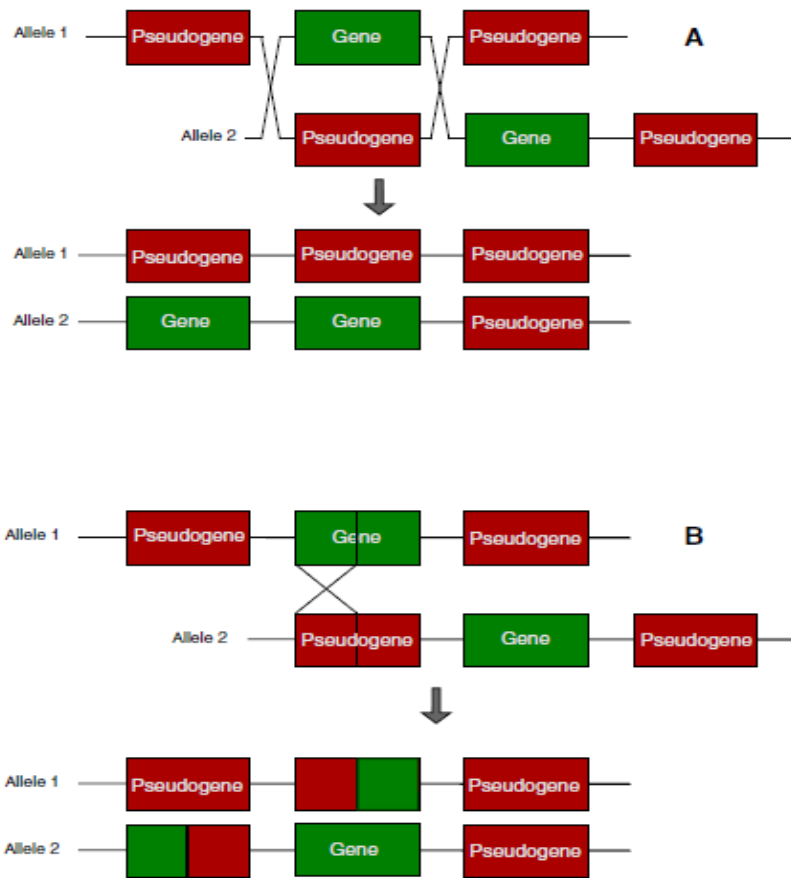
Single-nucleotide substitutions (missense or nonsense mutations including splicing or not) account for 58% of the defects; small deletions, insertions, and insertion–deletions account for 26% and large deletions and insertions for 14%. However, insertions in *CYBB* are less frequent than deletions, in accordance with findings in other genes (Cooper DN & Krawczak M., 1991), these results show that X linked CGD is a very heterogeneous disease, caused by a large variety of mutations, except gene conversions. It should be emphasized that only three polymorphisms caused by missense mutations located in the encoding region of the *CYBB* gene have been reported (Heyworth et al., 2001). Most of the time, mutations in the *CYBB* gene lead to a lack of NOX2 expression because of the instability of the corresponding mRNA or protein. In these patients, NADPH oxidase activity is always totally abolished. This phenotype, called X91⁰ CGD, is the most frequent. It is usually caused by nonsense, missense, splice mutations, small deletions, and insertions, sometimes associated with frameshift and early termination of protein synthesis. In addition, large insertions or large deletions removing part of or the entire gene lead to X91⁰ CGD (Stenson et al., 2003; Piirilä et al., 2006).

Generally, small deletions and insertions, often associated with frameshift in *CYBB*, lead to a sharp decrease in mRNA stability associated with the absence of NOX2 synthesis. This type of mutation is often caused by slipped mispairing during DNA replication at the replication fork, which often accounts for single base pair deletions or insertions. In addition, deletions are often situated in very rich GC regions (Roos et al., 1996; Krawczak et al., 1991). Mutations near or in the splice-junction sites in *CYBB* also cause CGD, with a mRNA processing defect (exon skipping) and a decrease in its stability (Krawczak et al., 2007).

Nonsense mutations, which introduce a stop codon, affect the mRNA level to various degrees (Roos et al., 1996; Rae et al., 1998). When mRNA is stably transcribed, the corresponding truncated NOX2 protein is never immunodetected by Western blot analysis, suggesting either the absence of the specific epitope recognized by monoclonal antibodies, or, more probably, the instability of the mutated protein. Approximately 50% of the point mutations in 13 exons of *CYBB* are missense mutations responsible for replacement of a single amino acid. Generally, these mutations do not affect mRNA stability but act on the level of NOX2 expression in phagocytic cells, leading to either X91⁰, X91⁻, or X91⁺ CGD variants. The superscripts minus or plus mean that NOX2 expression is diminished or normal, respectively. NADPH oxidase activity is always totally abolished in X91⁰ and X91⁺ CGD, while in X91⁻ CGD neutrophils, this activity can be residual (Stasia et al., 2003).

b. NCF1 And Pseudogenes:

The cytoplasmic p47phox subunit (frequency, 30%) of the NADPH oxidase enzyme is encoded by *NCF1* (OMIM number 233700), (Stasia & Li, 2008). This gene is located on chromosome 7 at location 11.23 and encodes a protein of 390 amino acids. The *NCF1* gene is 15 kb long and consists of 11 exons varying from 55 to 165 bp in length. In healthy individuals, the *NCF1* gene locus contains one *NCF1* gene and two pseudo-*NCF1* (Ψ -*NCF1*) genes, one on either side of *NCF1* (Görlach et al., 1997; Antonell et al., 2006), one having the same orientation as *NCF1*, the other one having a reverse orientation (Antonell et al., 2005). The 5' upstream region has been identified and no TATA and CAAT boxes were found, unlike the promoter region of *CYBB*. The pseudogenes are >99% homologous to *NCF1* but differ from *NCF1* in one important aspect: they both contain a GT deletion (Δ GT) at the start of exon 2, causing a frameshift and premature termination of protein synthesis. In addition, some single nucleotide polymorphisms (SNPs) distinguish *NCF1* from Ψ -*NCF1* at various locations (Chanock et al., 2000). These SNPs are used as segregation points to distinguish *NCF1* from its pseudogenes and can be used to analyze DNA from CGD patients. The mutations found in *NCF1* in autosomal p47phox-deficient (A47⁰) CGD patients are not as heterogeneous as those found in other CGD subtypes. More than 90% of all A47⁰ CGD patients lack an intact *NCF1* exon 2, meaning they only have Ψ -*NCF1* exon 2 sequences, containing the GT deletion (Casimir et al., 1991; Iwata et al., 1994). This is caused by unequal cross-over events between *NCF1* and Ψ -*NCF1* during DNA replication or repair (Roesler et al., 2000; Vázquez N et al., 2001), this unequal cross-over can take place between *NCF1* and its pseudogenes (Fig. 4.1A) or within *NCF1* and a pseudogene (Fig. 4.1B). The first mechanism results in the deletion of *NCF1* from one allele. A child inheriting such an allele from both of its parents will suffer from a total deletion of *NCF1* and thus from a lack of p47phox. In the second mechanism, the result will be the formation of a fusion gene, with one part derived from an *NCF1* pseudogene and another part derived from the *NCF1* gene. If the 5' end of such a fusion gene is derived from a pseudogene, thus lacking an intact exon 2, the fusion gene will not encode a functional protein (Fig. 1.4B, allele 1). A child inheriting such alleles from both parents will also be a p47phox-deficient CGD patient. If the 5' end of the fusion gene is derived from *NCF1*, the fusion gene might encode a functional p47phox protein (Heyworth et al., 2002) (Fig. 1.4B, allele 2), but we have obtained indications that in such situations the mRNA splicing is disturbed, again disrupting production of functional p47phox.



Adopted from: Hayrapetyan A. et al., (2013)

Figure (1.4): A. Crossing over between *NCF1* (allele 1, top) and one of its pseudogenes (allele 2, top), resulting in complete removal of functional *NCF1* from one allele (allele 1, bottom) and addition of *NCF1* on the other allele (allele 2, bottom). B. Crossing over within *NCF1* (allele 1, top) and one of its pseudogenes (allele 2, top), leading to the formation of fusion genes.

Most patients have a homozygous GT deletion, which predicts a frameshift within a premature stop codon at amino acid 51, leading to a complete absence of p47phox protein from the patients' neutrophils (A47⁰ CGD). Of approximately 100 patients investigated in previous studies, only 12 patients were compound heterozygote for the Δ GT and one additional mutation; five patients were homozygote for a point mutation different from the Δ GT, and two patients had two different mutations on both alleles of *NCF1* but other than Δ GT (Roos D et al., 1996; Cross AR et al., 2000, B; Jurkowska et al., 2004, B).

The mutations other than the classical Δ GT at the beginning of exon 2 were small mutations (nonsense, missense mutations, and small deletion) and always led to A47⁰ CGD (Görlach et al., 1997). Because of the presence of these Ψ -*NCF1* and the extreme homology between them and *NCF1*, it is hardly possible to detect carriers for A47⁰ CGD by normal PCR and sequencing methods. However, the pseudogenes are characterized by a single 30-bp block in intron 1, which is duplicated in the functional gene, and by a 20-bp duplication in intron 2, where *NCF1* has a single 20-bp stretch. A number of single nucleotides are also

different between *NCF1* and Ψ -*NCF1s*. Therefore, gene and pseudogene-specific PCR, starting from cDNA or from genomic DNA, have been used (Roesler et al., 2000; Noack et al., 2001; Heyworth et al., 2002; De Boer et al., 2002).

c. CYBA Gene:

Mutations in the *CYBA* gene encoding p22phox are extremely rare (frequency <5%). The *CYBA* gene (OMIM number 233690) mapped to 16q24 has 6 exons. The promoter region of *CYBA* contains TATA and CCAC boxes and Sp1, γ -interferon, and nuclear factor κ B sites (Moreno et al., 2003).

Studies on *CYBA* showed 26 different mutations (Cross et al., 2000, B; Dinauer et al., 1990; Roos et al., 1996; Ishibashi et al., 2000; Moreno et al., 2003; Bakri et al., 2008), most of the mutations (15/28) are missense or nonsense. Only one mutation is a large deletion (>10 kb); three of them are real splice-site mutations caused by a base change in the GT 5' donor sequence of the intron. Most of the small insertions or deletions led to a frameshift, and in one mutation the entire exon 2 and exon 3 were deleted from the genomic DNA, the genetic reason for this exon's skipping was not determined (Rae et al., 2000).

In 2000 two new mutations have been described in *CYBA* (Stasia et al., 2002; Bakri et al., 2008), the first one is a 36-bp deletion in the intron 4–exon 5 junction leading to abnormal intronic sequence incorporation in the p22phox mRNA. The second one is a 7-bp deletion in exon 5 leading to a frameshift and a premature stop codon at position 188 (El Kares et al., 2006; Bakri et al., 2008).

Missense mutations leading to A22⁰ CGD are principally located in the potential transmembrane passages of p22phox. This includes the amino acids and the sequences involved in the structural stability of p22phox. Perhaps some of these regions are possible interaction sites with NOX2. Finally, the only missense mutation, Pro156Gln, leading to the unique A22⁺ CGD, is located in the potential cytosolic C-terminal tail of p22phox (Dinauer et al., 1991; Leusen et al., 1994, A). The proline 156 to glutamine substitution inhibits the ex vivo and in vitro p47phox and p67phox translocation from the cytosol to the plasma membranes. Most likely, binding of p47phox is disturbed because p47phox is thought to interact first with cytochrome b558 (and p22phox more precisely) (Kleinberg et al., 1990; Sumimoto et al., 1996).

d. NCF2 Gene:

Mutations in the *NCF2* gene encoding *p67phox*, accounting for approximately 5% of CGD cases. The *NCF2* gene (OMIM number 233710) mapped to 1q25 possesses 16 exons (Eklund & Kakar, 1999; Ammons et al., 2007). Its promoter region has been well defined. It contains PU.1, IRF1, and ICSBP transcriptional activation sequences, like the *CYBB* gene (Eklund & Kakar, 1999). Because of the homologous cis-element in the *CYBB* and *NCF2* genes, they are regulated by common transcription factors (Lindsey et al., 2007; Ammons et al., 2007).

Most A67 CGD patients had no expression of the p67phox protein with normal levels of mRNA (Roos et al., 2003). However, an A67⁰ CGD mutation (a T-to-C transition in the conservative 5' splice site of intron 3) resulted in a deletion in mRNA from 174 to 258 bp, leading to a dramatic reduction in mRNA expression. This mutation generated a premature

TGA stop codon at position 60, resulting in the absence of p67phox in the patient containing this T–C transition (Tanugi-Cholley et al., 1995)

Deletion, insertion, missense and nonsense mutations are cause of A67 CGD. All the missense mutations led to A67⁰ CGD and were located in the tetratricopeptide repeat (TPR) domains of p67phox. This demonstrated that the TPR domains are structurally important for p67phox protein stability. Another mutation was described, it is involves exon 9 and exon 10 and is the result of tandem duplication of approximately 1.1 kb caused by the juxta position of intron 8 to intron 10 (Borgato et al., 2001). In this case, the mRNA is dramatically reduced, but using RT-PCR two abnormal bands were found, one containing the duplication of exons 9 and 10, the other one revealing the presence of a second exon 10 between exons 8 and 10. Unfortunately, the authors did not determine the subtypes of this mutation (0, –, or +). The absence of p67phox protein expression leads to the absence or the reduction of p40phox expression. (Stasia MJ & Li XJ, 2008). This confirms that p67phox and p40phox protein stability are related (Vergnaud et al., 2000; Tsunawaki et al., 2002).

1.1.4 Diagnosis of CGD:

The functional diagnosis of CGD can be made by demonstrating the inability of phagocytes from affected individuals to produce a normal respiratory burst. The other phagocyte functions, including chemotaxis, adhesion, phagocytosis, and degranulation of intra cytoplasmic granule populations, are normal. This is conveniently done by the phorbol myristate acetate-stimulated nitroblue tetrazolium (NBT) test (Repine et al., 1979).

In this test, incubation of activated neutrophils with the yellow dye NBT results in the accumulation of dark blue pigment, formazan, within normal phagocytes, although proper interpretation relies on an experienced observer. For X-CGD, carrier status can be determined by observing a mixed population of NBT-positive and NBT-negative cells (Taga et al., 1985). However, a control blood sample carried and preserved in the same manner as the patient's sample and a control fresh blood sample are needed to ascertain the results. More sensitive techniques such as luminol or lucigenine chemiluminescence exist, where fewer than 10⁵ cells can be taken for one test, to measure hydrogen peroxide or superoxide, respectively. The major disadvantage is the expression of the results in arbitrary units (relative luminescence unit [RLU]) and the calculation method (maximum RLU or peak or the sum of total RLU's during a total measurement time that varies depending on the stimuli used). Then fresh purified neutrophils must be used for reproducible results (Stasia & Li, 2008).

A flow cytometric test for superoxide production was first described in 1985 (Taga et al., 1985), being subsequently refined by many groups (Perticarari et al., 1994).

It relies on the reduction of dihydrorhodamine by stimulated phagocytes in heparinized whole blood and provides a quick and convenient method for semi quantitatively determining NADPH oxidase function. It can also accurately detect carrier status in X-CGD. Immunoblotting for individual components of the NADPH oxidase can help identify the defective protein in the majority of cases (remembering that mutations in either subunit of flavocytochrome *b₅₅₈* usually result in the absence of both), while confirmation of the molecular defect can be obtained by sequencing of the relevant gene (Roos et al., 1996).

DHR is preferable because of its relative ease of use, its ability to distinguish X-linked from autosomal patterns of CGD on flow cytometry, and its sensitivity to even very low numbers of functional neutrophils (Elloumi & Holland, 2007).

Immunoblot and flow cytometry can be used to infer the specific genotype. However, molecular determination of specific mutations, available from various research and commercial laboratories, is necessary for prenatal diagnosis, (Holland, 2010).

Prenatal diagnosis can be made on tissue obtained by chorionic villus sampling in the first trimester. This strategy is dependent on identification of specific family based mutations or on informative polymorphisms (Muhlebach et al., 1990). It may also be possible to detect the presence of individual NADPH-oxidase components in chorion-derived macrophages with specific antibody (Nakamura et al., 1990). Alternatively, prenatal diagnosis can be reliably determined by measurement of NADPH oxidase activity in fetal blood samples taken during the second trimester (Goldblatt & Thrasher, 2000).

1.1.5 Correlation between Genetic Defect and Clinical Course:

As a group, patients with X-linked CGD, A22 CGD, and A67 CGD tend to have a more severe clinical course compared to patients with A47 CGD (Dinauer, 2003; Winkelstein, 2000). This may reflect residual superoxide formation by p47*phox*-deficient neutrophils, which can be detected using sensitive fluorescent probes. Some X91 patients have a partially functional gp91*phox*, associated in some cases with a milder clinical course (Dinauer, 2003). However, despite the fact that more than 90% of patients with non-p47*phox*-deficient forms of CGD have undetectable levels of O₂⁻ production, there is a surprising clinical heterogeneity (Dinauer, 2003; Winkelstein, 2000). At one end of the spectrum are patients who develop severe and recurrent bacterial and fungal infections beginning during infancy. At the other end of the spectrum are patients who are well for many years and then unexpectedly develop a serious infection typical of CGD. Polymorphisms in oxygen independent antimicrobial systems or other components regulating the innate immune response are likely to play an important role in modifying disease severity. These remain to be fully defined, although specific polymorphisms in the myeloperoxidase, mannose binding lectin, and FcγRIIa genes are associated with a higher risk for granulomatous or autoimmune complications in CGD (Foster et al., 1998).

1.1.6 Clinical Features, Infections, Treatment and Drugs Toxicity in CGD Patients:

Many CGD patients also develop chronic inflammatory granulomas, which are a distinctive hallmark of this disorder. Symptomatic disease can include colitis, enteritis or granulomatous obstruction of either the gastric outlet or urinary tract. An analysis of 140 patients with CGD followed at the National Institutes of Health (NIH) revealed inflammatory involvement of the gastrointestinal tract in 8% of patients, (Barese et al., 2004), 89% of them had X-linked inheritance (Marciano et al., 2004, A).

In some cases, granuloma formation is a response to active infection, but in many cases it is believed to reflect a dysregulated inflammatory response or inefficient degradation of inflammatory mediators and debris in the absence of respiratory burst derived oxidants (Morgenstern et al., 1997; Segal et al., 2002). Production of oxidants appears to be an important trigger of neutrophil apoptosis at sites of inflammation, which is also important

for resolution of the inflammatory response. Studies have shown that apoptosis is delayed in CGD neutrophils (Hiraoka et al., 1998; Kobayashi et al., 2004).

Ocular manifestations of CGD have been described since 1965 and include dermatitis of the eyelids, conjunctivitis, keratitis, corneal ulcers, optic nerve atrophy, and chorioretinal lesions (Palestine et al., 1983; Carson et al., 1965). A study (Carson et al., 1965) reported 2 of 13 CGD patients presenting with chorioretinal lesions. Subsequently, 11 patients with CGD and chorioretinal lesions were described in scattered studies that reported the lesions were perivascular, nonprogressive, and spared the macula (Palestine et al., 1983; Martyn et al., 1971; Rodrigues et al., 1983). Other reports have suggested that chorioretinal lesions are more common than previously thought and occur primarily in X-linked patients and female carriers (Goldblatt et al., 1999). In some patients, the disease caused severe vision loss (Goldblatt et al., 1999; Kim et al., 2003)

Despite the significant progress made in antibiotic and antifungal therapy and prophylaxis, patients with CGD still have serious infections. Most large studies have shown an infection rate of around 0.15 to 0.3 per year (Martire et al., 2008; Marciano et al., 2004, A).

NIH has followed more than 250 patients with CGD over almost 40 years, the majority of whom were given diagnoses after infections of the skin, lymph node, lung, or liver. A small group of patients (approximately 5%) were identified because of inflammatory lesions being their primary clinical event. The diagnosis was usually established early in life (median age of diagnosis, 5.4 years), although a small proportion were given diagnoses as adults. Notably, the majority of these later diagnoses were due to autosomal recessive forms of CGD. Isolation of the microorganism causing infection in patients with CGD is essential to rational and appropriate treatment but is not always feasible. About 80% of patients with CGD at the NIH with a pulmonary infection underwent some type of diagnostic procedure, either needle biopsy or bronchial lavage. Of these procedures, 52% were successful in identifying a pathogen. Co infection, such as fungal plus bacterial infection, was found in less than 10% of biopsy specimens. Viral infections appeared at similar rates as in the general population. The majority of infections in patients with CGD are due to 4 bacterial organisms (*Staphylococcus aureus*, *Serratia marcescens*, *Burkholderia cepacia* complex, and *Nocardia* species), as well as species of the fungus *Aspergillus*. Invasive aspergillosis has been a major cause of morbidity and mortality in patients with CGD, but the advent of the newer azole antifungal agents has dramatically changed the treatment and outcome of these infections (Segal et al., 1998; Winkelstein et al., 2000; Vinh et al., 2009, A).

Patients with CGD might present without symptoms or with low grade fevers and only mild constitutional symptoms inconsistent with the extent of disease seen by using imaging studies. Consequently, frequent imaging studies (eg, computed tomography and magnetic resonance imaging) are recommended for clinical monitoring. The lung was the most common site of disease in the NIH, and *Aspergillus* species was responsible for approximately 40% of the culture-positive cases. Chest scans and markers of acute inflammation (eg, C-reactive protein and erythrocyte sedimentation rate) have proved useful in the diagnosis and monitoring of fungal disease.

North American studies have identified a much higher incidence of *Burkholderia* and *Nocardia* species infections than in European reports, which in part might reflect the differences in diagnostic approaches and might also reflect environmental differences (Martire et al., 2008; van den Berg et al., 2009).

Emerging pathogens in patients with CGD include gram negative pathogens (eg: *Granulibacter bethesdensis* (Greenberg et al., 2006), gram positive pathogens (eg: *Actinomyces* species (Reichenbach et al., 2009), and fungi (eg, *Neosartorya udagawae* (Vinh et al., 2009, B). Occurrence of these uncommon pathogens in patients with CGD might provide clues to the critical pathways and functions of the NADPH oxidase (Messina et al., 2002; Brechard & Tschirhart, 2008).

Liver abscesses are common in patients with CGD (Lublin et al., 2002). Thirty percent of NIH patients had liver abscesses, with 25% of these occurring more than once. *S aureus* was the organism most frequently cultured, and surgical resection was the usual treatment. Percutaneous drainage was usually not helpful because liver abscesses associated with CGD tend to develop multiple loculations. When resected, the lesions are a collection of micro abscesses (Lublin et al., 2002). Corticosteroids have been reported to be helpful in 2 cases of liver abscess (Yamazaki-Nakashimada et al., 2006).

Other staphylococcal infections are typically confined to the skin or lymph nodes (Segal et al., 2000).

Patients compliant with prophylaxis still have skin infections, but these infrequently spread. Skin and soft tissue infections are caused by *S aureus*, *Klebsiella* species, *S marcescens*, *B cepacia* complex, and some fungi. Lymph node and skin infections have decreased overall and constitute only about 20% of the infections seen in NIH patients.

Antibacterial (trimethoprim- sulfamethoxazole) and antifungal (itraconazole) prophylaxis has significantly reduced the rates and severity of infections in patients with CGD, but breakthrough infections still occur (Gallin et al., 2003; Mouy et al., 1994). Prophylactic antibiotics were used in 93% of NIH patients with CGD, with trimethoprim-sulfamethoxazole the most frequent. Intolerance to sulfamethoxazole or other adverse events typically led to use of trimethoprim alone, cephalosporins, or quinolones.

Fungal prophylaxis was used by only 68% of the patients, although it was recommended for all patients with CGD. Of these, 55% were receiving itraconazole, 30% were receiving posaconazole, and 15% were receiving voriconazole. Typically, patients receiving the latter 2 agents were receiving them after having been treated for an invasive fungal infection. A single-center transplantation study did show better outcomes with posaconazole compared with itraconazole; however, direct extrapolation to patients with CGD might not be appropriate (Sanchez-Ortega et al., 2010).

Mild toxicity related to drugs was recorded in 36% of the overall NIH, 15% of whom had photosensitivity, most likely caused by voriconazole or trimethoprim-sulfamethoxazole. Severe photosensitivity leading to squamous cell carcinoma and melanoma has been reported with long-term voriconazole (Cowen et al., 2010; Miller et al., 2010).

Patients receiving voriconazole should use aggressive sun protection. For patients with severe voriconazole-induced photosensitivity despite sun avoidance, posaconazole causes less photoreactivity.

IFN- γ was shown in 1991 to be effective prophylaxis for CGD. The use of prophylactic antibiotics and interferon- γ (IFN- γ), coupled with aggressive treatment of acute infections. Prophylactic IFN- γ is another mainstay of current management, although its use is not accompanied by any measurable improvement in phagocyte NADPH oxidase activity in the majority of CGD patients. The clinical benefit of IFN- γ is probably related to enhanced phagocyte function and killing by non-oxidative mechanisms. A large, multicenter trial initially established that recipients of IFN- γ had 70% fewer and less severe infections (The International CGD Cooperative Study, 1991). Another study reinforced these findings,

reporting only 0.30 serious bacterial infections and 0.12 serious fungal infections observed per patient-year, in patients observed for up to 9 years, with a total observation period of 328.4 patient-years. Where the mortality rate was 1.5% per patient - year (Marciano et al., 2004, B). The most common side effects were fever and flu-like symptoms. Importantly, there was no increase in the incidence of chronic inflammatory complications of CGD in patients receiving IFN- γ , (Gallin et al., 2003).

Hence, for all patients with CGD, regardless of genetic subgroup, the current recommendation is to use prophylaxis with trimethoprim- sulfamethoxazole, itraconazole, and IFN- γ . Corticosteroids are used to treat clinically significant granulomatous complications of CGD. The prognosis of CGD has improved dramatically in the past two decades with the advent of prophylactic antimicrobials and IFN- γ . (Dinauer, 2003).

However, use in Europe has been less than in the United States because non randomized European data suggested less benefit from IFN- γ (Mouy et al., 1991) with the advent of better antifungal agents and more active oral antibiotics, the percentage receiving IFN- γ is only 36% because of intolerance or lack of access. Fevers, myalgias, and irritability were reported as reasons for stopping the IFN- γ in 13% of patients in 1 study (Marciano et al., 2004, B).

1.1.7 Hematopoietic Cell Transplantation for Patients with CGD:

Currently, the only known cure for CGD is allogeneic hematopoietic cell transplantation. Historically, this has only reluctantly offered because of the risks of procedure-related morbidity and mortality. Additionally, unrelated donor transplantations were riskier than sibling transplantations, and the pool of donors was limited. From 1973, when the first CGD bone marrow transplant was performed, until 2011(Kang et al., 2011) the results of 99 transplantations, not including cord blood recipients, have been published, with the majority being single-case reports (Gungor et al., 2005; Soncini et al., 2008).

However, of the 99 patients undergoing transplantations, 50 occurred in the last 10 years compared with 49 in the prior 27 years. With the advent of nonmyeloablative regimens, the risks surrounding transplantation have decreased and have permitted transplantation in patients with ongoing infections. Additionally, more transplantations are being performed with unrelated donors. Notably, the first transplantation ever performed for CGD used an unrelated donor, and up to 2000, 22 patients have undergone transplantation with unrelated donor transplants, with the majority performed within the last 10 years.

Hematopoietic stem cell transplantation has been more frequently offered to European patients with CGD than North American patients. The first large report of bone marrow transplantation for CGD was from a group of European centers describing the results in 27 patients undergoing transplantation from 1985 to 2000 (Seger et al., 2002). HLA-matched sibling donors were used for 25 of these cases, and the majority received a myeloablative, busulfan-based regimen. In 9 patients undergoing transplantation during a refractory infection, there were 2 graft failures and severe graft-versus-host disease (GvHD) in 3 patients, with 1 patient dying as a result. In the North American study (Horwitz et al., 2001), reported the outcomes of 10 patients who received a fully matched sibling donor transplant with a nonmyeloablative conditioning regimen of fludarabine, cyclophosphamide, and anti thymocyte globulin (ATG). Stem cell products were T-cell depleted, and donor lymphocyte infusions were given after transplantation to augment engraftment. Eight patients were engrafted, but 1 had significant GvHD resulting in death, with 1

additional patient dying 18 months after transplantation with pneumococcal sepsis despite full myeloid engraftment. Of the non engrafted patients, both survived and went on to retransplantation, with 1 dying subsequently. Long-term follow-up in the engrafted patients showed stable mixed chimerism in 2 patients, including donor lymphoid engraftment of less than 50% in 1 patient but continued myeloid engraftment, with more than 10 years' follow-up. All surviving patients with engraftment remain phenotypically well, with no evidence of CGD-related autoimmune complications or infections.

Two other studies, both from European centers, (Soncini et al., 2008) described the results in 20 patients undergoing transplantation from 1998 to 2007. Patients ranged in age from 15 months to 21 years. Ten of those were with matched sibling donors, 9 receiving bone marrow and 1 receiving cord blood. The remainder received transplants from matched and single mismatched unrelated donors, including 1 cord blood transplantation. The follow-up ranged from 4 to 117 months; 18 (90%) patients survived with continued normal neutrophil function, and 2 died from pretransplantation fungal infections. The majority of the patients received a busulphan- cyclophosphamide conditioning regimen, with alemtuzumab added for those receiving unrelated donor products. (Schuetz et al., 2009), also reported 12 patients, 9 of whom received grafts from unrelated donors. The majority received busulfan-cyclophosphamide with or without either ATG or alemtuzumab. Two patients had graft failure, and 5 patients had grade 1 or 2 acute GvHD. At a mean follow-up of 53 months, 9 of the 12 were alive, including 7 of the 9 recipients of matched unrelated transplants, all with stable engraftment, including 1 patient with mixed chimerism.

The first cord blood transplantation for CGD was an 8-year-old boy undergoing transplantation with an unrelated donor matching at 5 of 6 loci published in 1999 by (Nakano et al., 1999). He was conditioned with 10 Gy of total-body irradiation, ATG, and cyclophosphamide but died at day 51 from infection. Seven subsequent patients have been reported as having received cord blood products, either from related or unrelated donors (Kikuta et al., 2006; Suzuki et al., 2007; Soncini et al., 2008; Jaing et al., 2010; Bhattacharya et al., 2003), three of the patients have required second transplantations. One patient received his initial cord blood product for his retransplantation. All appear to have done well, even when a cord product was used for both transplantations. More recently, with advanced genetic and fertility techniques, 3 cases of pre implantation selection have resulted in live births of siblings who have provided cord blood, bone marrow, or both. The patients who received these products appear to be doing well (Reichenbach et al., 2008; Goussetis et al., 2010).

1.1.8 Gene Therapy of CGD:

CGD is also a candidate disease for gene therapy targeted at hematopoietic stem cells (HSCs) (Barese et al., 2004). Observations on female carriers of X-linked CGD, variant X-linked CGD patients with residual enzyme activity, and preclinical studies in murine CGD models suggest that complete correction of respiratory burst activity in ~10% of circulating neutrophils would lead to clinically relevant improvements in host defense, particularly against *Aspergillus* (Barese et al., 2004). However, correction of > 20% of neutrophils will likely provide broadest protection against bacterial infection and granulomatous complications (Dinauer et al., 2001; Goebel et al., 2005). The relative level of superoxide within individual neutrophils may also be an important factor, and only partial correction of

cellular NADPH oxidase activity may not restore full antimicrobial activity (Dinauer et al., 2001).

The majority of preclinical studies in CGD have used gamma-retroviral vectors, although lentiviral vectors have attracted increasing attention. Lentiviral vectors can transduce quiescent cells, which is an advantage for future use in human hematopoietic stem cells. “Self-inactivating” lentiviral vectors with deleted viral enhancer sequences may also provide safety advantages over gamma-retroviral vectors, because the former tend to insert into the body of the gene rather than near gene promoters, with less chance of activating expression of neighboring genes (Baum et al., 2004).

Several phase I CGD gene therapy clinical trials using cytokine-mobilized peripheral blood CD34⁺ cells have either been completed or are ongoing. In initial trials by (Malech et al., 1997) at the NIH and by Mary C. Dinauer at the Indiana University School of Medicine, retrovirally transduced autologous peripheral blood CD34⁺ cells were reinfused into patients without any bone marrow conditioning. Oxidase positive peripheral blood neutrophils were observed over months, although numbers were very low (at most, 0.2% of neutrophils) and disappeared altogether within a year. These studies suggested that, not surprisingly, marrow conditioning prior to reinfusion of transduced cells was going to be important in order to achieve higher level engraftment of corrected stem progenitor cells.

A new trial being conducted in Europe for X-linked CGD patients utilizes moderate dose busulfan as conditioning prior to infusion of CD34⁺ cells transduced with a gamma-retroviral vector for gp91phox expression (Grez et al., 2005). The two patients reported in this study, higher than expected numbers of oxidase-positive granulocytes were seen post-transplant, which then increased in the months following reinfusion, reaching over 35% in one patient and 15% in the second. Both patients are currently well, with normal peripheral blood counts, and chronic infections associated with CGD have resolved. Analysis of peripheral blood granulocyte DNA showed that the majority of proviral insertions were non-random, and the authors postulated that vector-mediated activation of genes at the insertion sites contributed to the increase in oxidase-positive neutrophils (Schmidt et al., 2005). Another study using the mouse transplant model also suggested that retroviral integration might trigger nonmalignant expansion in murine hematopoiesis due to transcriptional activation of neighboring genes (Kustikova et al., 2005).

1.1.9 Inflammatory Complications and Autoimmunity in Patients with CGD:

Dysregulated inflammation in patients with CGD typically occurs in response to a trigger and might be due to either increased proinflammatory or decreased anti-inflammatory mediators. Patients with CGD frequently experience inflammatory complications, and some might have autoimmune problems (De Ravin et al., 2008). Other than infection, a characteristic feature of CGD is granulomatous inflammation. CGD granulomas are typically non caseating, are composed of multinucleated giant cells, and can be found in multiple organs, including the brain, lungs, liver, spleen, and gastrointestinal tract. When present in hollow viscera, they can lead to obstruction, such as obstruction of the gastric outlet or ureteral obstruction, which are relatively common in patients with X-linked CGD. For most of these granulomas, no pathogen is identified, and they respond rapidly to steroids, suggesting that the inciting event is not an invasive infectious one. Surgical intervention should be avoided, and corticosteroids, when used, are usually started at doses of 1 mg/kg/d and then tapered after 1 week. In many patients the symptoms recur when the

steroid dose is reduced, and thus the corticosteroid dose should be gradually reduced to around 0.1 mg/kg/d on alternate days. Patients with recurring problems can be kept on low-dose prednisone for years, which does not appear to increase infection rates or impair growth (Marciano et al., 2004, A).

A unique presentation in CGD is an acute pneumonitis caused by the inhalation of mulch or other decayed organic matter (eg, potting soil, hay, and leaves). Exposure to a large burden of fungal elements and spores triggers an acute inflammatory response, leading to fever, hypoxia, and diffuse infiltrates, usually beginning within 1 week of the exposure (Ameratunga et al., 2010). Similar responses are seen in mice with CGD exposed to live or even dead fungi (Morgenstern et al., 1997), indicating that some of this pathology is due to dysregulated inflammation rather than infection per se. Bronchoscopy and lung biopsy specimens might yield 1 or more fungal pathogens, especially *Aspergillus* species. In addition to rapid institution of antifungal agents, moderately high doses of prednisone (1 mg/kg/d) help prevent respiratory failure and might facilitate more successful healing (Ameratunga et al., 2010; Siddiqui et al., 2007). Inflammatory lesions without demonstrated pathogens have also been noted in the lungs of patients with CGD and are characterized by discrete infiltrates on chest computed tomography that wax and wane without intervention. In some patients diffuse pulmonary inflammation can progress to hypoxia and functional limitation (Brown et al., 2008). It is difficult to exclude infection despite negative cultures, cytology, nucleic acid testing, and the lack of improvement in response to antibacterial or antifungal agents. However, in some cases empiric treatment beyond corticosteroids has included methotrexate (Segal et al., 2010).

Inflammatory bowel disease characterized by granulomatous involvement of the bowel, especially in the perirectal area, is hard to distinguish pathologically from Crohn disease. However, the inflammatory bowel disease seen in patients with CGD is typically limited to the bowel and unassociated with any of the extra intestinal manifestations often seen in patients with Crohn disease. In the NIH series 43% of X-linked and 11% of p47phox-deficient patients had biopsy-proved symptomatic bowel disease (Marciano et al., 2004, A). Other autoimmune diseases in patients with CGD and carriers have included IgA nephropathy, antiphospholipid syndrome, systemic lupus erythematosus, idiopathic thrombocytopenic purpura, and juvenile idiopathic arthritis (Winkelstein et al., 2000).

Dysregulated inflammation might play a role in the development of autoimmune complications in patients with CGD. For example, normal NADPH oxidase activity plays regulatory roles in apoptosis (Yamamoto et al., 2002; Arroyo et al., 2002) and macrophage clearance of apoptotic cells (Fernandez-Boyanapalli et al., 2010; Fernandez-Boyanapalli et al., 2009). Altered NADPH oxidase function can therefore lead to aberrant macrophage programming, impaired clearance of antigen, and intracellular elements, with further recruitment of neutrophils and prolonged production of IL-8, IL-1b, caspases, and other proinflammatory cytokines (Lekstrom-Himes et al., 2005; Fadok et al., 2001).

Persistence of CGD phagocytes during induced inflammation was reported in human X-linked CGD (Gallin et al., 1983) and in murine CGD-related peritonitis (Jackson et al., 1995; Segal et al., 2002)

These diverse studies suggest that the role of the NADPH oxidase in patients with CGD extends far beyond the simple predisposition to infection. Treatment for inflammatory and autoimmune complications in patients with CGD is problematic because most agents are immune suppressive and immunity is already impaired in patients with CGD. Many patients respond well to corticosteroids, but they might require prolonged courses.

Sulphasalazine and azathioprine are useful steroid-sparing agents. TNF- α inhibitors, such as infliximab, are effective anti-inflammatory agents but might significantly increase the risk of severe and even fatal infections (Uzel et al., 2010).

1.2 Aims of Study:

- Molecular detection of the defected gene and type of mutation(s).
- If it is X-linked or autosomal, hence the percentage of each type among the pediatric patients in Benghazi.

2. Subjects and Methods:

2.1. patients and samples:

2.1.1. Patients:

Blood samples were obtained from 14 patients (8 males and 6 females) who were admitted to Immunology Department at Pediatric Hospital of Benghazi, the samples were collected from July 2013 to April 2014 with appropriate institutional consent; the prevalence of the patients was as the following: 3 patients from Benghazi, 1 patient from Ijdabia, 2 patients from Albyda, 4 patients for Alabiar, 2 patients from Almarj, 1 patient from Cidi-Khalifa and 1 from Tuckra.

Some patients were confirmed as CGD cases and others were only clinically diagnosed; family pedigree and history were taken from patients; some biochemical tests were done for patients depending on their cases.

The patients' samples numbered from (p1 to p14), while the control's samples numbered as (C1, C2, C3).

Patient No. 1:

Gender: female. Age: 4,5 years.

Approved CGD, - NBT test.

Diagnosis:

Left side neck swelling, lymphadenopathy and abdominal sepleenomegally.

History:

Parents are relatives. Complained of fever, lymphadenopathy and bloody diarrhea after vaccinations.

Treatment history:

Septrin syrup

Treatment:

Cloxacillin I.V, Rocephine I.V

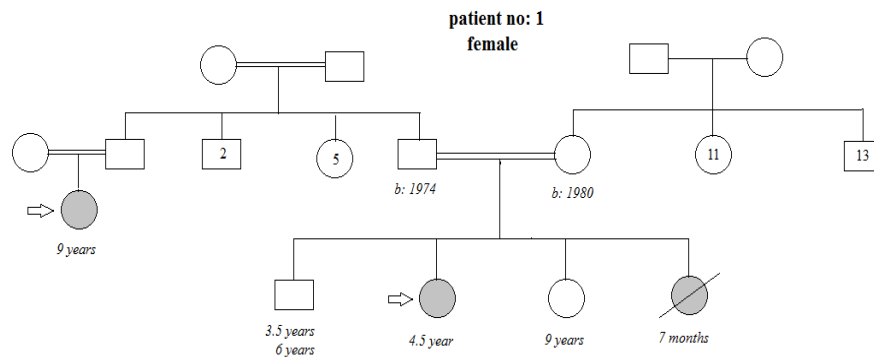


Figure (2.1): Family Pedigree of patient No. 1.

Patient No. 2:

Gender: male. Age: 8 months. Wt: 6.5 KG.

Approved CGD, - NBT test.

Diagnosis:

CGD, osteomyelitis in the left forearm and right ankle.

History:

Parents are not relatives. At 1 month of age patient had lymphadenitis, recurrent infections is continued.

Treatment:

I.V Ciprofloxacin, I.V Gentamicin.

USS report:

Spleen enlarged in size, evidence of large amount of subcutaneous Particular fluid collection (abscess) another focal area of fluid collection seen at Rt. Ankle joint.

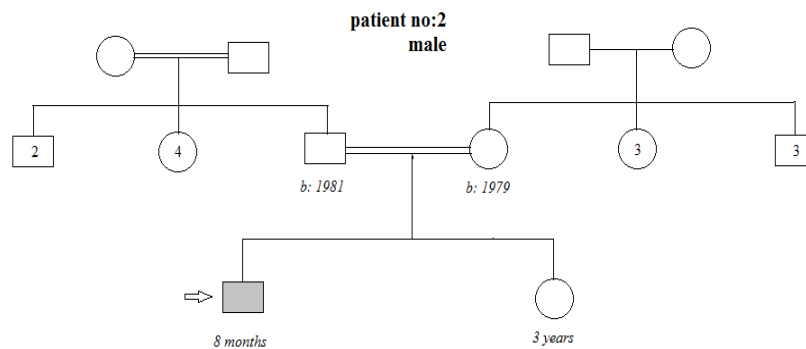


Figure (2.2): Family Pedigree of patient No. 2.

Patient No. 3:

Gender: male. Age : 11months. Wt: 7 KG

Approved CGD, - NBT test, + DHR test

Diagnosis:

Lung pneumonia " fungal", admitted with fever, persistent vomiting, rickets, sepsis, diarrhea, skin rash and anemia.

History:

Parents are not relatives, his brother died before at age 1.5 year with the same symptoms. Symptoms started at 15 days of age. Admitted before to hospital at 3 months of age due to pneumonia, hepatomegally, distended abdomen.

Treatment history:

Sporanox syrup 1x1, Septrin syrup 1x1

Treatment:

Oxygen inhalation every 2 hours, I.V cloxacillin, I.V amphotericin, I.V hydrocortisone.

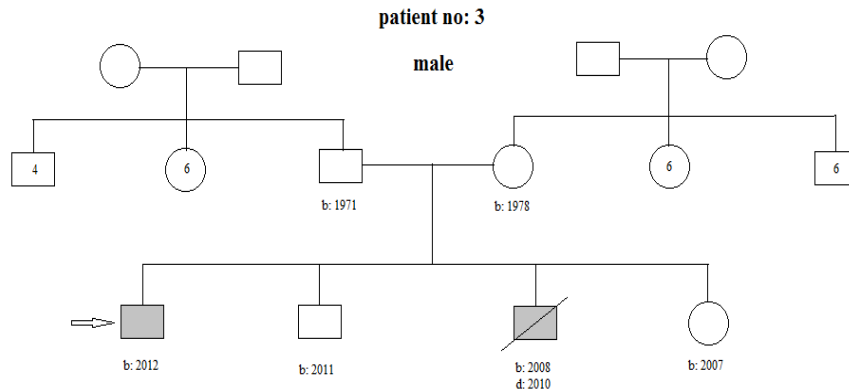


Figure (2.3): Family Pedigree of patient No. 3.

Patients No. 4:

Gender: female. Age: 5 months. Wt: 5.3 KG.

Approved CGD. - NBT test.

Diagnosis:

Patient admitted with liver abscess.

History:

Recurrent infection started from 2 months. Parents are relatives. Another child infected in the family.

Treatment history:

Septin syrup 1x1

Treatment:

I.V meronem → 7 days, I.V vancomycin → 7 days.

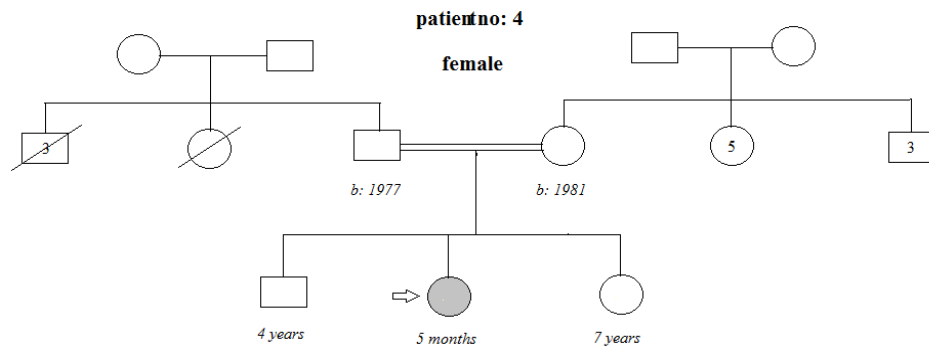


Figure (2.4): Family Pedigree of patient No. 4.

Patient no: 5

Gender: female. Age: 13 yrs. Wt: 30.

Approved CGD. - NBT test.

Admission with cough for one week .

Diagnosis: bronchopneumonia.

History:

Recurrent infection started from 3-4 month of age.

She subjected to bone marrow transplantation in 2/2012.

Parent are first degree relatives, she has two sisters and one brother dayed from the same cause.

Treatment:

Septtrin tap. 1/3 days.

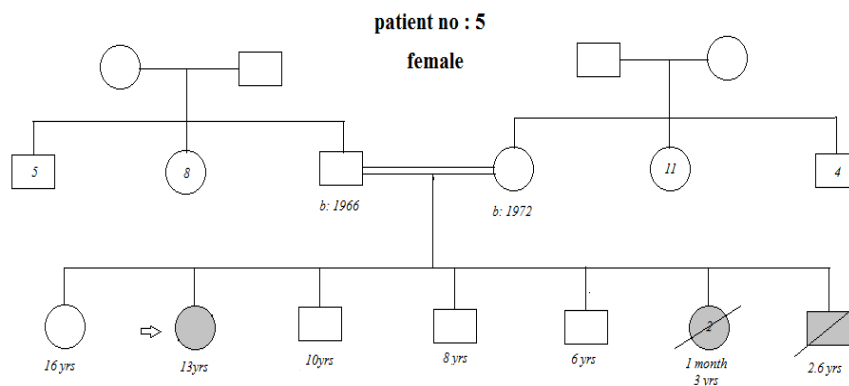


Figure (2.5): Family Pedigree of patient No. 5.

Patient No. : 6

Gender: male. Age : 4 months. Wt: 5KG. Ht : 61Cm

Suspected CGD.

Diagnosis: admission with left ring finger swelling (osteomyelitis), on ampiclox treatment for 10 days without improvement.

History:

Left axillary swelling and liver slightly enlarged after BCG vaccine.

Treatment:

Claforam I.V, Ampicillin I.V, Cloxacillin I.V

Multi vit. Syrup, Ferrus sulphate syrup.

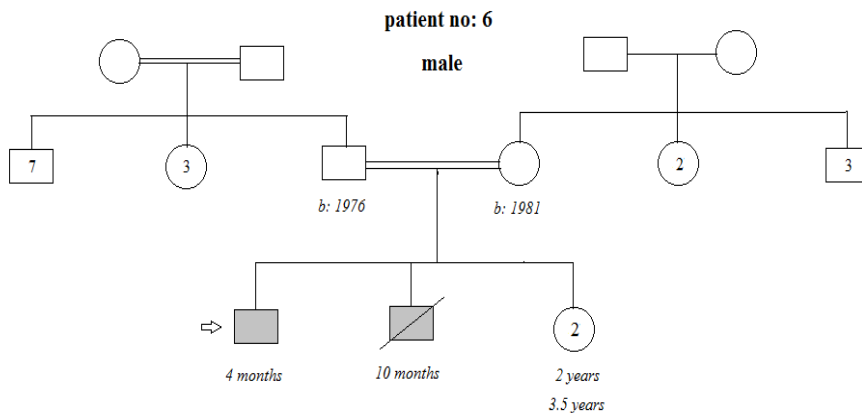


Figure (2.6): Family Pedigree of patient No. 6.

Patient No. 7:

Gender: male. Age 5 years.

Approved CGD. - NBT test.

History:

Parents first degree relatives.

Recurrent infection since 13 days of age , after BCG vaccine.

At 2 months of age abscess in neck and face, fever and diarrhea at 11months of age.

Treatment history:

Sporanox 1×1, Septrin 1×1

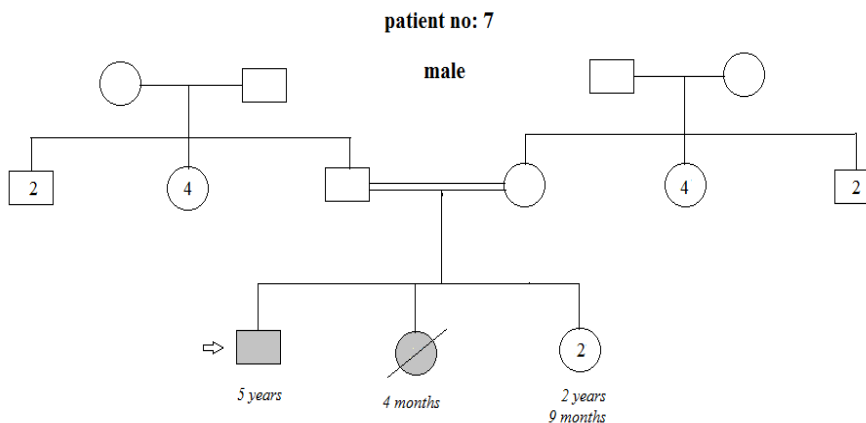


Figure (2.7): Family Pedigree of patient No. 7.

Patient No. 8:

Gender: female. Age: 2 years old. Wt: 10 KG

Suspected CGD.

Admitted with fever and mouth rash for 1 week .

History:

Parents first degree relatives.

At 6 months admitted to hospital with lymphadenitis, hepatomegaly, pneumonia and splenomegaly.

Ultrasound:

Liver wildy enlarged with normal echo.

Treatment:

Ampicillin I.V, Cloxacillin I.V.

Treatment history:

Seprtrin syrupe 1×1.

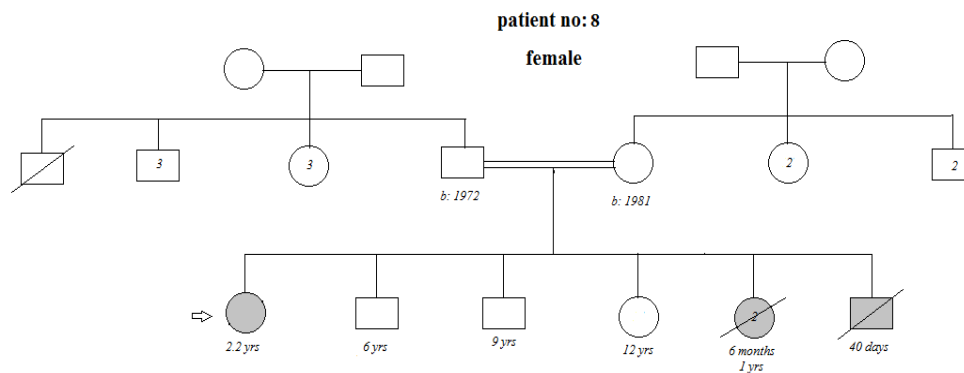


Figure (2.8): Family Pedigree of patient No. 8.

Patient No. 9:

Gender: male. Age: 5 months. Wt: 5,2 KG. Ht: 57 CM.

Suspected CGD.

Admitted to hospital complains of fever and breathlessness.

Diagnosis:

Bronchopneumonia.

Histo. Analysis:

RBC: moderate microcytic hypochromic RBC, aminocytosis, anisochromia.

Platelet: adequate to increase.

WBC: leukocytosis mainly neutrophils cytoplasmic vacuole.

Treatment:

Claforam I.V, Cloxacillin I.V, Gentamycin I.V, Ventolin nebulizer, Nystatin oral suspension.

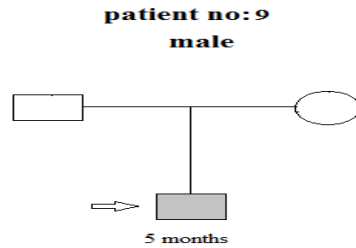


Figure (2.9): Family Pedigree of patient No. 9.

patient No. 10:

Gender: female. Age: 10 years. Wt: 19 KG.

Approved CGD. - NBT test.

Admitted to hospital complain of cough, fever.

Diagnosis: CGD, bronchopneumonia.

History:

Parents are first degree relatives, her cousins daughter is CGD patient also. Second day after birth she was complain of fever, pneumonia, spleen and lymph node enlargement. In 2006 diagnosed as CGD case in Tunisia.

Treatment history:

Septin syrupe 1×1, Sporanox syrupe 1×1

Treatment:

Hydrocortisone I.V 60 mg, Ventolin nebulizer, Claforam for 4 days.

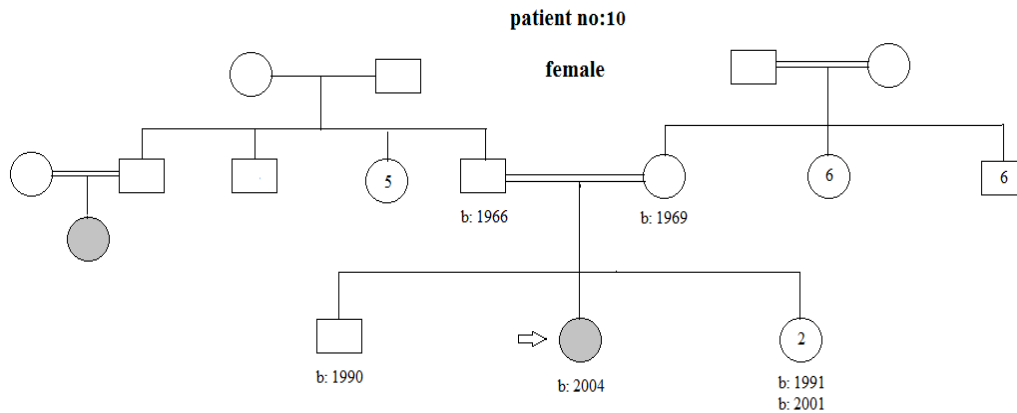


Figure (2.10): Family Pedigree of patient No. 10.

Patient No. 11:

Gender: female. Age: 2 months.

Approved CGD. + NBT

History:

Admitted to hospital with cervical lymphadenitis

Parents are relatives.

Recurrent infections

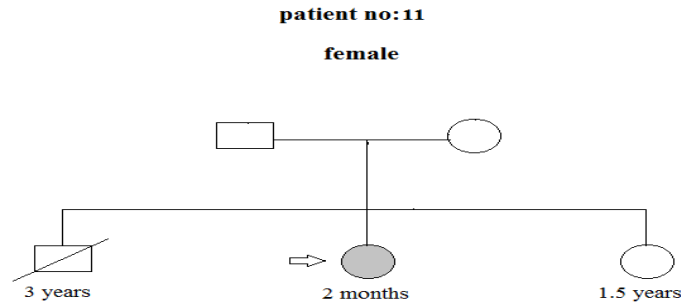


Figure (2.11): Family Pedigree of patient No. 11.

Patient No. 12:

Gender: male. Age: 3 years. Wt: 12 KG.

Suspected CGD.

Diagnosis:

Lymphadenopathy in axilla and inguinal lymph node.

Hepatomegally, spleenomegally.

History:

Parents are relatives.

Recurrent infections are started from 40 days of age until last admission.

Treatment history:

No medication is taken.

Treatment:

I.V Rocephine, I.V Flagyl

Histo. Analysis:

RBC: Hypomicrocytic with mild change

Platelet low with giant forms

WBC: mainly neutrophils with few toxic granules and vacuoles, few reactive lymphocyte.

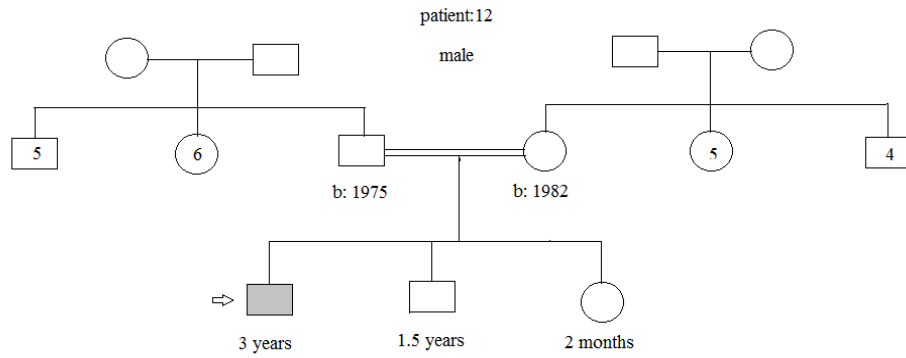


Figure (2.12): Family Pedigree of patient No. 12.

Patient No. 13:

Gender: male. Age: 9 years. Wt: 21 KG. Ht: 121 cm.

Approved CGD. + NBT test.

Diagnosis:

Complain of neck swelling

History:

Parent are not relative

Patient has one brother died in 2011 with unknown cause.

Recurrent infections started from birth . pneumonia, fever, lymphadenitis, anemia.

Treatment history:

Seprine 1×1, Sporanox 1×1, α interferon injection 3/w.

Treatment:

Ciprofloxacin I.V, Rociphen I.V (for 18 days before admission to hospital)

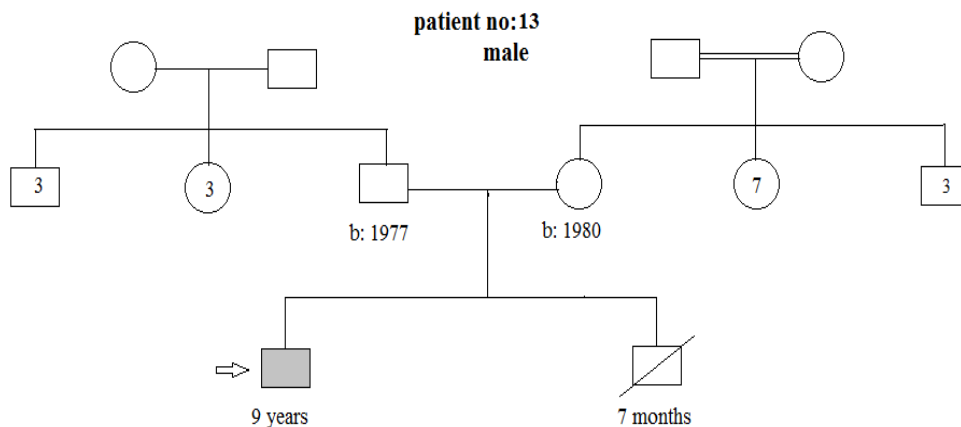


Figure (2.13): Family Pedigree of patient No. 13.

Patient No. 14:

Gender: male. Age: 6 months.

Suspected CGD.

Diagnosis: sever pneumonia, (he's an ICU patient).

History:

Parents are relatives, he has two prothers and one sister died because of CGD.

Treatment:

I.V antibiotic.

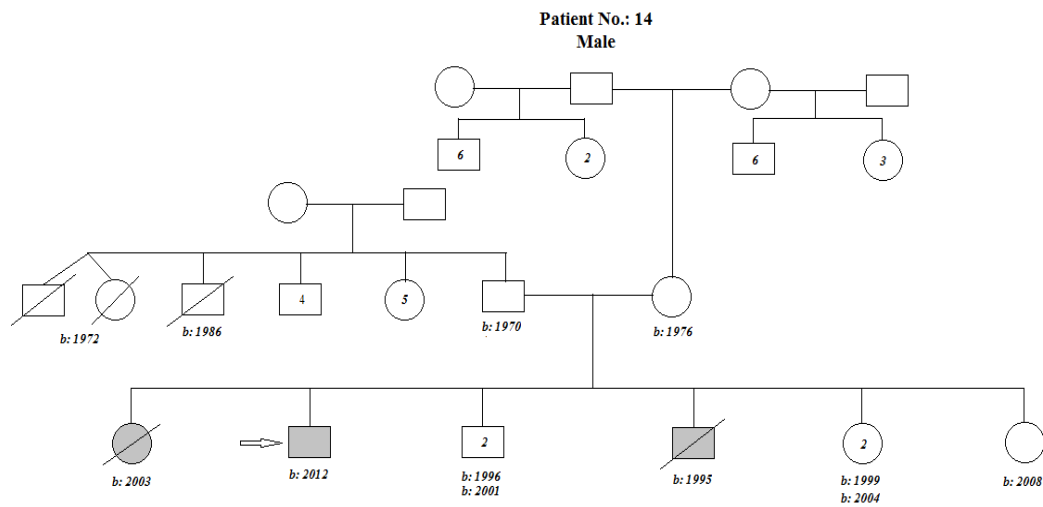


Figure (2.14): Family Pedigree of patient No. 14.

2.1.2. Blood sampling

Samples were collected from the affected individuals. Blood was obtained from the subjects by veinopuncture after obtaining informed written consent from the patient. Blood was obtained from the subjects by veinopuncture in CBC tube containing EDTA to prevent blood clotting. The collection of the whole blood samples in the Benghazi pediatric hospital.

2.2. Extraction of DNA

Genomic DNA from all patients was isolated from whole blood using QIAamp DNA Mini Kit (QIAGEN, USA) in 200 µl of total volume according to user protocol.

2.2.1. The QIAamp Mini Principles:

QIAamp DNA Blood Mini Kits are intended for fast and efficient purification of total genomic DNA from human blood from a donor for reliable PCR. Total genomic DNA can be purified from 200 µl, of whole blood. QIAamp DNA Blood Mini Kits are suitable for use with whole blood that has been treated with EDTA or heparin, and samples may be fresh or frozen. After lysis, the lysate is loaded onto the QIAamp spin column. DNA binds to the QIAamp membrane while impurities are effectively washed away in two centrifugation steps. Finally, DNA is eluted in Buffer AE or water and is ready for direct addition to PCR reactions, or it can be safely stored at – 20°C.

2.2.2. Materials: Equipment and Reagents

- Ethanol (96 – 100%).
- 1.5 ml microcentrifuge tubes.
- Pipets tips with aerosol barrier.
- Microcentrifuge (with rotor for 2 ml tubes).
- Vortexer.
- Heating block at 56°C.
- QIA amp DNA Blood Mini Kit (50):

QIAGEN Protease: (Pipet 1.2 ml protease solvent into a vial).

Buffer AL :(Mix Buffer AL thoroughly by shaking before use).

Buffer AW1: (add 25 ml of ethanol), Buffer AW2: (30 ml of ethanol were added).

2.2.3. Procedure for the extraction of DNA:

1. 20 µl of QIAGEN Protease (or proteinase K) Pipeted into the bottom of a 1.5 ml microcentrifuge tube.
2. 200 µl of the sample added to the microcentrifuge tube.
3. 200 µl of Buffer AL added to the sample. Content of the tube mixed by pulse- vortexing for 15 s.
4. The tube incubated at 56°C for 10 min in heating block. DNA yield reaches a maximum after lysis for 10 min at 56°C.

5. The 1.5 ml microcentrifuge tube briefly centrifuged to remove drops from the inside of the lid.
6. 200 µl ethanol (96–100%) added to the sample, and mixed again by pulse-vortex for 15 s. After mixing, the 1.5 ml microcentrifuge tube briefly centrifuged to remove drops from the inside of the lid.
7. The mixture from step 6 applied to the QIAamp Mini spin column (in a 2 ml collection tube) without wetting the rim. the cap closed, and centrifuged at 6000 x g (8000 rpm) for 1 min. the QIAamp Mini spin column placed in a clean 2 ml collection tube (provided), and the tube containing the filtrate discarded.
If the lysate had not completely passed through the column after centrifugation, the QIAamp Mini spin column centrifuged again at higher speed until it is became empty.
8. The QIAamp Mini spin column carefully opened and 500 µl Buffer AW1 added without wetting the rim. The cap closed and centrifuged at 6000 x g (8000 rpm) for 1min.
The QIAamp Mini spin column placed in a clean 2 ml collection tube (provided), and the collection tube containing the filtrate discarded.
9. The QIAamp Mini spin column carefully opened and 500 µl Buffer AW2 added without wetting the rim. the cap closed and centrifuged at full speed (20,000 x g; 14,000 rpm) for 3 min.
10. The QIAamp Mini spin column Placed in a new 2 ml collection tube (not provided) and the old collection tube discarded with the filtrate. The QIAamp Mini spin column centrifuged at full speed for 1 min.
11. The QIAamp Mini spin column Placed in a clean 1.5 ml microcentrifuge tube (not provided), and the collection tube containing the filtrate discarded. The QIAamp Mini spin column carefully opened and 200 µl Buffer AE added.
The QIAamp Mini spin column incubated at room temperature (15–25°C) for 1 min, and then centrifuged at 6000 x g (8000 rpm) for 1 min.
The QIAamp Mini spin column loaded with Buffer AE incubated for 5 min at room temperature before centrifugation to increase DNA yield.

- A second elution step with a further 200 µl Buffer AE will increase yields by up to 15%.
- The elution stored at –20°C for long term storage.
- A 200 µl sample of whole human blood (approximately 5 x 10⁶ leukocytes/ml) typically yields 6 µg of DNA in 200 µl water (30 ng/µl) with an A260/A280 ratio of 1.7–1.9.

2.3. Measuring of DNA purity and concentration:

DNA concentration and purity measured by two methods: absorbance (optical density) by spectrophotometer, agarose gel electrophoresis.

DNA purity measured by spectrophotometer in which Pure DNA samples have an A260/A280 ratio of greater than or equal to 1.8.

DNA purity of 6 samples measured by spectrophotometer:

1. 100ul taken from each sample and putted in cuvette tube.
2. The volume completed to 1.5 ml by distilled water.
3. Distilled water sample used as reference sample.
4. The optical density measured at 260 nm, 280 nm.

2.4. Agarose gel electrophoretic analysis of extracted DNA:

2.4.1. Principles for the agarose gel electrophoresis:

gel electrophoresis is the standard lab procedure for separating DNA molecules and their fragments, based on their size (e.g. length in base pairs) for visualization and purification.

Electrophoresis uses an electrical field to move the negatively charged DNA toward a positive electrode through an agarose gel matrix (When heated agarose solution becomes gel with pore size from 50nm to 200nm).

The migration rates are determined by the length of the DNA, voltage of the electrophoresis and the concentration of the agarose.

The DNA is visualised in the gel by addition of ethidium bromide. This binds strongly to DNA by intercalating between the bases and is fluorescent meaning that it absorbs invisible UV light and transmits the energy as visible orange light. Thus, we can accurately determine the length of a DNA segment by running it on an agarose gel alongside a DNA ladder.

- DNA electrophoresis apparatus: TECHNE multisub, Horizontal agarose (Power supply, Gel tank, comb, cover, Electrical leads, casting tray)
- Electronic balance: aeADAM, Agarose Powder: SCHARLAU__ Agarose high EEO, electyrophoresis grade.
- Deionized Water producing Machine: GFL_2104 Water Stills 2002-2012, 250 ml capped bottle: clear-borosilicate glass, 500 ml beaker, 100 ml measuring cylinder.
- Microwave: LG.
- loading stain, 50X loading buffer, DNA ladder (Gelpilot 100 bp Ladder, QIAGEN), Pipet: (VWR Signature™ Ergonomic High-Performance pipettor), loading tip: (Brand), eppendrof tubes.
- UV photographing Apparatus: Chemi Image - Advanced Molecular Vision, UK

2.4.2. Preparation protocols:

- A. 50X TAE (pH 8.0): 242 g of Tris base, 57.1 ml of glacial acetic acid, 37.2 g Na₂ EDTA.2H₂O to 1 liter deionized water .The agarose solvent should be the same with the running buffer.
- B. Loading Dye (5X): bromophenol blue 25mg, glycerol 3.3 ml, to 6.7 ml with deionized water.
- C. 1 Kb DNA Ladder (a collection of DNA fragments of known lengths) Store markers ready-mixed with loading buffer at 4°C.
- D. Ethidium Bromide: store in a dark bottle at 4° C (carcinogenic, so wear proper protection when handling).

2.4.3. Procedure for the agarose gel electrophoresis:

1. The edges of the casting tray was sealed and putted in the comb then the casting tray was placed on a level surface.
2. 50X Tris-Acetate were diluted 50 times for a final concentration of 1X.by adding 2 ml of 50X TAE and 98 ml of deionized water into the beaker.
3. 0.9% agarose gel was prepared by weighing out 0.9g of the agarose powder and dissolving it with 100ml 1X TAE buffer in a microwave bottle. The bottle was swirl to ensure homogeneous distribution of the agarose powder in the TAE buffer.
4. The agarose-TAE buffer mixture was heated in microwave until it began to boil. The bottle was swirled very well in intervals to ensure all agarose was completely dissolved in the buffer and a clear translucent solution was formed.
5. The agarose solution was allowed to cool slightly and the solution was carefully poured into the casting tray. Air bubbles were avoided.
6. While letting the gel solution to cool, the gel chamber was filled with 400 ml 1X TAE buffer (8 ml of 50X TAE and 392 ml of deionized water).
7. After the gel had cooled completely and solidified, the comb and tape were removed and the tray inserted properly into the gel chamber with the wells closest to the cathode (black) end and the TAE buffer covering the gel and filling the wells.
8. The DNA samples were kept on ice, 8 µl of each sample were pipetted into labeled eppendorf tubes with 2µl loading dye and mixed by filling and emptying the pipette a few times. This loading dye allowed the samples to be seen when loaded onto the gel, and increased the density of the samples, caused them to sink into the gel wells.
9. Samples were carefully and gently expelled into the wells of the gel from left to right. I had been careful not to puncture the gel with the pipette tip.
10. 2µl marker was loaded in the last well (not mixed with loading buffer).
11. A cover was placed on the electrophoresis chamber and electrical leads were connected to the power supply.
12. The gel was allowed to run at 100V for 30min. DNA was migrated toward the anode (red). Every time the power turned on, bubbles were formed on the electrodes in the electrophoresis chamber. The run was always stopped before the bromophenol blue loading dye front exited the gel.

13. After the power pack was turned off, the gel was removed and placed in a stain tray with 9µl ethidium bromide and 100 ml 1X TAE for approximately 20 minutes to allow the gel to stain.
14. Water was replaced several times to remove excess stain.
The agarose gel was put in an UV photographing Apparatus and all the images were recorded and saved by date.
- Five samples were stored in ethanol (99%) which must be removed before running in the gel :
 1. NaAC, PH 5, 3M added to the samples as in Table (2.1).
 2. Samples centrifuged for 10 min, then 500ul of ethanol 70% added to the samples after removal of supernatant.
 3. Samples centrifuged again for 10 min. (this step used to remove the salt NaAC from the samples).
 4. Ethanol removed after centrifugation and 200 ul of distilled water added and mixed with the samples

Table (2.1): amount of NaAC added to the samples:

Sample number	NaAC / 3M
1	150 ul
2	75 ul
3	75 ul
4	125 ul
5	125 ul

2.5. PCR (polymerase chain reaction)

PCR was done for two genes *NCF1* and *CYBB*.

2.5.1. Primers:

Primers of the Homo sapiens *NCF1* gene was obtained from (Noack D. et al, 2001) study. The primers sequences used for *NCF1* exon (exon 2, that had the most common mutation Δ GT deletion) are shown in Table (2.2), In which two forward primer was used, 2LB2 primer covering GTGT sequence at the start of exon 2, and il-3' F primer started at intron 2.

Table (2.2): *NCF1* gene PCR Primers:

<i>CYBB</i>	Primer Name	Primers for long-range PCR (5'→3'direction)	L	Tm	GC%	AF
Exon2	2LB2	F: GTGCACACAGCAAAGCCTCT	20	60	55	190
	2RB2	R: CTAAGGTCCTTCCCAAAGGGT	21	61	52.4	
	il-3' F	F: GGTCCACGTTTGTGCCCT	18	58	61.1	287
	2RB2	R: CTAAGGTCCTTCCCAAAGGGT	21	61	52.4	

F - Forward primer; R - Reverse primer; L-Length of primer; AF-Amplified fragment; Tm-Annealing temperature.

Primers of the Homo sapiens *CYBB* gene was obtained from (Hill et al, 2010) study. the primer sequences used for *CYBB* exons (exons 2, 3, 5, 7, 10 that has the most common mutations in another studies) are shown in (Table 2.3).

Table (2.3): *CYBB* gene PCR Primers

<i>CYBB</i>	Primers for long-range PCR (5'→3'direction)	L	Tm	GC%	AF
Exon2	F: CTACTGTGGAAATGCGGA	18	54	50	214
	R: AGCCAATATTGCATGGGAT	19	53	42	
Exon3	F: GGACAGGGCATATTCTGTG	19	57	52	249
	R: GCCTTTGAAAATTAGAGGAAGTCTAGTA	27	62	33	
Exon5	F: TCATACCCTTCATTCTCTTTGTTT	24	58	33	281
	R: AGTCCTCAATTGTAATGGCCTA	22	58	41	
Exon7	F: TTAATTTCCCTATTACTAAATGATCTGGACTT	31	63	26	255
	R: TGTCAGTAATGAACTGTAATAACAAC	27	61	30	
Exon10	F: GAGCAAGACATCTCTGTAAC	21	57	43	276
	R: CTCTAAGGCCCTCCGAT	17	55	59	

F - Forward primer; R - Reverse primer; L-Length of primer; AF-Amplified fragment; Tm-Annealing temperature .

2.5.2. Resuspending PCR Primers

When primer was received from manufacturer, there was a data sheet included indicating the mass of primer was synthesized.

First a master was created 100X stock (for each primer and then diluted it to a 10X working stock).

Master stock, 100 μ M

$100 \mu\text{M} = X \text{ nmoles primer} + (X \times 10 \mu\text{l nuclease free water})$

The number of nmol of primer in the tube was simply multiplied by 10 and that was the determined amount of H₂O added to make a 100 μ M primer stock.

The Forward and reverse primers 100 μ M stock solutions for *NCF1* exon 2 are shown in Table (2.4).

Table (2.4): The Forward and reverse primers 100 μ M stock solutions for *NCF1* exon:

<i>NCF1</i> exon2 primers	100 μ M forward primer stock.	100 μ M reverse primer stock.
2LB2	28.61 nmol+2861.5 μ l nuclease free water	---
il- 3'F	25.56 nmol+ 255.6 μ l nuclease free water	---
2RB2	---	19.01 nmol+ 190.1 μ l nuclease free water

The original primer tubes are often used for this 100 μ M stock. I mixed them well before making working stock dilutions.

Working stock, 10 μ M

The primer master stocks were diluted in a labeled sterile microcentrifuge tubes 1:10 with nuclease free water.

2.5.3. Polymerase chain reaction

The regions of interest (five exons of *CYBB* gene and exon 2 for *NCF1* gene) were amplified by PCR gradient thermal cycler TC-5000 made by Techne, Bibby scientific using. Each amplification reaction was performed using HotStarTaq Master Mix according to user protocol.

11 patient samples and 2 control samples was used in *NCF1* gene PCR.

13 patient samples and 2 control samples was used in *CYBB* gene PCR.

Procedure:

1. The primer solutions and templates nucleic acid were thawed on ice and mixed thoroughly before use.
2. The HotStarTaq Master Mix was thawed and mixed by vortexing briefly to avoid localized differences in salt concentration.
3. A reaction mix was prepared according to Table (2.5).
4. The reaction was mixed by pipetting up and down a few times. Appropriate volumes were dispensed into labeled PCR tubes.
5. Template DNA (<1 µg/50 µl reaction) was added to the individual labeled PCR tubes.
6. The thermal cycler was program according to the manufacturer's instructions. Each PCR program was start with an initial heat-activation step at 95°C for 15 min, a typical PCR cycling program is outlined in Table (2.6). For maximum yield and specificity, temperatures and cycling times were optimized for each new template target or primer pair.
7. The PCR tubes were promptly closed and placed in the thermal cycler and the cycling program was started. After amplification, samples were stored overnight at 2 –8°C or at 4 °C for few days if next step was not carried out, or at – 20°C for longer storage.

Table (2.5): Reaction setup using HotStarTaq Master Mix (QIAGEN Kit, USA)

Component	Volume/reaction	Final concentration
Reaction mix HotStarTaq Master Mix, 2x	25 µl	2.5 units HotStarTaq DNA Polymerase 1x PCR Buffer* 200 µM of each dNTP
10x primer mix (2 µM of each primer)	2 µl	0.2 µM of each primer
RNase-free water	18 µl	–
Template DNA (added at step 5)	5 µl	<1 µg/reaction
Total reaction volume	50 µl	

Table (2.6): Optimized cycling conditions (QIAGEN Kit, USA)

Step	Time	Temperature	Comment
Initial heat activation	15 min	95°C	Activates HotStarTaq DNA Polymerase.
3-step cycling: Denaturation	0.5–1 min	94°C	
Annealing	0.5–1 min	55–60°C	Approximately 1to 5°C below T_m of primers.
Extension	1 min	72°C	
Final extension	10 min	72°C	Number of cycles 30- 40.

2.5.4. Agarose gel electrophoresis:

Electrophoresis on a 1.4% agarose gel with amplification product 8 μ l and loading dye 2 μ l, the amplification products and marker were visualized with ethidium-bromide staining under ultraviolet light. The results images were saved by dates.

2.5.5. Purification of PCR products:

The PCR samples (five exons of *CYBB* gene and exon 2 for *NCF1* gene) were purified from primers, nucleotides, polymerases, and salts using QIAquick PCR Purification Kit according to user protocol.

Procedure:

1. 5 volumes Buffer PB was added to 1 volume of the PCR reaction and mixed together. The color of the mixture was orange to violet, 10 μ l 3 M sodium acetate was added, pH 5.0, and mixed. The color of the mixture turned yellow.
2. QIAquick column was labeled and placed in a 2 ml collection tube.
3. To bind DNA, the sample was applied to the labeled QIAquick column and centrifuged at (13,000 rpm) for 30–60 seconds. Flow-through was discarded and placed the QIAquick column back in the same tube.
4. To wash, 0.75 ml Buffer PE was added to the labeled QIAquick column and centrifuged for 30–60 s. Flow-through was discarded and placed the QIAquick column back in the same tube.
5. The labeled QIAquick column was centrifuged once more in the 2 ml collection tube for 1 min to remove residual wash buffer.
6. Each QIAquick column was placed in a clean labeled 1.5 ml microcentrifuge tube.
7. To elute DNA, 30 μ l elution buffer was added to the center of the QIAquick membrane, the column was let stand for 1 min, and centrifuged at (13,000 rpm) for 1 min.
8. To analyze the purified DNA on a gel, 5 volumes of purified DNA was added to 1 volume of loading dye. The solutions were mixed by pipetting up and down, they were loaded on a 1.4% agarose gel along with the marker and visualized with ethidium-bromide staining under ultraviolet light. The result images were saved by dates.

2.6. DNA Sequencing:

Sequencing the amplified DNA samples by 3130 Genetic analyzer by (Big dye sequencing kit from applied biosystem,USA), and the site of mutations that cause the disease will be identified.

2.6.1. Primer Preparation for the DNA Sequencing:

8 µl was pipetted from the previously prepared primer`s working stock of each primer and was diluted by 17µl of nuclease free water to give a concentration of 3.2pmol/µl which the concentration needed for the sequencing reaction.

2.6.2. Ethanol /EDTA Precipitation:

To precipitate 20 µl sequencing reactions

2.6.3. Procedure for the DNA Sequencing:

1. The PCR reaction tubes were removed from the thermal cycler and briefly spin.
2. Deionized water was added to the reaction.
3. The contents were transferred to a 1.5ml tube
4. 20µl of 125mM EDTA PH 8.0 was added and mixed by inverting 4-5 times.
5. 259µl of 100% ethanol was added to each tube.
6. The tubes were capped, mixed by inverting 4-5 times and incubated at room temperature for 20 min.
7. The tubes were spinned at 14000 rpm for 15 min and carefully discarded the supernatant.
8. 300µl of 70% ethanol was added to each tube and mixed by inverting 2-3 times.
9. The tubes were spinned at 14000 rpm for 5 min and carefully discarded the supernatant.
10. 300µl of 70% ethanol was added to each tube and mixed by inverting 2-3 times.
11. The tubes were spinned at 14000 rpm for 5 min and carefully discarded the supernatant.
12. The open tubes were inverted on tissue, to drain the remaining ethanol.
13. The pellet was dried at 45°C to 50°C till all alcohol evaporated.
14. The pellet was dissolved in 20µl of Hi-Di formamide, vortex and spinned briefly.
15. 15-The samples were loaded in 96-well plate for performing sequencing.

The reaction mixtures were prepared according to Table (2.7).

The samples were mixed by flicking and put in the thermocycler using the following thermal profile: 1cycle of 96°C: 1min, 25 cycles of 96°C: 10 sec., 53°C: 5 sec, 60°C: 4 min.

Table (2.7): Reagents measurements in the sequencing reaction (Big dye sequencing kit from applied biosystem,USA)

Reagent	Quantity
BDT v3.1 reaction mix	4µl
3.2pmol/ µl primer	1µl
Purified PCR product	1µl
Deionised H ₂ O	14µl
Total	20µl

2.7. Real time PCR (High Resolution Melting):

Principle:

High-resolution melting analysis is an innovative technique that is based on analysis of DNA melting. HRM characterizes DNA samples according to their dissociation behavior as they transition from double-stranded DNA (dsDNA) to single-stranded DNA (ssDNA) with increasing temperature.

Before performing HRM analysis, the target sequence must be amplified to a high-copy number in the presence of the dsDNA-binding fluorescent dye, EvaGreen. The dye does not interact with ssDNA but actively binds to dsDNA and fluoresces brightly when bound. Change in fluorescence can be used to measure the increase in DNA concentration during PCR and then to directly measure thermally-induced DNA melting by HRM.

To perform high-resolution melting analysis, the temperature is increased from a lower to a higher temperature. The fluorescence of EvaGreen is measured continuously as the temperature is increased and is plotted against the temperature. EvaGreen fluoresces as long as it is bound to dsDNA. Due to the amplification procedure before the HRM analysis, fluorescence will be high at the beginning of the HRM analysis. Upon melting of dsDNA, EvaGreen is released and the fluorescence is reduced to a background level.

2.7.1 primers:

primers of the Homo sapiens *NCF1* gene was obtained from (Noack et al, 2001) study. the primers used for *NCF1* exon (exon 2, that had the most common mutation Δ GT deletion) are shown in Table (2.8). In which tow forward primer was used, 2LB2 primer covering GTGT sequence at the start of exon 2, and il-3' F primer started at intron 2.

Table (2.8): *NCF1* PCR Primers

<i>CYBB</i>	Primer Name	Primers for long-range PCR (5'→ 3'direction)	L	Tm	GC%	AF
Exon 2	2LB2	F: GTGCACACAGCAAAGCCTCT	20	60	55	190
	2RB2	R: CTAAGGTCCTTCCCAAAGGGT	21	61	52.4	
	il-3' F	F: GGTCCACGTTTGTGCCCT	18	58	61.1	287
	2RB2	R: CTAAGGTCCTTCCCAAAGGGT	21	61	52.4	

F - forward primer; R - reverse primer; L-length of primer; AF-amplified fragment ;Tm- annealing temperature .

2.5.2. Resuspending PCR Primers

When primer was received from manufacturer, there was a data sheet included indicating the mass of primer was synthesized.

First a master was created 100X stock (for each primer and then diluted it to a 10X working stock).

Master stock, 100 μ M

$100 \mu\text{M} = X \text{ nmoles primer} + (X \times 10 \mu\text{l nuclease free water})$

The number of nmol of primer in the tube was simply multiplied by 10 and that was the determined amount of H₂O added to make a 100 μ M primer stock.

The Forward and reverse primers 100 μ M stock solutions for *NCF1* exon 2 are shown in Table (2.9).

Table (2.9): The Forward and reverse primers 100 μ M stock solutions for *NCF1* exon:

<i>NCF1</i> exon2 primers	100 μ M forward primer stock.	100 μ M reverse primer stock.
2LB2	28.61 nmol+2861.5 μ l nuclease free water	---
il- 3'F	25.56 nmol+ 255.6 μ l nuclease free water	---
2RB2	---	19.01 nmol+ 190.1 μ l nuclease free water

The original primer tubes are often used for this 100 μ M stock. I mixed them well before making working stock dilutions.

Working stock, 10 μ M

The primer master stocks were diluted in a labeled sterile microcentrifuge tubes 1:10 with nuclease free water.

Procedure of RT-PCR by HRM:

1. 2x HRM PCR Master Mix, primer solutions, RNase-free water, template DNAs, are thawed.
It is important to mix the solutions completely before use to avoid localized concentrations of salt.
2. The reaction mix prepared according to Table (2.10).
It is recommended to prepare a volume of reaction mix 10% greater than that required for the total number of reactions to be performed.
Reaction setup can be done at room temperature (15–25°C). However, it is recommended to keep the individual reagents, samples, and controls on ice.
3. The reaction mix was mixed thoroughly, and appropriate volumes were dispensed into PCR tubes or the wells of a PCR plate.
4. Equal amounts and volumes of template DNA (1–50 ng genomic DNA or 1–50 pg microbial DNA, same amount for each sample) was added to the individual PCR tubes or wells and mixed thoroughly.
5. the real-time cycler programed according to Table (2.11).
6. The PCR tubes or plate was placed in the real-time cycler, and the PCR cycling program started, followed by HRM analysis.
7. The data analysis was performed.

Table (2.10): preparation of reaction mixture, (QIAGENE Kit, USA)

Component	Volume per 25ul Reaction	Final concentration
Reaction mix 2x HRM PCR master mix	12.5 µl	1x
10 µM primer mix	1.75 µl	0.7 µM forward primer 0.7 µM reverse primer
Rnase-free water	Variable	---
Template DNA (added at step 4)	Variable	Eukaryotic: 1-50 ng DNA/ reaction Microbial: 1-50 pg DNA/ reaction (equal volume for all reactions)

Table (2.11): the real-time cycler program (QIAGEN Kit, USA)

Step	Time	Temp	Additional comments
Initial PCR activation step	5 min	95°C	HotStarTaq plus DNA polymerase is activated by this heating step
3-step cycling:			Important: optimal performance is only assured using these cycling conditions
Denaturation	15 s	95°C	
Annealing	20 s	55°C	
Extension	25 s	72°C	Activate fluorescence data acquisition on the green channel. Suitable for PCR products up to 350 bp. For PCR >350 bp, use 1s extension time per 25 bp of PCR product length.
Number of cycles	35		
HRM	2 s	65-95°C 0.1°C increments	

2.8. Blast Alignment:

BLAST, or the Basic Local Alignment Search Tool, was specifically designed to search nucleotide and protein databases. It takes a query (DNA or protein sequence) and searches either DNA or protein databases for levels of identity that range from perfect matches to very low similarity. Using statistics, it reports back what it finds, in order of decreasing significance, and in the form of graphics, tables, and alignments.

2.8.1. Steps of Blast alignment of patient's DNA sequence (CYBB Gene) with Gene Bank:

1. Select the BLAST program from the NCBI Website, ncbi.nlm.nih.gov.
2. Enter a query sequence.
3. Select the database to search.
4. Select the algorithm and the parameters of the algorithm for the search.
5. Run the BLAST program.

2.8.2. Blast alignment of patient's DNA sequence (CYBB Gene) with control sample:

1. Select the BLAST program the NCBI Website, ncbi.nlm.nih.gov.
2. Enter a query sequence and the subject (control) sequence.
3. Select the algorithm and the parameters of the algorithm for the search.
4. Run the BLAST program.

3. Results:

The current study is an attempt to elucidate the causative mutations of chronic granulomatous disease using different means of molecular techniques. The study involved 14 patients admitted in the Immunology Department of the Pediatric Hospital of Benghazi. They were eight males and six females, and their ages range from 2 months to 13 years old. All patients presented histories of recurrent infections and seven of them with positive family history. Parents often of the patients had consanguinity marriage.

1.3 the biochemical data:

a. **Hemoglobin (Hb):** Anemia was the major hematological abnormality seen in our CGD patients. The calculated mean Hb value was $9.9 \text{ g/dl} \pm 1.08$.

b. **White Blood Cells (WBC):** The estimated WBC numbers showed a high mean value of $12.2 \times 10^3/\text{ul} \pm 2.8$, which is higher than the report number used as a standard in clinical settings, (Table: 3.1).

c. **Red Blood Cells (RBC):** The estimated RBC numbers of our patients showed a mean value of $4.6 \times 10^6/\text{ul} \pm 1.1$, (Table: 3.1).

d. **Platelet (PLT):** The estimated numbers of PLT produced a calculated mean value of $356 \times 10^3/\text{ul} \pm 139$, which is within the normal range, (Table: 3.1).

e. **Erythrocyte Sedimentation Rate (ESR):** Most patients had high ESR, the mean of which reaching $37 \text{ mm/hr} \pm 19.7$, (Table: 3.1).

f. **Neutrophil:** The estimated numbers of neutrophils showed a mean of $47.4 \times 10^9/\text{L} \pm 30.6$, being higher than the estimated value, (Table: 3.2).

g. **Albumin:** The mean albumin value was in the normal levels ($4.7 \text{ g/dl} \pm 0.8$), but one patient (N0. 4) had high albumin value (6.3 g/dl), (Table: 3.2).

h. **Globulin:** All patients had high globulin value, the mean value being $2.7 \text{ g/dl} \pm 0.87$, (Table: 3.2).

j. **Lymphocyte:** The mean value was high ($32.56 \times 10^9/\text{l} \pm 14.5$), (Table: 3.2).

k. **Total Lymphocyte:** The estimated numbers of lymphocytes showed a high mean value of 4198.5 ± 632.8 , (Table: 3.2).

l. **C – Reactive Protein (CRP):** most patients had high CRP value (41.2 mg/l) and STDEV (38), (Table: 3.2).

m. Immunoglobulins:

- **IgA:** The mean value for immunoglobulin A was as high as $175.9 \text{ mg/dl} \pm 108.9$, (Table: 3.3).
- **IgE:** The mean value for immunoglobulin E was within the normal range ($80.41 \text{ KIU/L} \pm 141.5$), (Table: 3.3).

- **IgG:** Most patients had high immunoglobulin value showing a mean of 1628 mg/dl \pm 298.5. It is worth noting that it is the second hematological abnormality seen in our CGD patients after anemia, (Table: 3.3).
- **IgM:** Most patients had values but within the normal range, the mean value was 143.9 mg/dl \pm 38.28, (Table: 3.3).

n. Aspartate Transferase (AST): Some patients had high AST values and others had values within the normal range, with a high mean value of 91.7U/L \pm 84, (Table: 3.4).

o. Alanine Transferase (ALT): Some patients had high ALT values, but others had values within the normal range. The mean value was as high as 97.9U/L \pm 119.3, (Table: 3.4).

P. Urea: Most patients' urea values were within the normal range, where the mean value was 17.5mg/dl \pm 8.17, (Table: 3.4).

q. Creatinine: Most patients Creatinine values were within the normal range, where the mean value was 0.28 mg/dl \pm 0.1, (Table: 3.4).

r. Total protein: Most patients had normal values, with the mean value of 7.07g/dl \pm 1.9, (Table: 3.4).

s. Alkaline phosphatase: Alkaline phosphatase activity showed a high mean value of 279.5 U/L \pm 120.5, (Table: 3.4).

The high values reported here for IgG, WBC, CRP, Neutrophils associated with anemia may give an indication for CGD.

2.3 Measuring DNA purity and concentration:

Following DNA extraction other steps were taken to measure its purity and concentration, two methods were employed:

- Measuring the optical density by spectrophotometer:** The optical densities of 6 samples were measured as shown in table (3.5). The 260/280 ratio of the six samples was higher than 1.8, and this indicated good purity of DNA samples.
- Measuring the DNA purity and concentration by Agarose gel electrophoresis:** The DNA samples were blotted on 0.9% agarose gel as shown in figure (3.1), lanes from A to M represent the genomic DNA, while lanes 1 and 2 represent the 1kb molecular marker, where the DNA bands appeared with good concentration.

3.3 Size of DNA bands after PCR:

Following the PCR of the *NCF1* gene the DNA sample were blotted on 1.4% agarose gel to detect the desired band based on size of the samples as compared with the 100bp marker.

- Figure (3.2) shows the DNA bands of exon 2 of *NCF1* gene following the PCR by using the forward and reverse primers (F: 2LB2, R: 2RB2), where the lanes from A

to J represent DNA bands with the desired size of about 200 bp, and lanes 1, 2 represent the 100bp marker.

- b. Figure (3.3) shows the DNA bands of exon 2 of *NCF1* gene following the PCR by using forward and reverse primers (F: il-3'f, R: 2RB2), where the lanes from A to L represent DNA bands with the desired size of about 300bp, and lanes 1, 2 represent the 100bp marker.

4.3 Purification of PCR product:

Following the PCR the DNA samples of exon 2 of *NCF1* gene was purified from polymerase, primers, nucleotides and salts, and blotted again in 1.4% agarose gel to detect the desired bands.

- a. Figure (3.4) shows the DNA bands of exon 2 of the *NCF1* gene amplified using the primers (F: 2LB2, R: 2RB2) following their purification, where lanes from A to I represent the purified DNA bands with the desired size of about 200bp, and lanes 1, 2 represent the 100bp marker.
- b. Figure (3.5) show the DNA bands of exon 2 of *NCF1* gene, primers (F: il-3'f, R: 2RB2) after purification where lanes from A to G representing purified DNA bands with desired size about 200 bp, and lanes 1, 2 representing 100bp marker.

5.3 High Resolution melting analysis Real Time PCR (HRM Real Time PCR):

HRM Real Time PCR was used to detect mutations in exon 2 of *NCF1* gene based on analysis of DNA melting, following its amplification where the fluorescence of Eva Green dye that bind to ds DNA was blotted against the increasing temperature.

- a. Figure (3.6) shows the high resolution melting analysis of RT-PCR products of exon 2 of *NCF1* gene by using primers (F: il-3'f – R: 2RB2), where the melting curves of patients samples and controls had the same melting curves, and this shows that no mutation was detected.
- b. Figure (3.7) shows the high resolution melting analysis of Real-Time PCR products of exon 2 of *NCF1* gene by using primers (F:2LB2 – R: 2RB2), where the melting curves of patients' samples and controls had the same melting curves, and this shows that no mutation was detected.

6.3 chromatogram and sequences of patients and controls samples:

Following sequencing of the five exons (2, 3, 5, 7, 10) of *CYBB* gene, we compared between the sequencing chromatogram of patients and controls samples and align the sequences by the sequencer program, as a result no mutations were detected in the five exons of all patients.

7.3 Blast Alignment:

Following CYBB gene sequencing Blast Alignment Tool from the NCBI was used to align patients' DNA sequence and gene bank / control sequencing.

Blast alignment of patient's DNA sequence (*CYBB* Gene) with Gene Bank:

- a. Alignment of exon 2:** no mutation was found in exon 2 of all patients with identity value of 99- 100%.
- b. Alignment of exon 3:** no mutation was found in exon 3 of all patients with identity value of 99%.
- c. Alignment of exon 5:** no mutation was found in exon 5 of all patients with identity value of 98-99%.
- d. Alignment of exon 7:** no mutation was found in exon 7 of all patients with identity value of 97-99%.
- e. Alignment of exon 10:** no mutation was found in exon 10 of all patients with identity value of 99-100%.

Blast alignment of patient's DNA sequence (*CYBB* Gene) with control sample:

- a. Alignment of exon 2:** no mutation was found in exon 2 of all patients with identity value (99-100%).
- b. Alignment of exon 3:** no mutation was found in exon 3 of all patients with identity value (100%).
- c. Alignment of exon 5:** no mutation was found in exon 5 of all patients with identity value (99-100%).
- d. Alignment of exon 7:** no mutation was found in exon 7 of all patients with identity value (97-100%).
- e. Alignment of exon 10:** no mutation was found in exon 10 of all patients with identity value (99-100%).

Table (3.1): The biochemical data for patients recruited for this study.

<i>PT</i>	<i>HB</i>	<i>WBC</i>	<i>RBC</i>	<i>PLT</i>	<i>ESR</i>	<i>CRP</i>
	<i>11-13.3 g/dl</i>	<i>4.5-10 x10³/ul</i>	<i>4.2-5.2 x10⁶/μl</i>	<i>150-400 x10³/l</i>	<i>1-8 mm/hr</i>	<i>0-5 mg/l</i>
P1	10.6					
P2						100
P3	9.2	11.5		324	35	16
P4	9.8			265		16
P5	12.4	8.9		286	55	
P6	9.4	11.7	4.53	512	7	99
P7						
P8	9.2	14.5	5.49			17
P9	9.1	15.8	3.59			28
P10						
P11	9.3	8.7	3.46	205	55	48
P12						
P13	10.6	15.1	5.98	544	33	6.02
P14						
Mean	9.9	12.3	4.61	356	37	41.25
SD	1.08	2.8	1.1	139	19.7	38.

Table (3.2): The biochemical data for patients recruited for this study.

<i>PT</i>	<i>Neutrophil</i>	<i>Albumin</i>	<i>Globulin</i>	<i>Lymphocyte</i>	<i>Total Lymphocyte</i>
	<i>2-7.5 x10⁹/l</i>	<i>3.5-5g/dl</i>	<i>0.6-1g/dl</i>	<i>1.3-3.5x10⁹/l</i>	<i>690 - 2540</i>
P1					
P2		4.1	3.5		
P3		4.6	1.6		
P4		6.3	2.9		3751
P5	44.8	4.6	2.2	38.8	
P6	5.71			52.6	4646
P7					
P8				29.5	
P9					
P10					
P11	76	4.1	3.9	13	
P12					
P13	63.1	4.5	2.2	28.9	
P14					
Mean	47.4	4.7	2.7	32.56	4198.5
SD	30.6	0.8	0.87	14.5	632.8

Table (3.3): The biochemical data for patients recruited for this study.

<i>PT</i>	<i>IgA</i>	<i>IgE</i>	<i>IgG</i>	<i>IgM</i>
	<i>20 -100 mg/dl</i>	<i><295KIU/L</i>	<i>700 – 1411mg/dl</i>	<i>40-200 mg/dl</i>
P1				
P2				
P3				
P4	336	13.53	1971	156.3
P5	276	270		176.3
P6				
P7				
P8		38.02	1424	115
P9	89.94	<0.1	1490	179
P10				
P11				
P12				
P13	174			93
P14				
Mean	218.9	80.41	1628	143.9
SD	108.9	141.5	298.5	38.28

Table (3.4): The biochemical data for patients recruited for this study.

<i>PT</i>	<i>AST</i>	<i>ALT</i>	<i>Urea</i>	<i>Creatinine</i>	<i>Total protein</i>	<i>Alkaline Phosphatase</i>
	<i>5-38 U/L</i>	<i>5-41 U/L</i>	<i>10-50 mg/dl</i>	<i>0.1-1.5 mg/dl</i>	<i>6.4-8.3g/dl</i>	<i>40-129 U/L</i>
P1	32	16	14	0.2		
P2	211	352	15.8	0.2	7.7	230
P3	39.3	15.1		0.2	6.2	
P4	35	9			6.8	153
P5	13.8	8.9	28.1	0.5	10.7	437
P6	39	28.2	12.9	0.2		
P7						
P8	59	84	13	0.3	4.3	298
P9						
P10	220	233				
P11	222	236	8.8	0.3	7.1	
P12	105	69				
P13	33.5	26	30	0.4	6.7	
P14						
Mean	91.7	97.9	17.5	0.28	7.07	279.5
SD	84	119.3	8.17	0.1	1.9	120.5

Table (3.5): The optical density of DNA samples extracted from patients' blood

sample	260 nm	280 nm	260/280
P6	+ 0.0126	+ 0.004	3.1
P7	+ 0.0155	+ 0.0044	3.5
C1	+ 0.0311	+ 0.0125	2.488
C2	+ 0.0375	+ 0.0155	2.4
C3	+ 0.0372	+ 0.0168	2.2
P8	+ 0.0462	+ 0.02	2.31

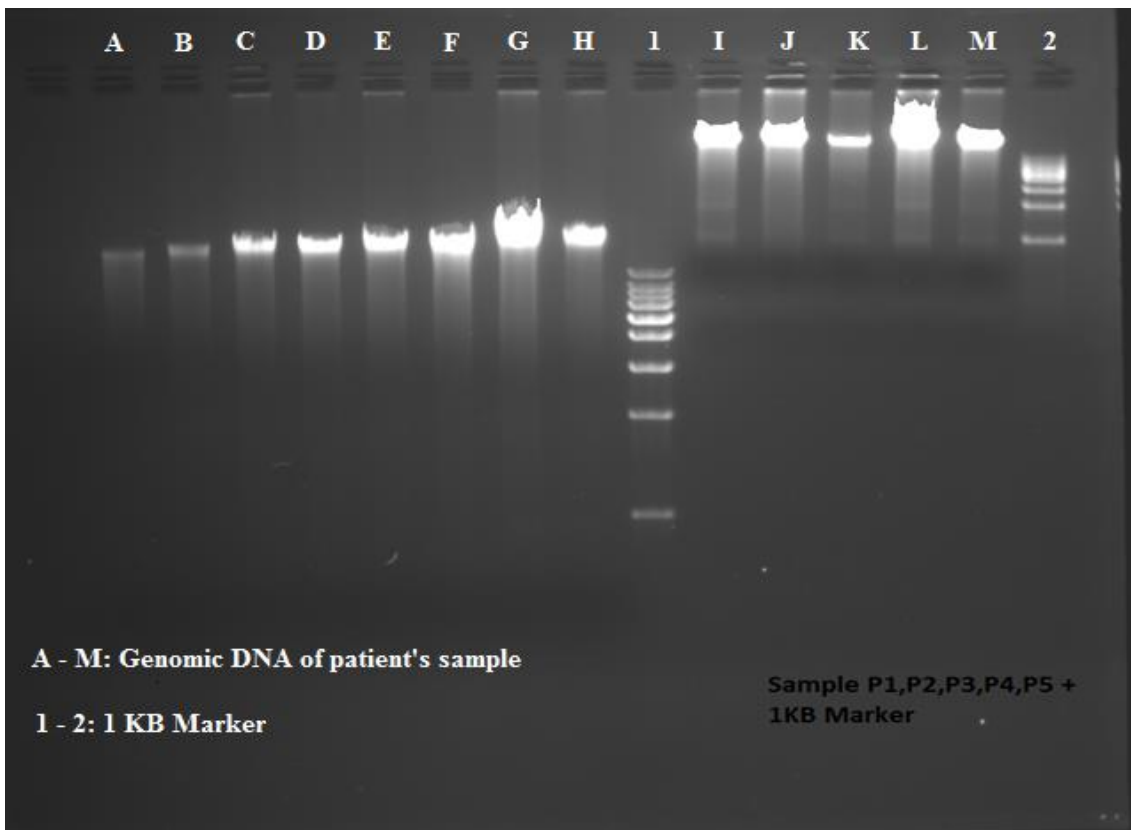


Figure (3.1): Photograph showing the bands that reflect the measured DNA purity and concentration by gel electrophoresis.



Figure (3.2): DNA bands on the gel following PCR for NCF1 gene using primers (F: 2LB2, R: 2RB2).

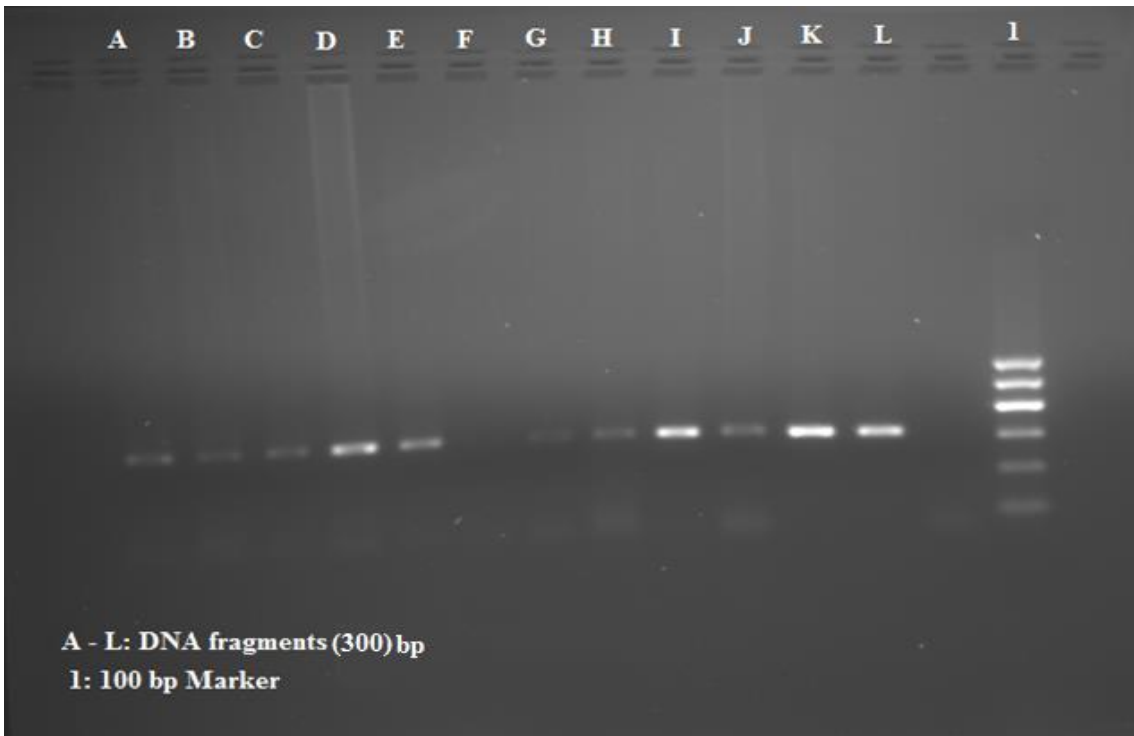


Figure (3.3): DNA bands on the gel following PCR for NCF1 gene using primers (F: il-3'f, R: 2RB2).

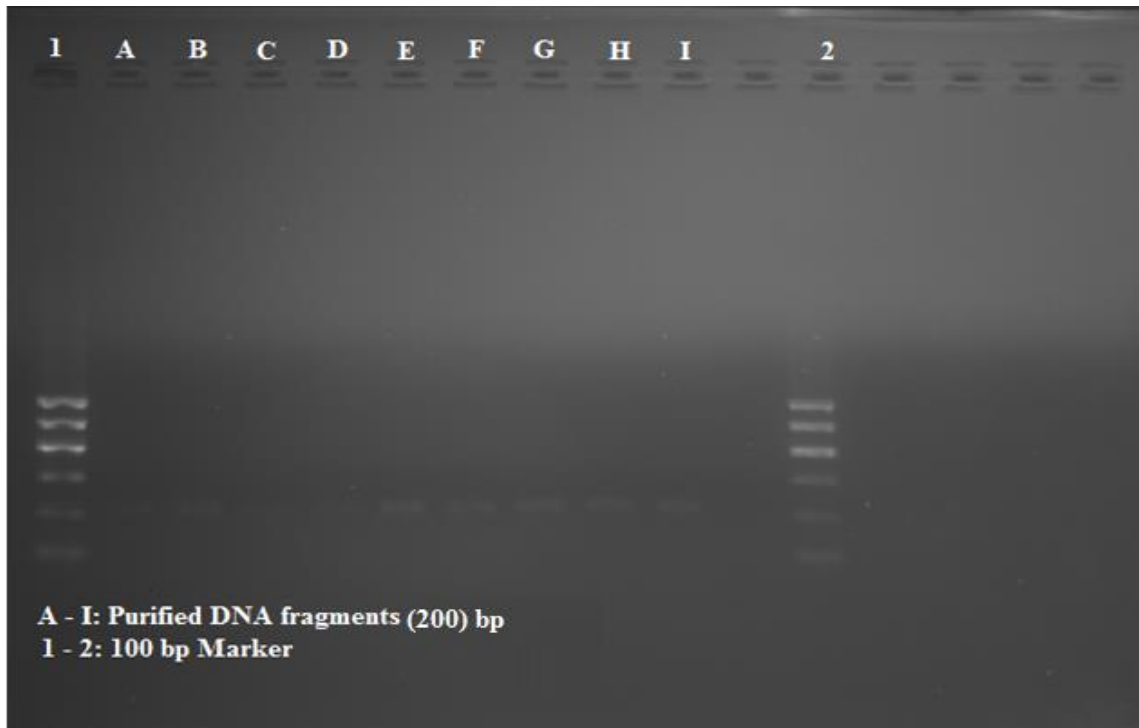


Figure (3.4): DNA bands of NCF1 gene following PCR using the primers (F: 2LB2, R: 2RB2), and after product purification



Figure (3.5): DNA bands of NCF1 gene after purification of PCR samples of primers (F: il-3'f, R: 2RB2)

No	color	Sample No.
1	Red	P1
2	Yellow	P2
3	Blue	P3
4	Purple	P4
5	Pink	P5
6	Cyan	P6
7	Teal	P7
8	Light Red	C1
9	Green	C2
19	Light Pink	C3
20	Red	P8
21	Brown	P9
22	Olive Green	P10
23	Teal	P11
24	Blue	P12
25	Dark Blue	P13
26	Purple	P14
27	Magenta	-C

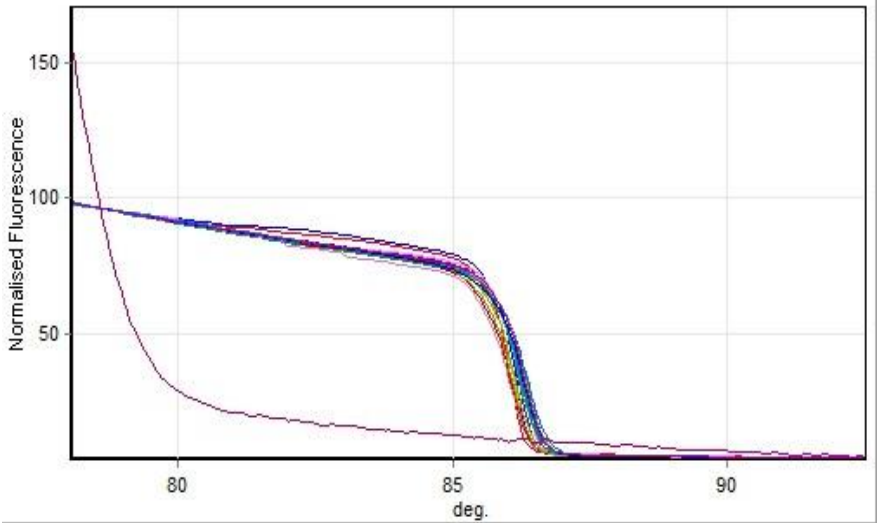


Figure (3.6): HRM, Primers F: il-3'f – R: 2RB2

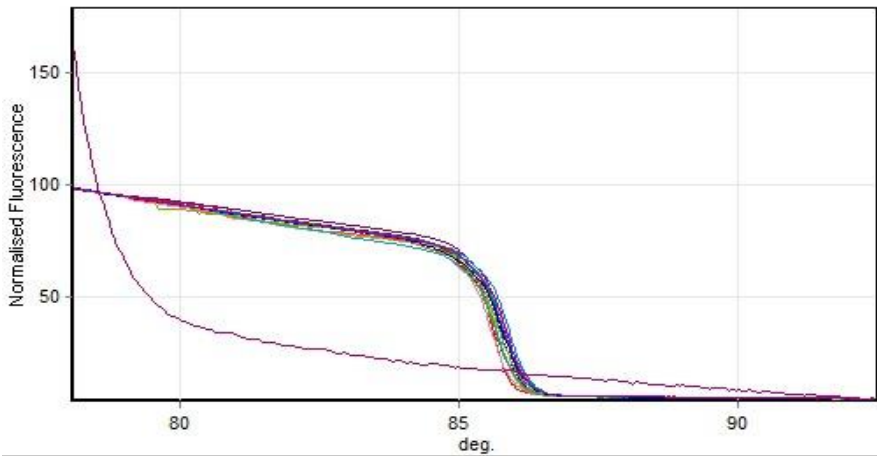


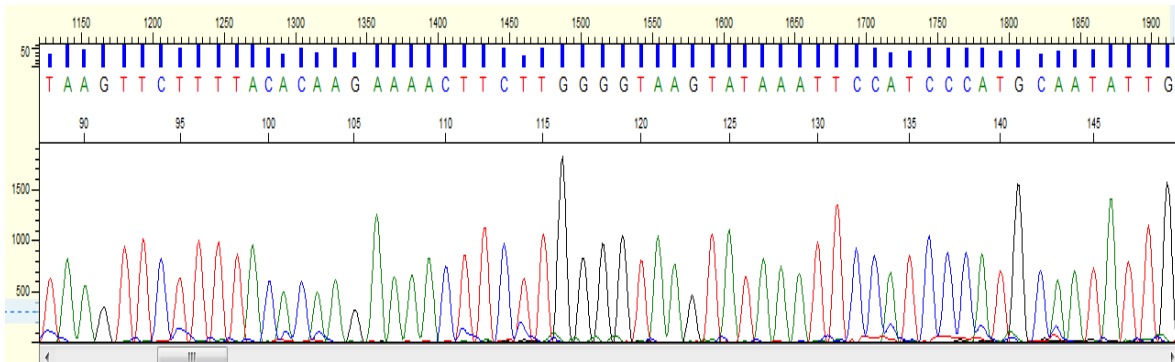
Figure (3.7): HRM, Primers F: 2LB2 – R: 2RB2.

Figures (3.6,3.7): The high resolution melting analysis of real time-PCR products of primers (F:il-3'f – R: 2RB2), (F: 2LB2 – R: 2RB2),respectively. The table indicates the color for each patient's sample.

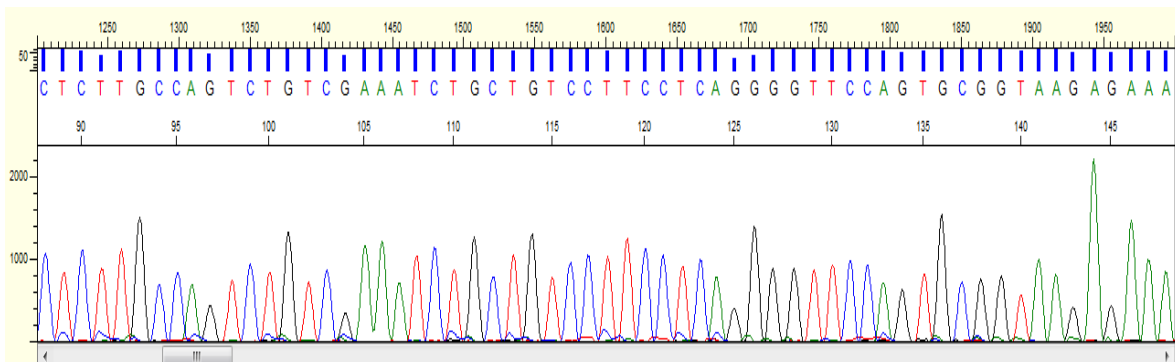
Chromatogram of patients and control samples:

Patient No. 1

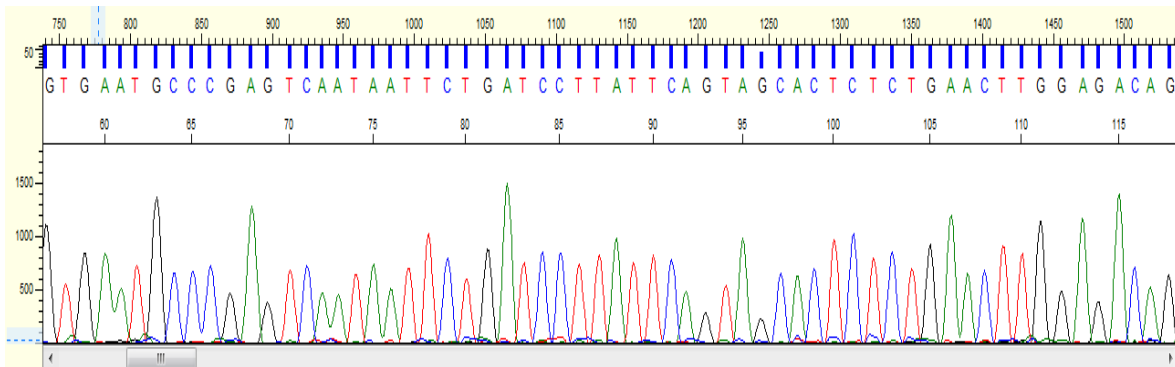
Chromatogram of Exon 2:



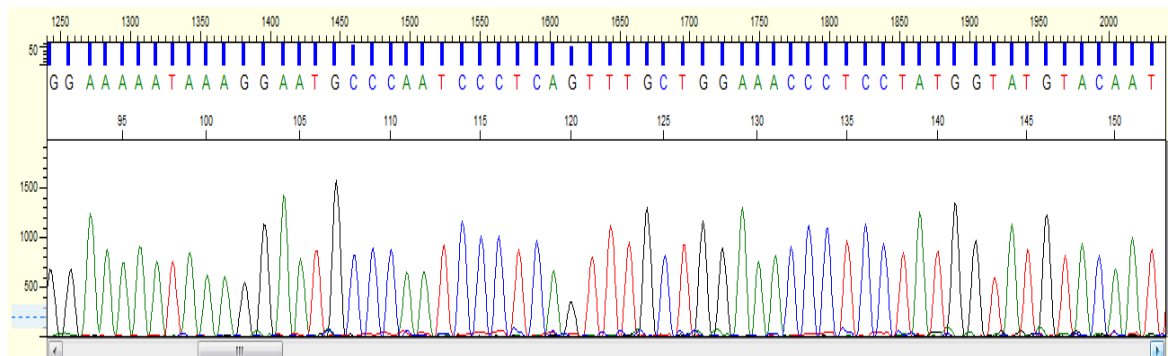
Chromatogram of Exon 3:



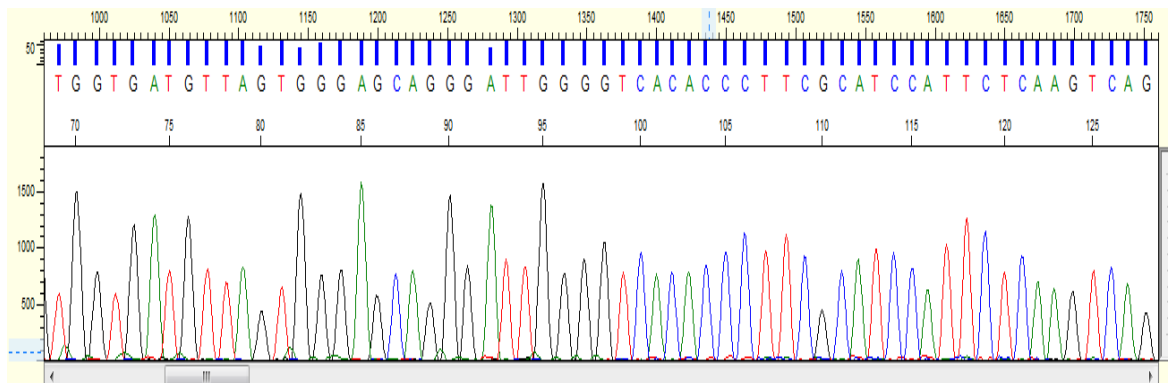
Chromatogram of Exon 5:



Chromatogram of Exon 7:

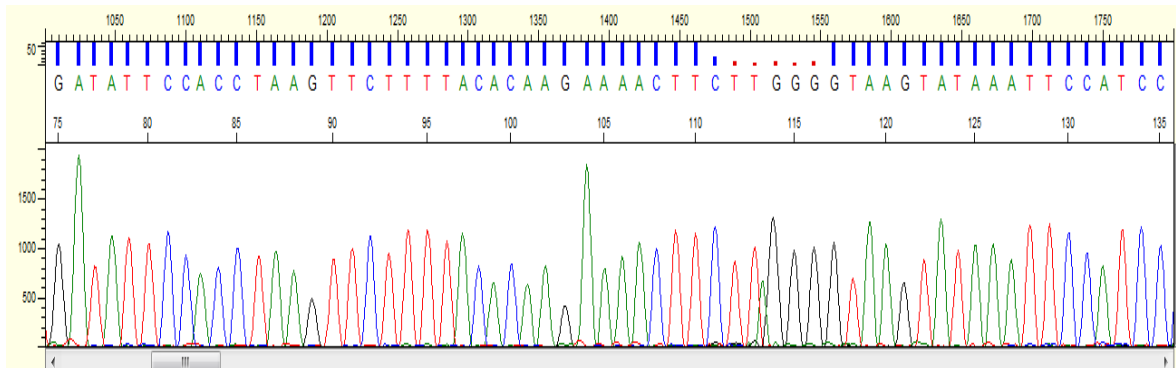


Chromatogram of Exon 10:

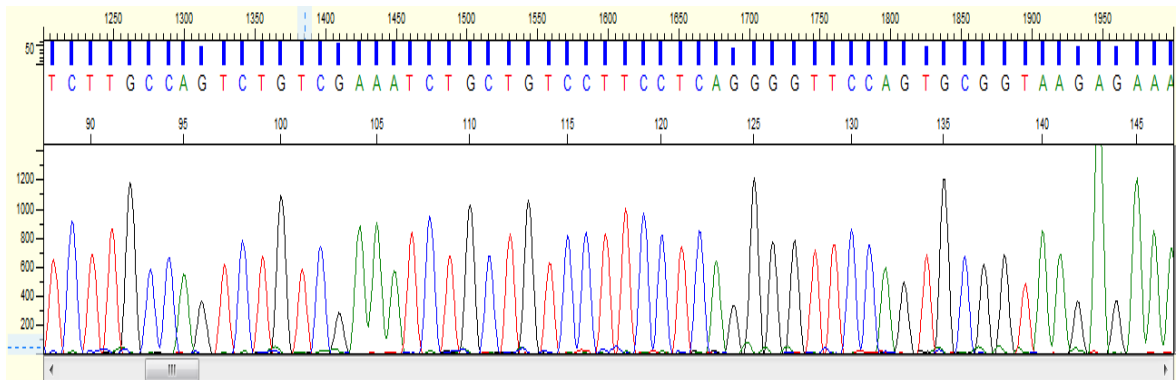


Patient No. 3

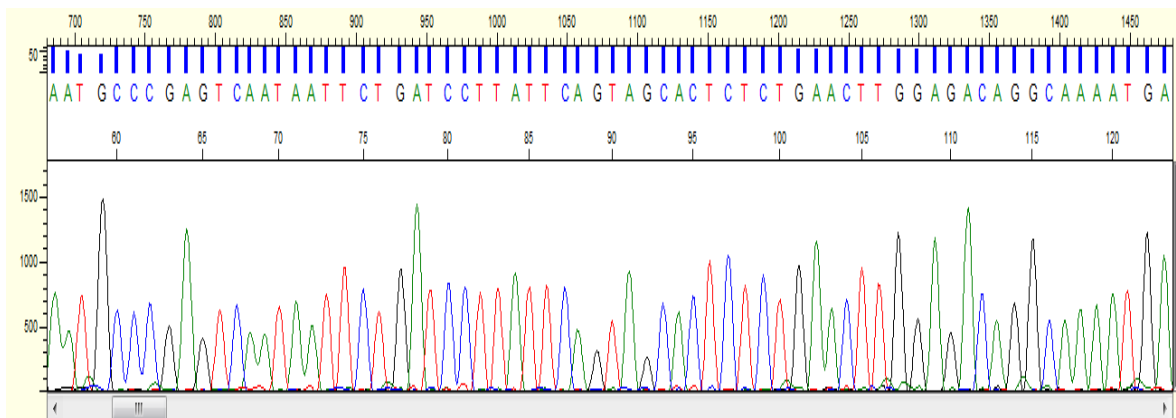
Chromatogram of Exon 2:



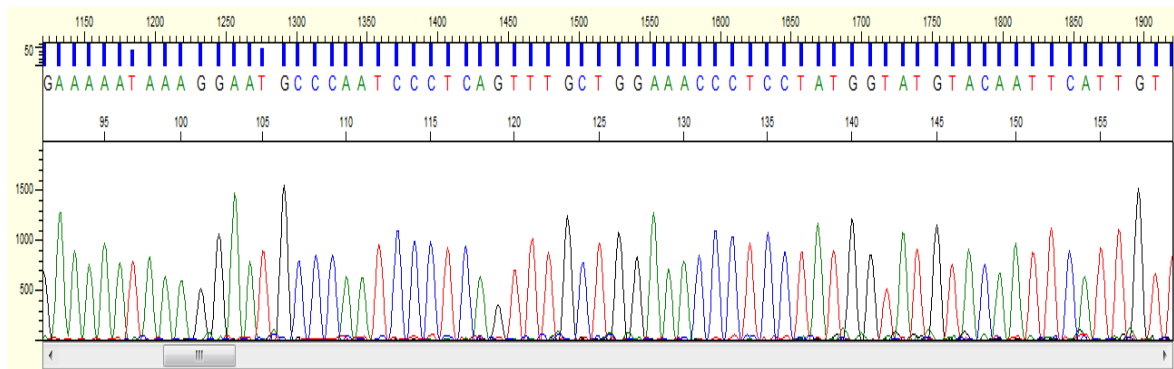
Chromatogram of Exon 3:



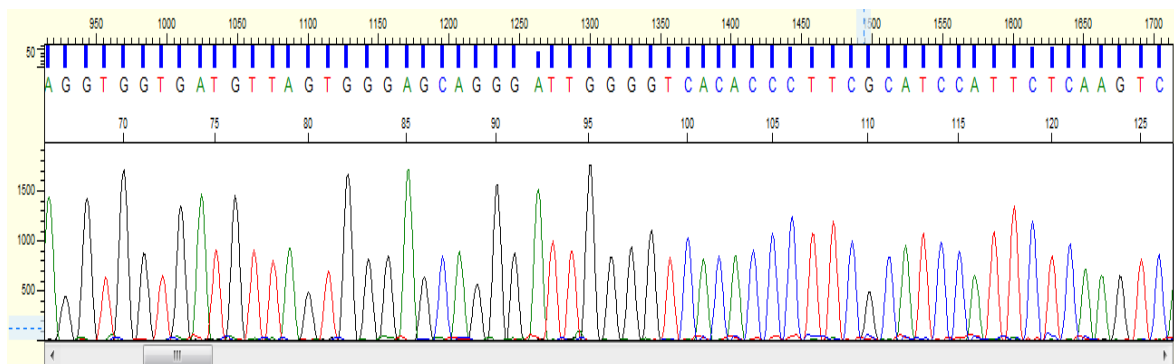
Chromatogram of Exon 5:



Chromatogram of Exon 7:

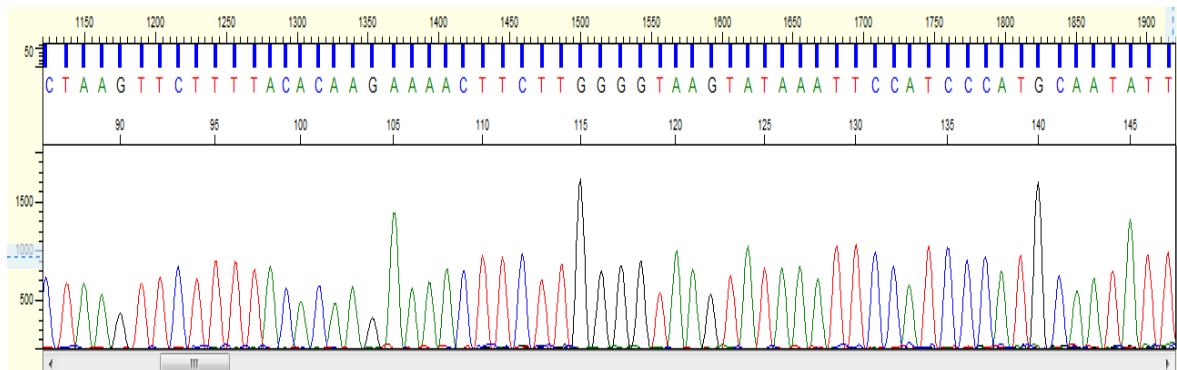


Chromatogram of Exon 10:

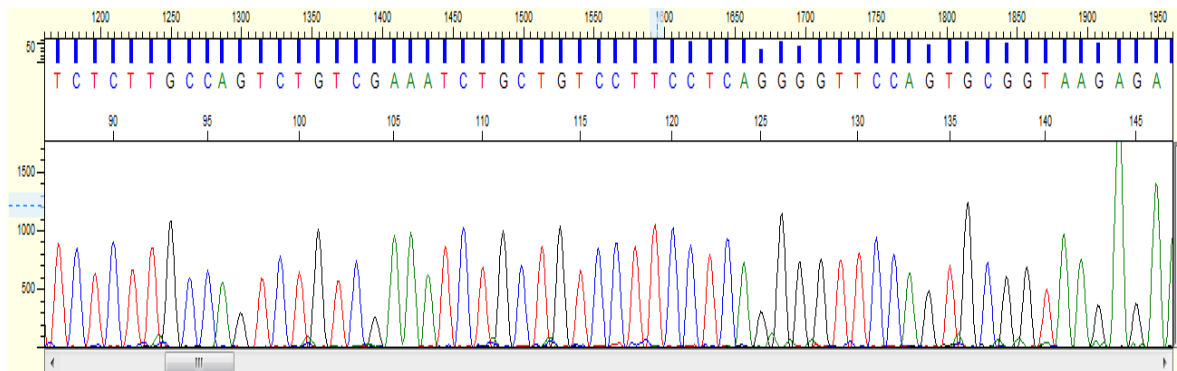


Patient No.6:

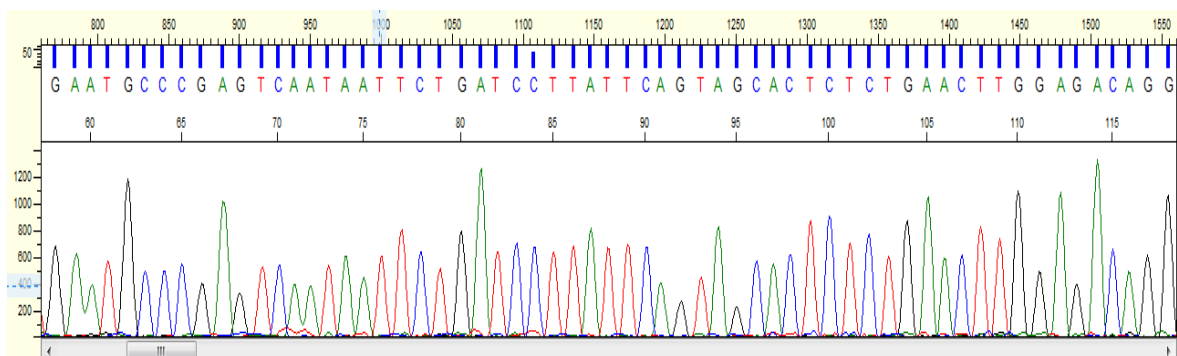
Chromatogram of Exon 2:



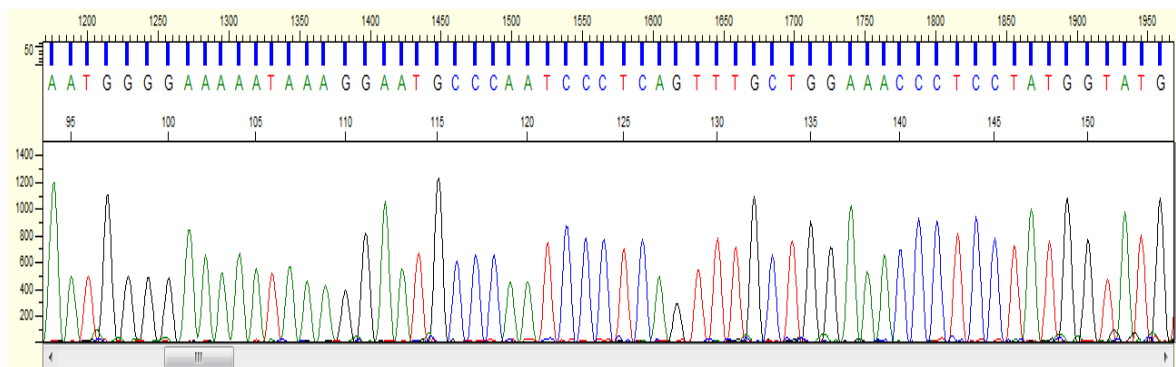
Chromatogram of Exon 3:



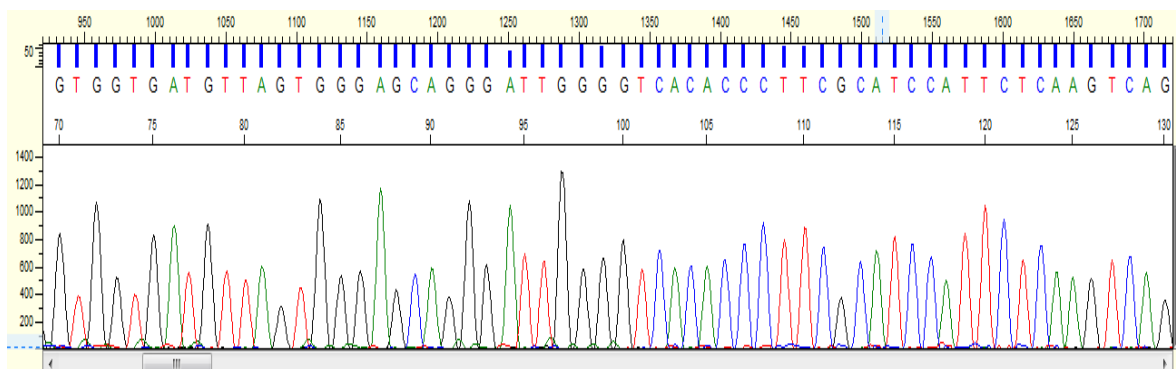
Chromatogram of Exon 5:



Chromatogram of Exon 7:

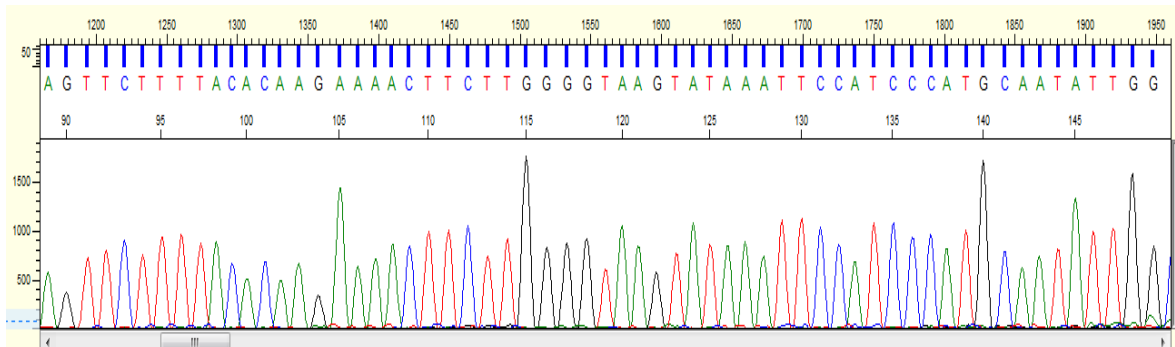


Chromatogram of Exon 10:

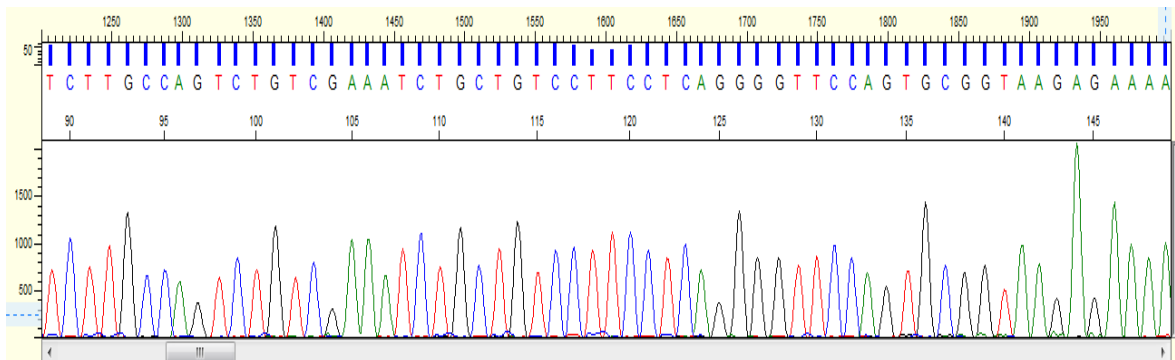


Patient No. 7:

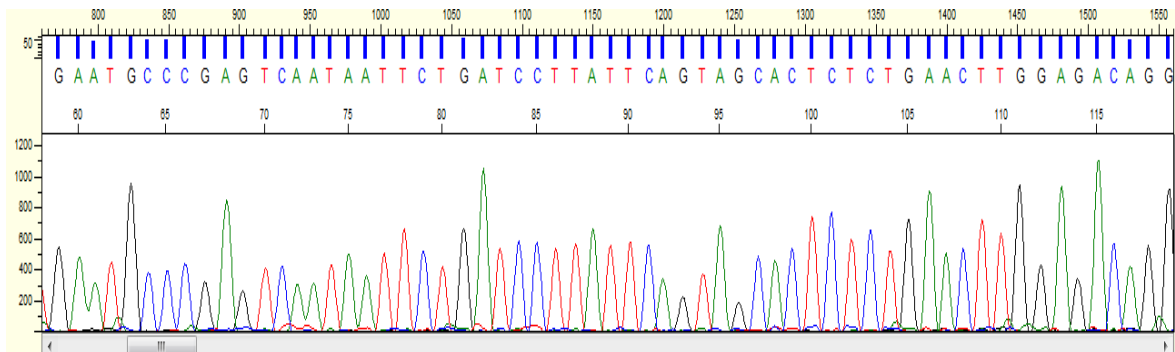
Chromatogram of Exon 2:



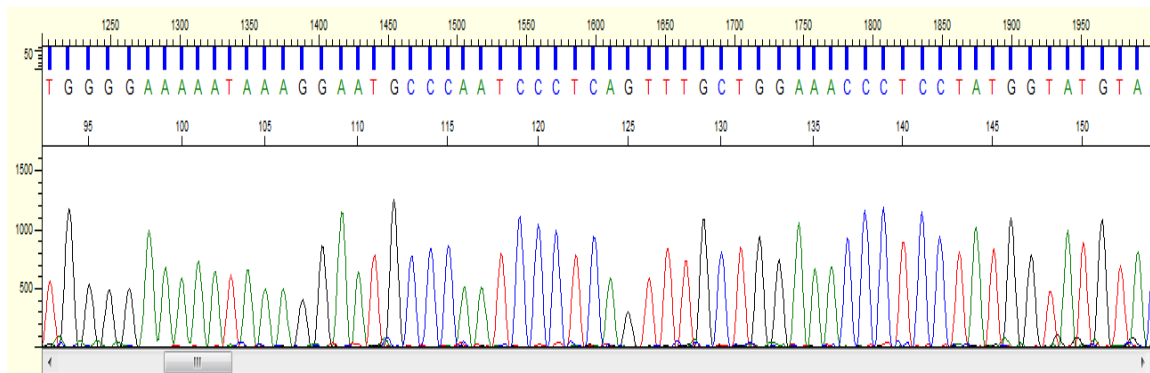
Chromatogram of Exon 3:



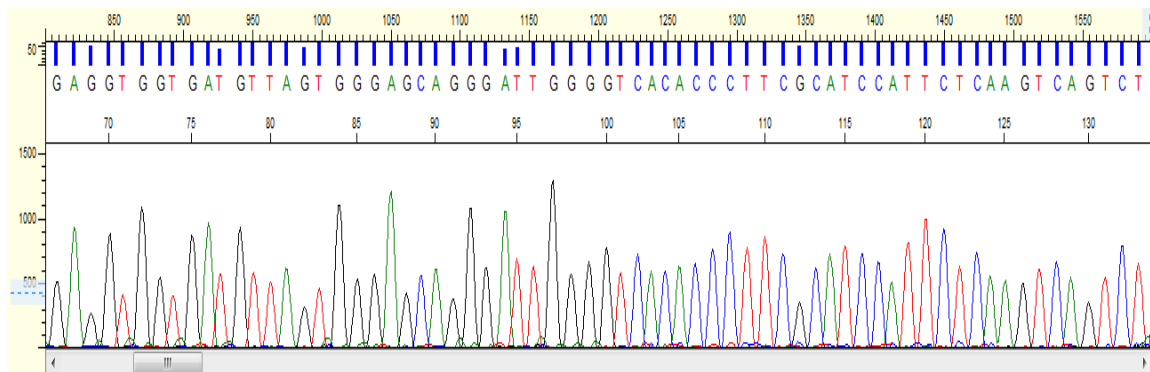
Chromatogram of Exon 5:



Chromatogram of Exon 7:

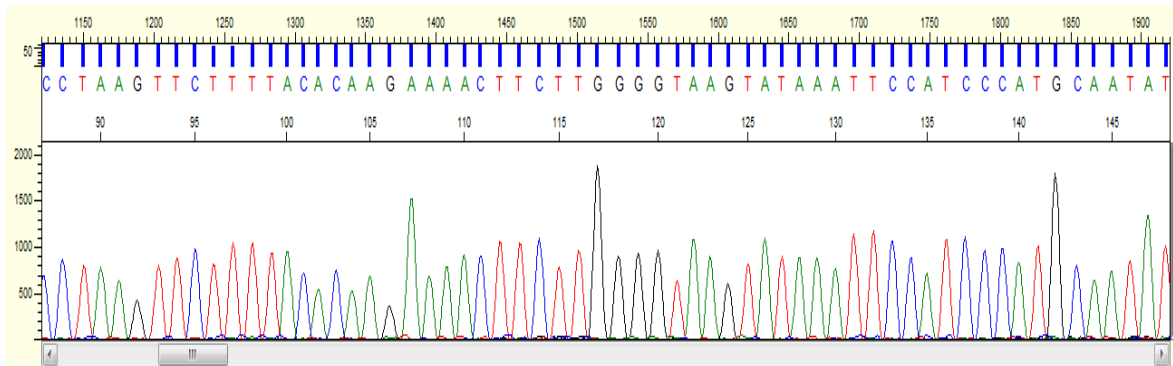


Chromatogram of Exon 10:

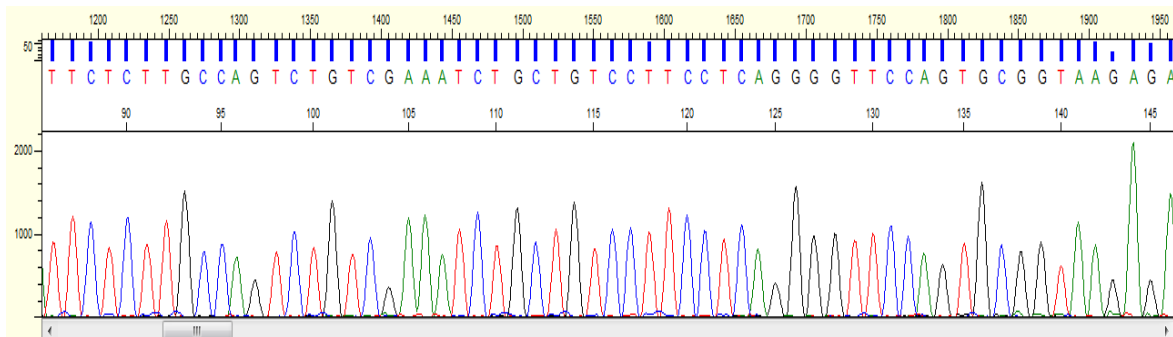


Patient No. 9:

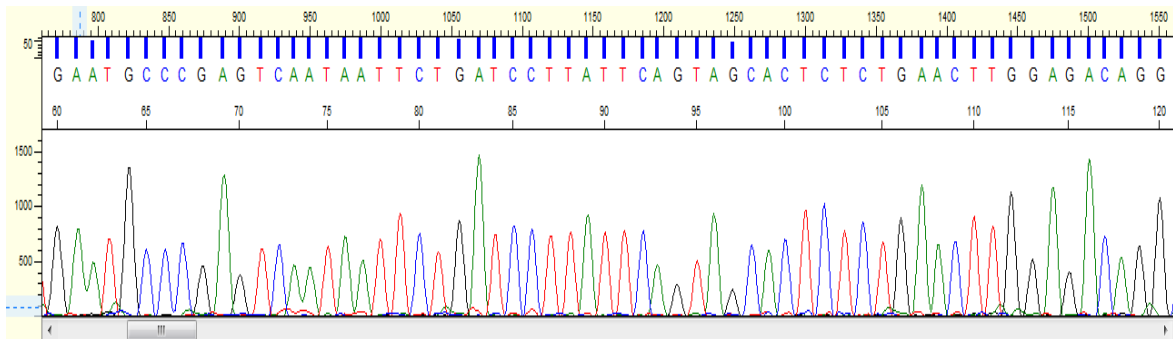
Chromatogram of Exon 2:



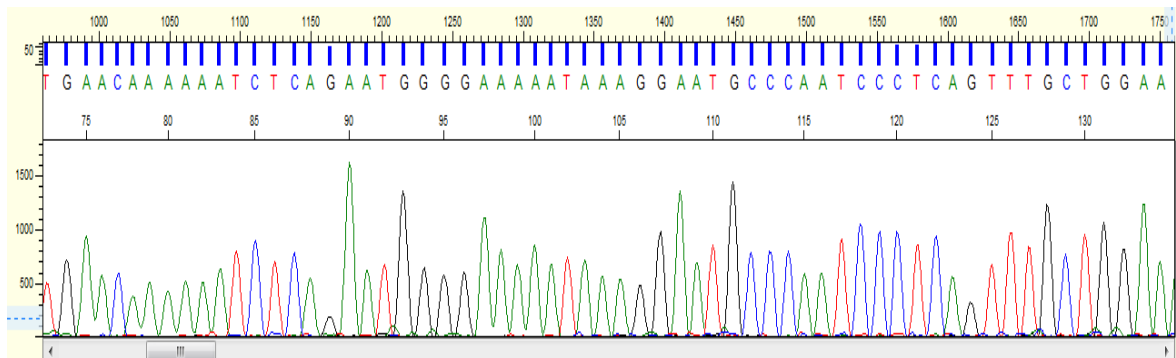
Chromatogram of Exon 3:



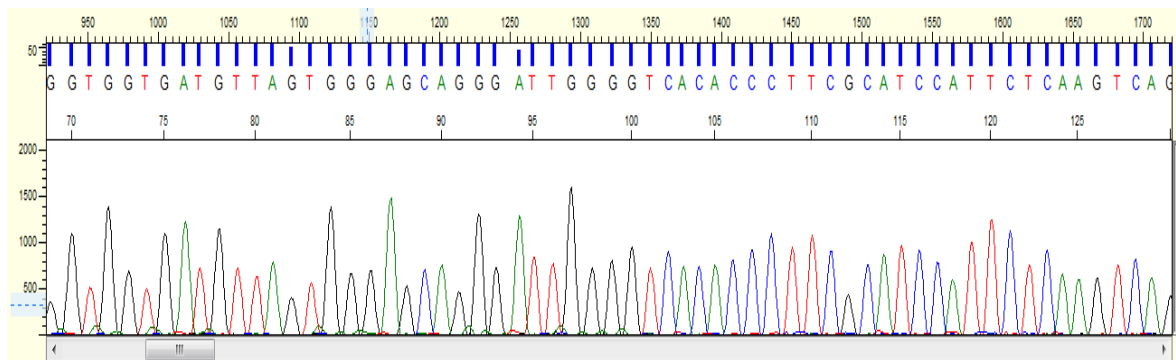
Chromatogram of Exon 5:



Chromatogram of Exon 7:

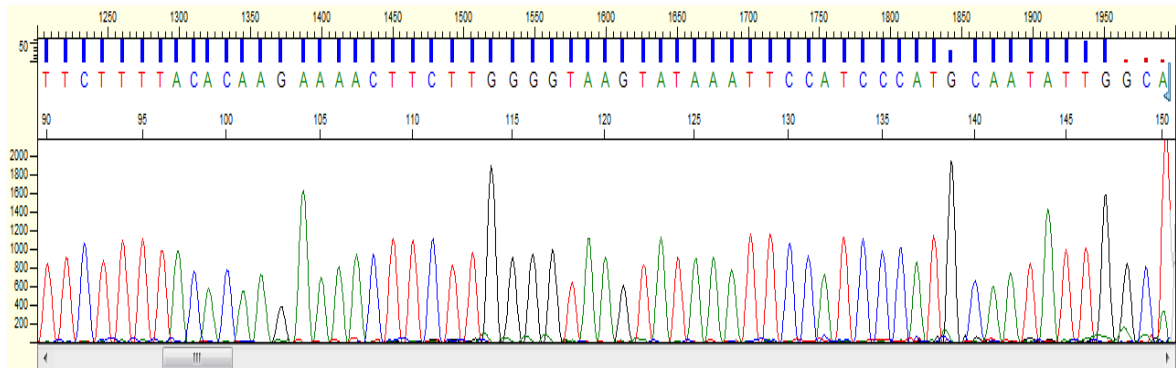


Chromatogram of Exon 10:

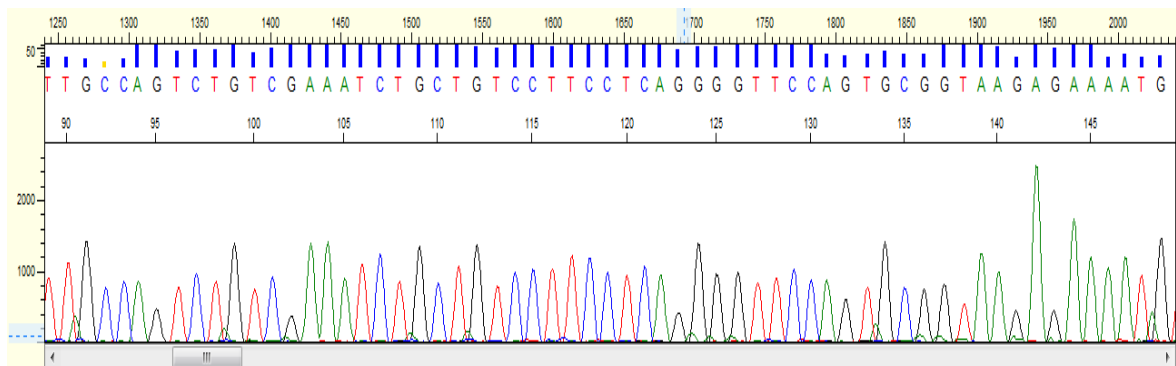


Patient No. 12:

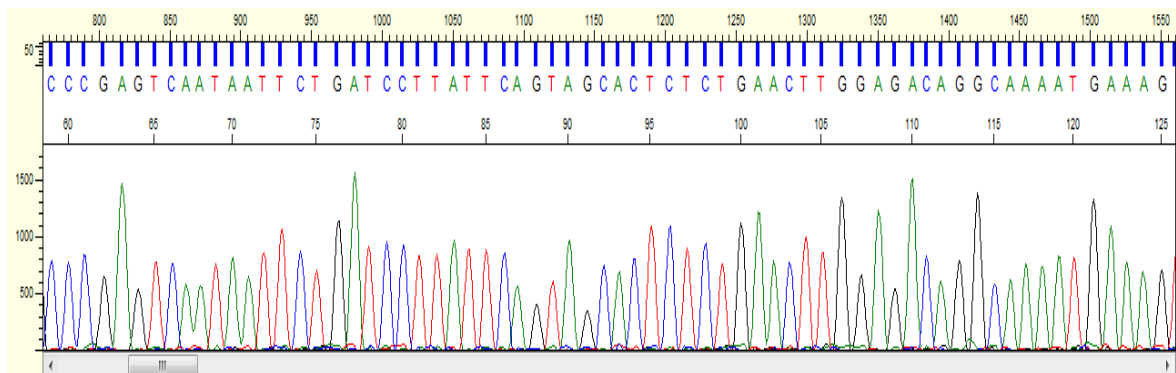
Chromatogram of Exon 2:



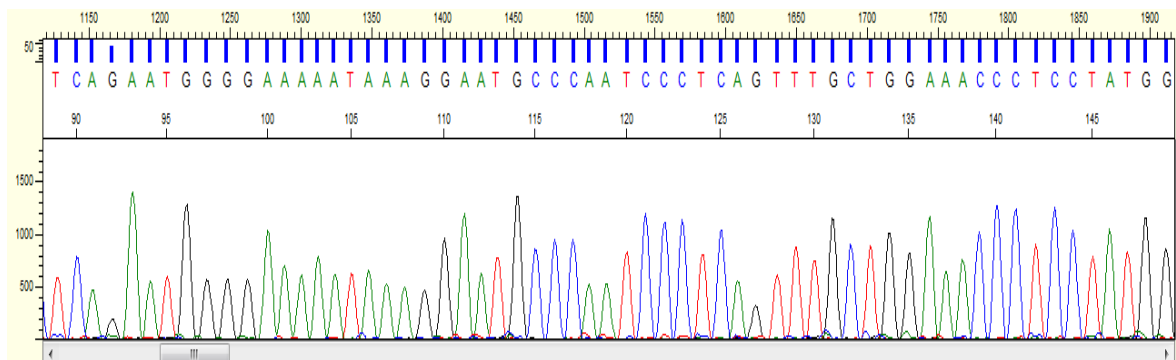
Chromatogram of Exon 3:



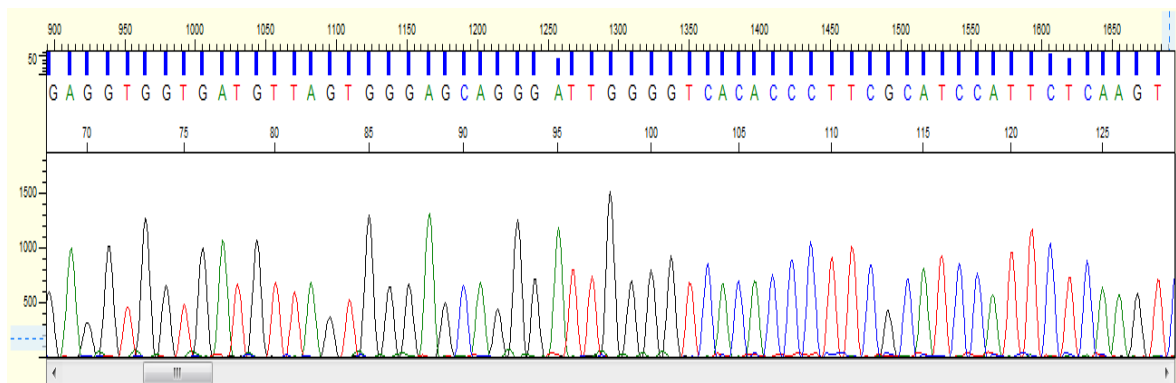
Chromatogram of Exon 5:



Chromatogram of Exon 7:

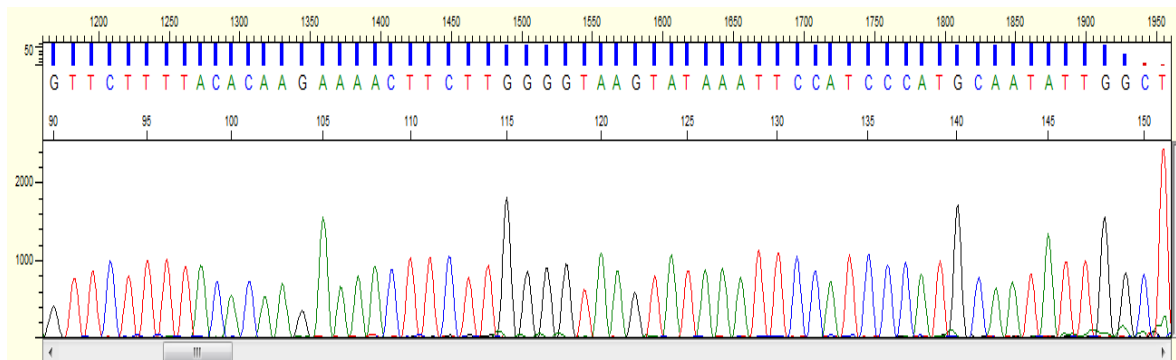


Chromatogram of Exon 10:

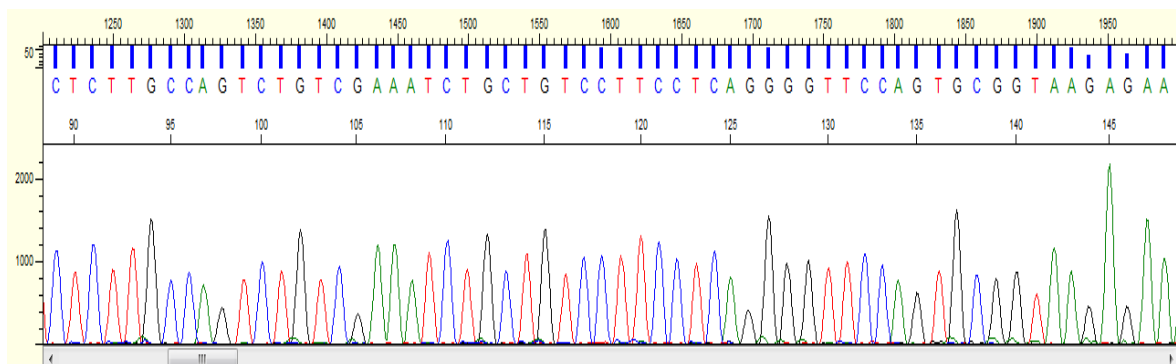


Patient No. 13:

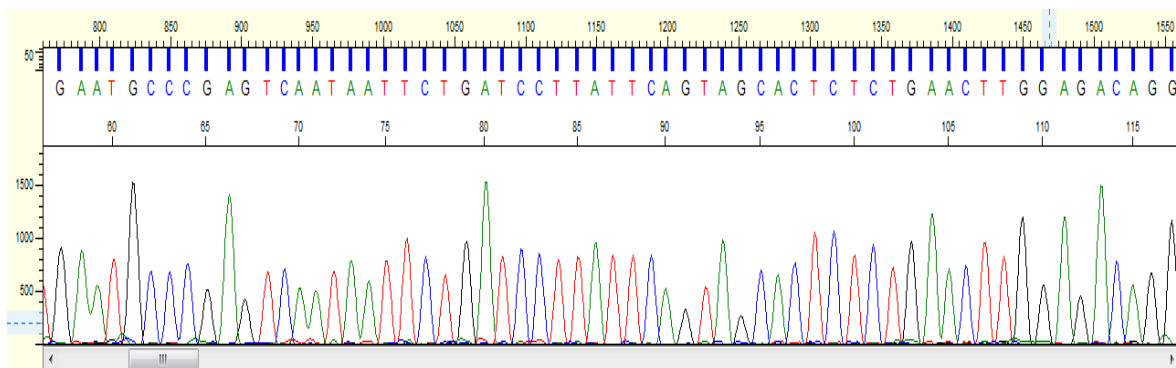
Chromatogram of Exon 2:



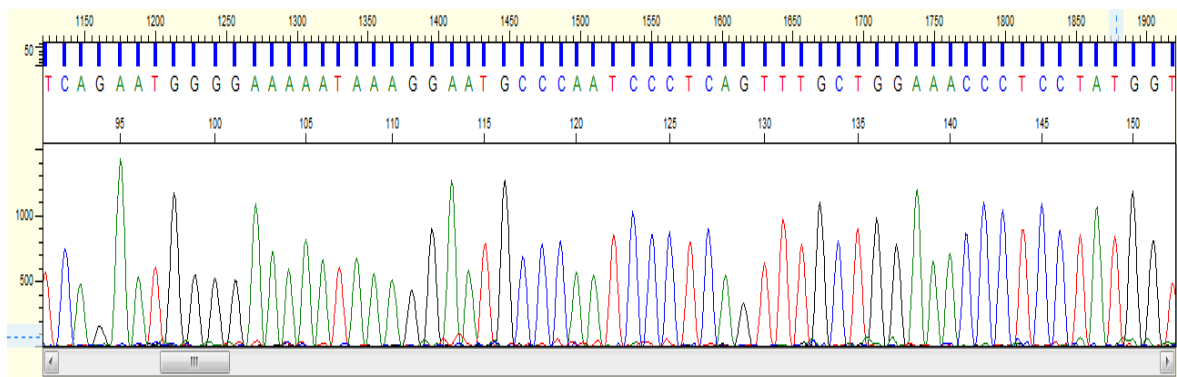
Chromatogram of Exon 3:



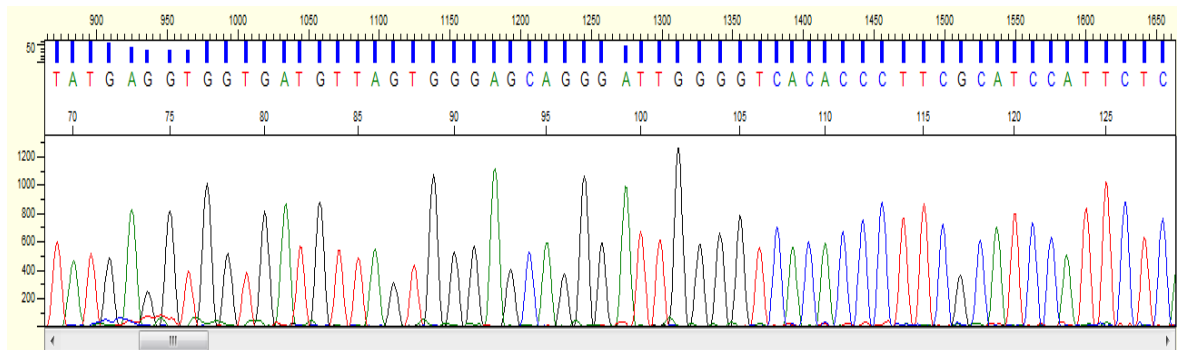
Chromatogram of Exon 5:



Chromatogram of Exon 7:

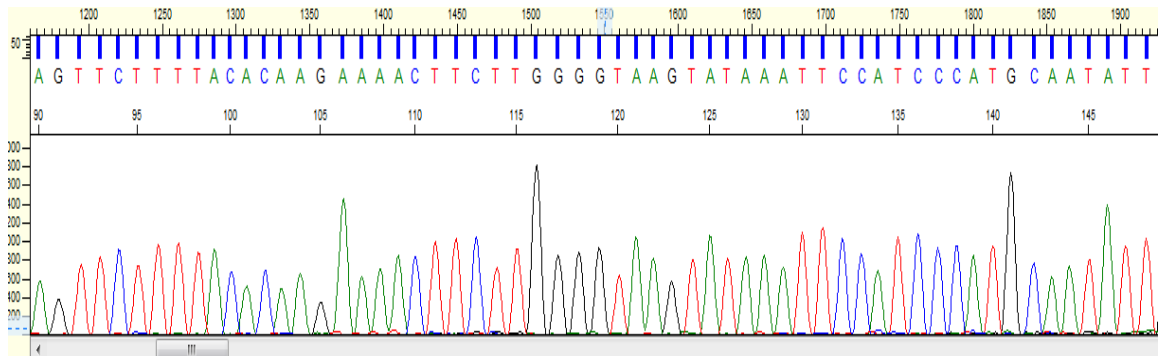


Chromatogram of Exon 10:

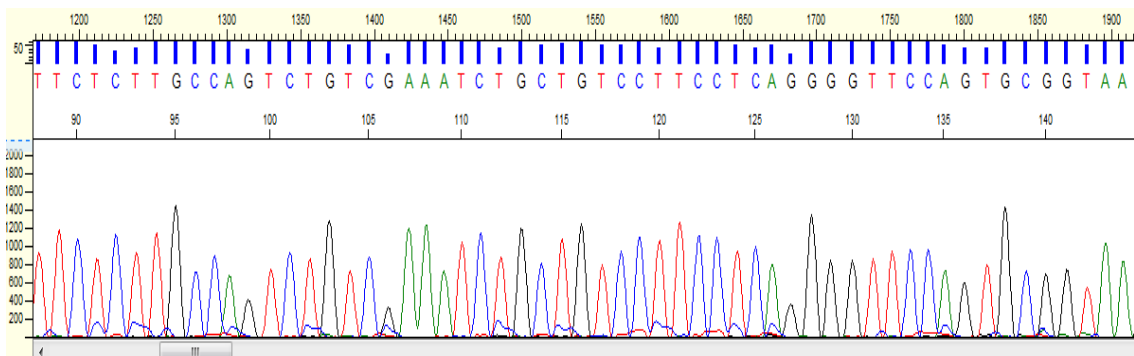


Control No. 2:

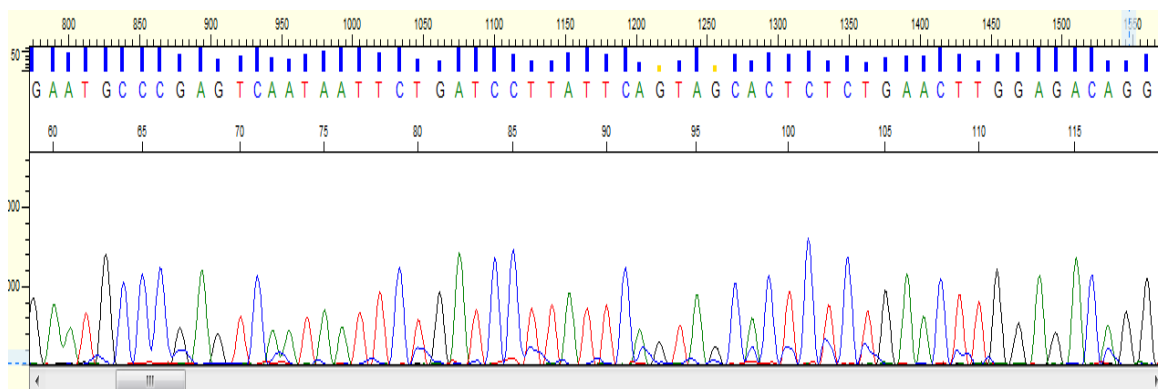
Chromatogram of Exon 2:



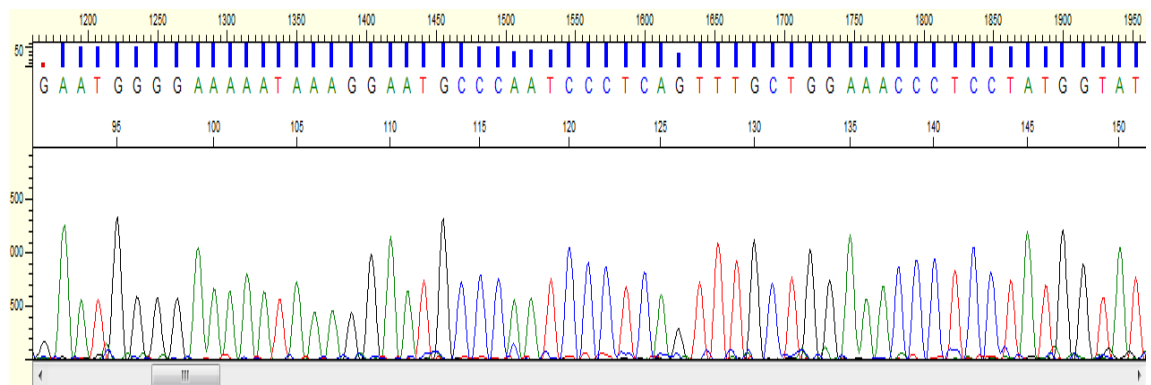
Chromatogram of Exon 3:



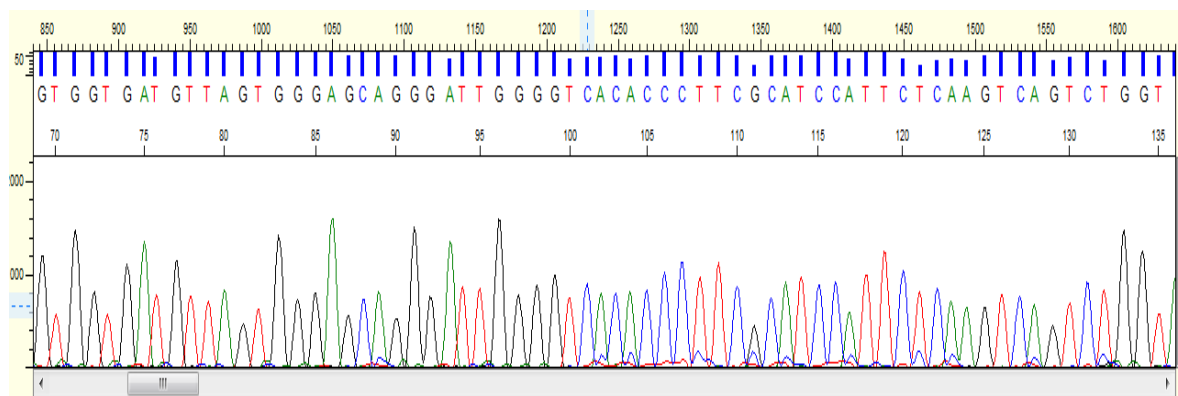
Chromatogram of Exon 5:



Chromatogram of Exon 7:



Chromatogram of Exon 10:



Sequencing and alignment of patients and controls samples by sequencer program:

Sequencing of Exon 2

Blast alignment of patient's DNA sequence (CYBB Gene) with Gene Bank sequence:

Patient 1:

Alignment of exon 2:

Homo sapiens cytochrome b-245 beta polypeptide (CYBB) gene, exon 2
Sequence ID: [gb|AF469758.1|F469757S02](#) Length: 230 Number of Matches: 1

Range 1: 83 to 226 [GenBank](#) [Graphics](#) ▼ Next Match ▲ Previous Match

Score	Expect	Identities	Gaps	Strand
267 bits(144)	5e-68	144/144(100%)	0/144(0%)	Plus/Plus
Query 9	TTCGTGTTGTCAGCTGGTTGGCTGGGGTTGAACGCTTCCTCTTGTCTGGTATTACC	68		
Sbjct 83	TTCGTGTTGTCAGCTGGTTGGCTGGGGTTGAACGCTTCCTCTTGTCTGGTATTACC	142		
Query 69	GGGTTTATGATATCCACCTAAGTCTTTTACACAAGAAAACCTCTTGGGGTAAAGTATAA	128		
Sbjct 143	GGGTTTATGATATCCACCTAAGTCTTTTACACAAGAAAACCTCTTGGGGTAAAGTATAA	202		
Query 129	ATTCCATCCCATGCAATATTGGCT	152		
Sbjct 203	ATTCCATCCCATGCAATATTGGCT	226		

Alignment of exon 3:

Homo sapiens cytochrome b-245 beta polypeptide (CYBB) gene, exon 3
Sequence ID: [gb|AF469759.1|F469757S03](#) Length: 256 Number of Matches: 1

Range 1: 80 to 250 [GenBank](#) [Graphics](#) ▼ Next Match ▲ Previous Match

Score	Expect	Identities	Gaps	Strand
309 bits(167)	1e-80	170/171(99%)	1/171(0%)	Plus/Plus
Query 11	CTTT-CCGCCTCTTCTAGTCAGCACTGGCACTGGCCAGGGCCCTGCAGCCTGCCTGAAT	69		
Sbjct 80	CTTTCCCGCCTCTTCTAGTCAGCACTGGCACTGGCCAGGGCCCTGCAGCCTGCCTGAAT	139		
Query 70	TTCAACTGCATGCTGATTCTCTTCCAGTCTGTCGAAATCTGCTGTCCTTCTCAGGGGT	129		
Sbjct 140	TTCAACTGCATGCTGATTCTCTTCCAGTCTGTCGAAATCTGCTGTCCTTCTCAGGGGT	199		
Query 130	TCCAGTGC GGTAAGAGAAAATGTTTACTAAGTTCCCTCTAATTTCAAAGG	180		
Sbjct 200	TCCAGTGC GGTAAGAGAAAATGTTTACTAAGTTCCCTCTAATTTCAAAGG	250		

Alignment of exon 5:

Homo sapiens cytochrome b-245 beta polypeptide (CYBB) gene, exon 5
Sequence ID: [gb|AF469761.1|F469757S05](#) Length: 311 Number of Matches: 1

Range 1: 71 to 277 [GenBank](#) [Graphics](#) ▼ Next Match ▲ Previous Match

Score	Expect	Identities	Gaps	Strand
375 bits(203)	1e-100	206/207(99%)	1/207(0%)	Plus/Plus
Query 10	TTTT-AGCGATTACACCAATTGCACATCTATTTAATGTGGAATGGTGTGTGAATGCCCGA	68		
Sbjct 71	TTTTAGCGATTACACCAATTGCACATCTATTTAATGTGGAATGGTGTGTGAATGCCCGA	130		
Query 69	GTCAATAATTCTGATCCTTATTAGTAGCACTCTCTGAACTTGAGACAGGCCAAAATGAA	128		
Sbjct 131	GTCAATAATTCTGATCCTTATTAGTAGCACTCTCTGAACTTGAGACAGGCCAAAATGAA	190		
Query 129	AGTTATCTCAATTTTGCTCGAAAAGAGAATAAAGGTAAGCCTCTCATTATCTGACTTAGAT	188		
Sbjct 191	AGTTATCTCAATTTTGCTCGAAAAGAGAATAAAGGTAAGCCTCTCATTATCTGACTTAGAT	250		
Query 189	ATTCTTAGGCCATTACAATTGAGGAC	215		
Sbjct 251	ATTCTTAGGCCATTACAATTGAGGAC	277		

Alignment of exon 7:

Homo sapiens cytochrome b-245 beta polypeptide (CYBB) gene, exon 7

Sequence ID: [gb|AF469763.1|F469757S07](#) Length: 244 Number of Matches: 1

Range 1: 28 to 214 [GenBank](#) [Graphics](#) ▼ Next Match ▲ Previous Match

Score	Expect	Identities	Gaps	Strand
333 bits(180)	7e-88	185/187(99%)	2/187(1%)	Plus/Plus
Query 1	ATTTTT-ACCCAGACG-ATTGTACGTGGGCAGACCCGAGAGAGTTTGGCTGTGCATAATA			58
Sbjct 28	ATTTTTACCCAGACGAATTGTACGTGGGCAGACCCGAGAGAGTTTGGCTGTGCATAATA			87
Query 59	TAACAGTTTGTGAACAAAAATCTCAGAATGGGGAAAAATAAAGGAATGCCCAATCCCTC			118
Sbjct 88	TAACAGTTTGTGAACAAAAATCTCAGAATGGGGAAAAATAAAGGAATGCCCAATCCCTC			147
Query 119	AGTTTGCTGGAAACCCTCCTATGGTATGTACAATTCATTGTTGTTATTACAGTTTCATTA			178
Sbjct 148	AGTTTGCTGGAAACCCTCCTATGGTATGTACAATTCATTGTTGTTATTACAGTTTCATTA			207
Query 179	CTGACAA 185			
Sbjct 208	CTGACAA 214			

Alignment of exon 10:

Homo sapiens cytochrome b-245 beta polypeptide (CYBB) gene, exon 10

Sequence ID: [gb|AF469766.1|F469757S10](#) Length: 258 Number of Matches: 1

Range 1: 49 to 249 [GenBank](#) [Graphics](#) ▼ Next Match ▲ Previous Match

Score	Expect	Identities	Gaps	Strand
361 bits(195)	4e-96	200/202(99%)	2/202(0%)	Plus/Plus
Query 9	TTC-GGATAGCGGTTGATGGGCCCTTTGGCACTGCCAGTGAAGATGTTTTCAGCTATGAG			67
Sbjct 49	TTCAGGATAGCGGTTGATGGGCCCTTTGGCACTGCCAGTGAAGATGTTTTCAGCTATGAG			108
Query 68	GTGGTGATGTTAGTGGGAGCAGGGATTGGGGTCACACCCTTCGCATCCATTCTCAAGTCA			127
Sbjct 109	GTGGTGATGTTAGTGGGAGCAGGGATTGGGGTCACACCCTTCGCATCCATTCTCAAGTCA			168
Query 128	GTCGGTACAAATATTGCAATAACGCCACCAATCTGAAGCTCAAAAAGGTAAGTCCTTTC			187
Sbjct 169	GTCGGTACAAATATTGCAATAACGCCACCAATCTGAAGCTCAAAAAGGTAAGTCCTTTC			228
Query 188	ATTTATCGGAGGGGCTTAGAG 209			
Sbjct 229	ATTTATCGGAGGG-CCTTAGAG 249			

Patient 2:

Alignment of exon 2

Homo sapiens cytochrome b-245 beta polypeptide (CYBB) gene, exon 2

Sequence ID: [gb|AF469758.1|F469757S02](#) Length: 230 Number of Matches: 1

Range 1: 84 to 226		GenBank	Graphics	Next Match	Previous Match
Score	Expect	Identities	Gaps	Strand	
265 bits(143)	2e-67	143/143(100%)	0/143(0%)	Plus/Plus	
Query	9	TCTGTTTGTGCAGCTGGTTTGGCTGGGGTTGAACGTCTTCCTCTTTGCTGGTATTACCG		68	
Sbjct	84	TCTGTTTGTGCAGCTGGTTTGGCTGGGGTTGAACGTCTTCCTCTTTGCTGGTATTACCG		143	
Query	69	GGTTTATGATATTCCACCTAAGTTCTTTTACACAAGAAAACCTCTTGGGGTAAGTATAAA		128	
Sbjct	144	GGTTTATGATATTCCACCTAAGTTCTTTTACACAAGAAAACCTCTTGGGGTAAGTATAAA		203	
Query	129	TTCCATCCCATGCAATATTGGCT	151		
Sbjct	204	TTCCATCCCATGCAATATTGGCT	226		

Alignment of exon 3

Homo sapiens cytochrome b-245 beta polypeptide (CYBB) gene, exon 3

Sequence ID: [gb|AF469759.1|F469757S03](#) Length: 256 Number of Matches: 1

Range 1: 75 to 250		GenBank	Graphics	Next Match	Previous Match
Score	Expect	Identities	Gaps	Strand	
313 bits(169)	7e-82	174/176(99%)	2/176(1%)	Plus/Plus	
Query	7	GCT-CCTTT-CCGCCTCTTCTAGTCAGCACTGGCACTGGCCAGGGCCCTGCAGCCTGCC		64	
Sbjct	75	GCTCCCTTCCCGCCTCTTCTAGTCAGCACTGGCACTGGCCAGGGCCCTGCAGCCTGCC		134	
Query	65	TGAATTTCAACTGCATGCTGATTCTCTTGCCAGTCTGTCGAAATCTGCTGTCCTTCCTCA		124	
Sbjct	135	TGAATTTCAACTGCATGCTGATTCTCTTGCCAGTCTGTCGAAATCTGCTGTCCTTCCTCA		194	
Query	125	GGGGTCCAGTGC GGTAAGAGAAAATGTTTTACTAAGTTCCTCTAATTTTCAAAGG	180		
Sbjct	195	GGGGTCCAGTGC GGTAAGAGAAAATGTTTTACTAAGTTCCTCTAATTTTCAAAGG	250		

Alignment of exon 5

Homo sapiens cytochrome b-245 beta polypeptide (CYBB) gene, exon 5

Sequence ID: [gb|AF469761.1|F469757S05](#) Length: 311 Number of Matches: 1

Range 1: 70 to 277		GenBank	Graphics	Next Match	Previous Match
Score	Expect	Identities	Gaps	Strand	
355 bits(192)	1e-94	204/209(98%)	3/209(1%)	Plus/Plus	
Query	7	CTTTTC-GCGATT-CACCATTGCACATCTATTTAATAGTGGAAAGGTGTGTGAAAGCCC		64	
Sbjct	70	CTTTTCAGCGATTACACCATTGCACATCTATTTAAT-GTGGAAATGGTGTGTGAATGCC		128	
Query	65	GAGTCAATAAATTCGATCCTTATTTCAGTAGCACTCTCTGAACTGGAGACAGGCAAAATG		124	
Sbjct	129	GAGTCAATAAATTCGATCCTTATTTCAGTAGCACTCTCTGAACTGGAGACAGGCAAAATG		188	
Query	125	AAAGTTATCTCAATTTTGTCTCGAAAGAGAATAAAGGTAAGCCCTCTCATTATCTGACTTAG		184	
Sbjct	189	AAAGTTATCTCAATTTTGTCTCGAAAGAGAATAAAGGTAAGCCCTCTCATTATCTGACTTAG		248	
Query	185	ATATTCTTAGGCCATTACAATTGAGGAC	213		
Sbjct	249	ATATTCTTAGGCCATTACAATTGAGGAC	277		

Alignment of exon 7

Homo sapiens cytochrome b-245 beta polypeptide (CYBB) gene, exon 7

Sequence ID: [gb|AF469763.1|F469757S07](#) Length: 244 Number of Matches: 1

Range 1: 29 to 214		GenBank	Graphics	Next Match	Previous Match
Score	Expect	Identities	Gaps	Strand	
331 bits(179)	2e-87	184/186(99%)	1/186(0%)	Plus/Plus	
Query 3	ttttttACCCAGACG-ATTGTACGTGGGCAGACCGCAGAGAGTTGGCTGTGCATAATAT			61	
Sbjct 29	TTTTTCACCCAGACGAATTGTACGTGGGCAGACCGCAGAGAGTTGGCTGTGCATAATAT			88	
Query 62	AACAGTTTGTGAACAAAAATCTCAGAATGGGGAAAAATAAAGGAATGCCCAATCCCTCA			121	
Sbjct 89	AACAGTTTGTGAACAAAAATCTCAGAATGGGGAAAAATAAAGGAATGCCCAATCCCTCA			148	
Query 122	GTTTGTGGAAACCCCTCCTATGGTATGTACAATTCATTGTTGTTATTACAGTTTCATTAC			181	
Sbjct 149	GTTTGTGGAAACCCCTCCTATGGTATGTACAATTCATTGTTGTTATTACAGTTTCATTAC			208	
Query 182	TGACAA 187				
Sbjct 209	TGACAA 214				

Alignment of exon 10:

Homo sapiens cytochrome b-245 beta polypeptide (CYBB) gene, exon 10

Sequence ID: [gb|AF469766.1|F469757S10](#) Length: 258 Number of Matches: 1

Range 1: 49 to 249		GenBank	Graphics	Next Match	Previous Match
Score	Expect	Identities	Gaps	Strand	
361 bits(195)	3e-96	200/202(99%)	2/202(0%)	Plus/Plus	
Query 9	TTC-GGATAGCGGTTGATGGGCCCTTTGGCACTGCCAGTGAAGATGTGTTTCAGCTATGAG			67	
Sbjct 49	TTCAGGATAGCGGTTGATGGGCCCTTTGGCACTGCCAGTGAAGATGTGTTTCAGCTATGAG			108	
Query 68	GTGGTGAIGTTAGTGGGAGCAGGGATTGGGGTCACACCCTTCGCATCCATTCTCAAGTCA			127	
Sbjct 109	GTGGTGAIGTTAGTGGGAGCAGGGATTGGGGTCACACCCTTCGCATCCATTCTCAAGTCA			168	
Query 128	GTCTGGTACAAATATTGCAATAACGCCACCAATCTGAAGCTCAAAAAGGTAAGTCCTTTC			187	
Sbjct 169	GTCTGGTACAAATATTGCAATAACGCCACCAATCTGAAGCTCAAAAAGGTAAGTCCTTTC			228	
Query 188	ATTTATCGGAGGGCCTTAGAG 209				
Sbjct 229	ATTTATCGGAGGG-CCTTAGAG 249				

Patient 3:

Alignment of exon 2:

Homo sapiens cytochrome b-245 beta polypeptide (CYBB) gene, exon 2

Sequence ID: [gb|AF469758.1|F469757S02](#) Length: 230 Number of Matches: 1

Range 1: 80 to 225		GenBank	Graphics	Next Match	Previous Match
Score	Expect	Identities	Gaps	Strand	
259 bits(140)	8e-66	145/147(99%)	1/147(0%)	Plus/Plus	
Query	3	TATATTCIGTTTTGTGCAGCTGGTTTGGCAGGGGTTGAACGTCCTCTTTGCTGGTAT		62	
Sbjct	80	TAT-TTCIGTTTTGTGCAGCTGGTTTGGCTGGGGTTGAACGTCCTCTTTGCTGGTAT		138	
Query	63	TACCGGGTTTATGATATCCACCTAAGTCTTTTACACAAGAAAACCTCTTGGGGTAAGT		122	
Sbjct	139	TACCGGGTTTATGATATCCACCTAAGTCTTTTACACAAGAAAACCTCTTGGGGTAAGT		198	
Query	123	ATAAATCCATCCCATGCAATATTGGC	149		
Sbjct	199	ATAAATCCATCCCATGCAATATTGGC	225		

Alignment of exon 3:

Homo sapiens cytochrome b-245 beta polypeptide (CYBB) gene, exon 3

Sequence ID: [gb|AF469759.1|F469757S03](#) Length: 256 Number of Matches: 1

Range 1: 80 to 250		GenBank	Graphics	Next Match	Previous Match
Score	Expect	Identities	Gaps	Strand	
309 bits(167)	9e-81	170/171(99%)	1/171(0%)	Plus/Plus	
Query	10	CTTT-CCGCCTCTTCTAGTCAGCACTGGCACTGGCCAGGGCCCTGCAGCCTGCCTGAAT		68	
Sbjct	80	CTTTCCCGCCTCTTCTAGTCAGCACTGGCACTGGCCAGGGCCCTGCAGCCTGCCTGAAT		139	
Query	69	TTCAACTGCATGCTGATCTCTTGCCAGTCTGTGCAAATCTGCTGCTTCCCTCAGGGGT		128	
Sbjct	140	TTCAACTGCATGCTGATCTCTTGCCAGTCTGTGCAAATCTGCTGCTTCCCTCAGGGGT		199	
Query	129	TCCAGTGCGGTAAGAGAAAATGTTTTACTAAGTTCCTCTAATTTCAAAGG	179		
Sbjct	200	TCCAGTGCGGTAAGAGAAAATGTTTTACTAAGTTCCTCTAATTTCAAAGG	250		

Alignment of exon 5:

Homo sapiens cytochrome b-245 beta polypeptide (CYBB) gene, exon 5

Sequence ID: [gb|AF469761.1|F469757S05](#) Length: 311 Number of Matches: 2

Range 1: 70 to 277		GenBank	Graphics	Next Match	Previous Match
Score	Expect	Identities	Gaps	Strand	
377 bits(204)	7e-101	207/208(99%)	1/208(0%)	Plus/Plus	
Query	5	CTTTT-AGCGATTACACCAATTGCACATCTATTTAATGTGGAATGGTGTGTAATGCCCG		63	
Sbjct	70	CTTTTCAGCGATTACACCAATTGCACATCTATTTAATGTGGAATGGTGTGTAATGCCCG		129	
Query	64	AGTCAATAATTCTGATCCTTATTTCAGTAGCACCTCTGAACTTGGAGACAGGCAAAATGA		123	
Sbjct	130	AGTCAATAATTCTGATCCTTATTTCAGTAGCACCTCTGAACTTGGAGACAGGCAAAATGA		189	
Query	124	AAGTTATCTCAATTTGCTCGAAAGAGAATAAAGGTAAGCCTCTCATTATCTGACTTAGA		183	
Sbjct	190	AAGTTATCTCAATTTGCTCGAAAGAGAATAAAGGTAAGCCTCTCATTATCTGACTTAGA		249	
Query	184	TATTCTTAGGCCATTACAATTGAGGAC	211		
Sbjct	250	TATTCTTAGGCCATTACAATTGAGGAC	277		

Alignment of exon 7:

Homo sapiens cytochrome b-245 beta polypeptide (CYBB) gene, exon 7

Sequence ID: [gb|AF469763.1|F469757S07](#) Length: 244 Number of Matches: 1

Range 1: 28 to 214		GenBank	Graphics	Next Match	Previous Match
Score	Expect	Identities	Gaps	Strand	
326 bits(176)	9e-86	184/187(98%)	3/187(1%)	Plus/Plus	
Query	1	ATTTTT-A-CCAGACG-ATTGTACGTGGGCAGACCGCAGAGAGTTTGGCTGTGCATAATA		57	
Sbjct	28	ATTTTTCACCCAGACGAATTGTACGTGGGCAGACCGCAGAGAGTTTGGCTGTGCATAATA		87	
Query	58	TAACAGTTTGTGAACAAAAAATCTCAGAATGGGGAAAAATAAAGGAATGCCCAATCCCTC		117	
Sbjct	88	TAACAGTTTGTGAACAAAAAATCTCAGAATGGGGAAAAATAAAGGAATGCCCAATCCCTC		147	
Query	118	AGTTTGTGGAACCCCTCCTAIGGTAIGTACAATTCATTGTTGTTATTACAGTTTCATTA		177	
Sbjct	148	AGTTTGTGGAACCCCTCCTAIGGTAIGTACAATTCATTGTTGTTATTACAGTTTCATTA		207	
Query	178	CTGACAA 184			
Sbjct	208	CTGACAA 214			

Alignment of exon 10:

Homo sapiens cytochrome b-245 beta polypeptide (CYBB) gene, exon 10

Sequence ID: [gb|AF469766.1|F469757S10](#) Length: 258 Number of Matches: 1

Range 1: 52 to 249		GenBank	Graphics	Next Match	Previous Match
Score	Expect	Identities	Gaps	Strand	
361 bits(195)	3e-96	198/199(99%)	1/199(0%)	Plus/Plus	
Query	11	AGGATAGCGGTTGATGGGCCCTTTGGCACTGCCAGTGAAGATGTGTTTCAGCTATGAGGTG		70	
Sbjct	52	AGGATAGCGGTTGATGGGCCCTTTGGCACTGCCAGTGAAGATGTGTTTCAGCTATGAGGTG		111	
Query	71	GTGATGTTAGTGGGAGCAGGGATTGGGGTCACACCCTTCGCATCCATTCTCAAGTCAGTC		130	
Sbjct	112	GTGATGTTAGTGGGAGCAGGGATTGGGGTCACACCCTTCGCATCCATTCTCAAGTCAGTC		171	
Query	131	TGGTACAAATATTGCAATAACGCCACCAATCTGAAGCTCAAAAAGGTAAGTCCTTTTCATT		190	
Sbjct	172	TGGTACAAATATTGCAATAACGCCACCAATCTGAAGCTCAAAAAGGTAAGTCCTTTTCATT		231	
Query	191	TATCGGAGGGGCCTTAGAG 209			
Sbjct	232	TATCGGAGGG-CCTTAGAG 249			

Patient 6:

Alignment of exon 2:

Homo sapiens cytochrome b-245 beta polypeptide (CYBB) gene, exon 2

Sequence ID: [gb|AF469758.1|F469757S02](#) Length: 230 Number of Matches: 1

Range 1: 83 to 226		GenBank	Graphics	Next Match	Previous Match
Score	Expect	Identities	Gaps	Strand	
267 bits(144)	5e-68	144/144(100%)	0/144(0%)	Plus/Plus	
Query	8	TTCTGTTTGTGCAGCTGGTTTGGCTGGGGTTGAACGCTCTTCTCTTTGCTCTGGTATTACC			67
Sbjct	83	TTCTGTTTGTGCAGCTGGTTTGGCTGGGGTTGAACGCTCTTCTCTTTGCTCTGGTATTACC			142
Query	68	GGGTTTATGATATTCCACCTAAGTTCTTTTACACAAGAAAACCTTCTGGGGTAAGTATAA			127
Sbjct	143	GGGTTTATGATATTCCACCTAAGTTCTTTTACACAAGAAAACCTTCTGGGGTAAGTATAA			202
Query	128	ATTCCATCCCATGCAATATTGGCT	151		
Sbjct	203	ATTCCATCCCATGCAATATTGGCT	226		

Alignment of exon 3:

Homo sapiens cytochrome b-245 beta polypeptide (CYBB) gene, exon 3

Sequence ID: [gb|AF469759.1|F469757S03](#) Length: 256 Number of Matches: 1

Range 1: 75 to 251		GenBank	Graphics	Next Match	Previous Match
Score	Expect	Identities	Gaps	Strand	
315 bits(170)	2e-82	175/177(99%)	1/177(0%)	Plus/Plus	
Query	6	GCTTCCTTT-CCGCCTCTTCTAGTCAGCACTGGCCAGGGCCCTGCAGCCTGCC			64
Sbjct	75	GCTTCCTTTCCCGCCTCTTCTAGTCAGCACTGGCCAGGGCCCTGCAGCCTGCC			134
Query	65	TGAATTTCAACTGCAIGCTGATTTCTTCCAGTCTGTGCGAAATCTGCTGTCTTCTCA			124
Sbjct	135	TGAATTTCAACTGCATGCTGATTTCTTCCAGTCTGTGCGAAATCTGCTGTCTTCTCA			194
Query	125	GGGGTCCAGTGCGGTAAGAGAAAATGTTTTACTAAGTTCCTCTAATTTTCAAAGGC	181		
Sbjct	195	GGGGTCCAGTGCGGTAAGAGAAAATGTTTTACTAAGTTCCTCTAATTTTCAAAGGC	251		

Alignment of exon 5:

Homo sapiens cytochrome b-245 beta polypeptide (CYBB) gene, exon 5

Sequence ID: [gb|AF469761.1|F469757S05](#) Length: 311 Number of Matches: 1

Range 1: 69 to 277		GenBank	Graphics	Next Match	Previous Match
Score	Expect	Identities	Gaps	Strand	
379 bits(205)	9e-102	208/209(99%)	1/209(0%)	Plus/Plus	
Query	7	CCITTT-AGCGATTACACCAATTGCACATCTAATTTAATGTGGAATGGTGTGTAATGCC			65
Sbjct	69	CCITTTACAGCGATTACACCAATTGCACATCTAATTTAATGTGGAATGGTGTGTAATGCC			128
Query	66	GAGTCAATAAATCTGATCCTTATTTCAGTAGCACTCTCTGAACTTGGAGACAGGCAAATG			125
Sbjct	129	GAGTCAATAAATCTGATCCTTATTTCAGTAGCACTCTCTGAACTTGGAGACAGGCAAATG			188
Query	126	AAAGTTAICTCAATTTTGTCTCGAAAGAGAATAAAGGTAAGCCTCTCATTATCTGACTTAG			185
Sbjct	189	AAAGTTAICTCAATTTTGTCTCGAAAGAGAATAAAGGTAAGCCTCTCATTATCTGACTTAG			248
Query	186	ATATTCTTAGGCCATTACAATTGAGGAC	214		
Sbjct	249	ATATTCTTAGGCCATTACAATTGAGGAC	277		

Alignment of exon 7:

Homo sapiens cytochrome b-245 beta polypeptide (CYBB) gene, exon 7

Sequence ID: [gb|AF469763.1|F469757S07](#) Length: 244 Number of Matches: 1

Range 1: 29 to 214		GenBank	Graphics	Next Match	Previous Match
Score	Expect	Identities	Gaps	Strand	
329 bits(178)	8e-87	186/189(98%)	3/189(1%)	Plus/Plus	
Query	5	tttttCACCCCAAGACGAAATTTGTACGTGGGCAGACCCGCAGAGAGTTTGGCTGTGCATAA			64
Sbjct	29	TTTTTCA-CCC-AGACG-AATTGTACGTGGGCAGACCCGCAGAGAGTTTGGCTGTGCATAA			85
Query	65	TATAACAGTTTGTGAACAAAAAATCTCAGAATGGGGAAAAATAAAGGAATGCCCAATCCC			124
Sbjct	86	TATAACAGTTTGTGAACAAAAAATCTCAGAATGGGGAAAAATAAAGGAATGCCCAATCCC			145
Query	125	TCAGTTTGTCTGGAACCCCTCCTATGGTATGTACAATTCATTGTTGTTATTACAGTTTCAT			184
Sbjct	146	TCAGTTTGTCTGGAACCCCTCCTATGGTATGTACAATTCATTGTTGTTATTACAGTTTCAT			205
Query	185	TACTGACAA 193			
Sbjct	206	TACTGACAA 214			

Alignment of exon 10:

Homo sapiens cytochrome b-245 beta polypeptide (CYBB) gene, exon 10

Sequence ID: [gb|AF469766.1|F469757S10](#) Length: 258 Number of Matches: 1

Range 1: 43 to 249		GenBank	Graphics	Next Match	Previous Match
Score	Expect	Identities	Gaps	Strand	
366 bits(198)	7e-98	204/207(99%)	0/207(0%)	Plus/Plus	
Query	4	TTTCCTTTTCGGATAGCGGTTGATGGGCCCTTTGGCACTGCCAGTGAAGATGTGTTTCAGC			63
Sbjct	43	TTTCCTTTCAGGATAGCGGTTGATGGGCCCTTTGGCACTGCCAGTGAAGATGTGTTTCAGC			102
Query	64	TATGAGGTGGTGAATGTTAGTGGGAGCAGGGATTGGGGTCACACCCTTCGCATCCATTCTC			123
Sbjct	103	TATGAGGTGGTGAATGTTAGTGGGAGCAGGGATTGGGGTCACACCCTTCGCATCCATTCTC			162
Query	124	AAGTCAGTCTGGTACAAATATTGCAATAACGCCACCAATCTGAAGCTCAAAAAGGTAAGT			183
Sbjct	163	AAGTCAGTCTGGTACAAATATTGCAATAACGCCACCAATCTGAAGCTCAAAAAGGTAAGT			222
Query	184	CCTTTCATTTATCGGAGGGCCTTAGAG 210			
Sbjct	223	CCTTTCATTTATCGGAGGGCCTTAGAG 249			

Patient 7:

Alignment of exon 2:

Homo sapiens cytochrome b-245 beta polypeptide (CYBB) gene, exon 2

Sequence ID: [gb|AF469758.1|F469757S02](#) Length: 230 Number of Matches: 1

Range 1: 84 to 226		GenBank	Graphics	Next Match	Previous Match
Score	Expect	Identities	Gaps	Strand	
265 bits(143)	2e-67	143/143(100%)	0/143(0%)	Plus/Plus	
Query	9	TCIGTTTGTGCAGCTGGTTTGGCTGGGGTTGAACGCTTCCTCTTTGTCTGGTATTACCG		68	
Sbjct	84	TCIGTTTGTGCAGCTGGTTTGGCTGGGGTTGAACGCTTCCTCTTTGTCTGGTATTACCG		143	
Query	69	GGTTTATGATATCCACCTAAGTTCTTTTACACAAGAAAACCTTCTTGGGGTAAGTATAAA		128	
Sbjct	144	GGTTTATGATATCCACCTAAGTTCTTTTACACAAGAAAACCTTCTTGGGGTAAGTATAAA		203	
Query	129	TTCCATCCCATGCAATATTGGCT	151		
Sbjct	204	TTCCATCCCATGCAATATTGGCT	226		

Alignment of exon 3:

Homo sapiens cytochrome b-245 beta polypeptide (CYBB) gene, exon 3

Sequence ID: [gb|AF469759.1|F469757S03](#) Length: 256 Number of Matches: 1

Range 1: 74 to 251		GenBank	Graphics	Next Match	Previous Match
Score	Expect	Identities	Gaps	Strand	
316 bits(171)	6e-83	176/178(99%)	2/178(1%)	Plus/Plus	
Query	6	TGCT-CCITT-CCGCCTCTTCTAGTCAGCACTGGCACTGGCCAGGGCCCCCTGCAGCCTGC		63	
Sbjct	74	TGCTCCCTTTCCCGCCTCTTCTAGTCAGCACTGGCACTGGCCAGGGCCCCCTGCAGCCTGC		133	
Query	64	CTGAATTTCAACTGCAIGCTGATTCTCTTGCCAGTCTGTGAAATCTGCTGTCCTTCCTC		123	
Sbjct	134	CTGAATTTCAACTGCAIGCTGATTCTCTTGCCAGTCTGTGAAATCTGCTGTCCTTCCTC		193	
Query	124	AGGGTTCCAGTGC GGTAAGAGAAAATGTTTTACTAAGTTCCCTAATTTCAAAGGC	181		
Sbjct	194	AGGGTTCCAGTGC GGTAAGAGAAAATGTTTTACTAAGTTCCCTAATTTCAAAGGC	251		

Alignment of exon 5:

Homo sapiens cytochrome b-245 beta polypeptide (CYBB) gene, exon 5

Sequence ID: [gb|AF469761.1|F469757S05](#) Length: 311 Number of Matches: 1

Range 1: 69 to 277		GenBank	Graphics	Next Match	Previous Match
Score	Expect	Identities	Gaps	Strand	
374 bits(202)	4e-100	207/209(99%)	1/209(0%)	Plus/Plus	
Query	8	CCTTTTTCAGCGATTTCACACCATTGCACATCTATTTAATGTGGAATGGTGTGTAATGCC		66	
Sbjct	69	CCTTTTTCAGCGATTTCACACCATTGCACATCTATTTAATGTGGAATGGTGTGTAATGCC		128	
Query	67	GAGTCAATAAATTCGATCCTTATTAGTAGCACTCTCTGAACTTGGAGACAGGCAAATG		126	
Sbjct	129	GAGTCAATAAATTCGATCCTTATTAGTAGCACTCTCTGAACTTGGAGACAGGCAAATG		188	
Query	127	AAAGTTATCTCAATTTTGCTCGAAAGAGAATAAAGGTAAGCCTCTCATTATCTGACTTAG		186	
Sbjct	189	AAAGTTATCTCAATTTTGCTCGAAAGAGAATAAAGGTAAGCCTCTCATTATCTGACTTAG		248	
Query	187	ATATTCTTAGGCCATTACAATTGAGGAC	215		
Sbjct	249	ATATTCTTAGGCCATTACAATTGAGGAC	277		

Alignment of exon 7:

Homo sapiens cytochrome b-245 beta polypeptide (CYBB) gene, exon 7

Sequence ID: [gb|AF469763.1|F469757S07](#) Length: 244 Number of Matches: 1

Range 1: 29 to 214		GenBank	Graphics	Next Match	Previous Match
Score	Expect	Identities	Gaps	Strand	
339 bits(183)	1e-89	185/186(99%)	0/186(0%)	Plus/Plus	
Query	5	tttttCCCCCAGACGAATTGTACGTGGGCAGACCGCAGAGAGTTTGGCTGTGCATAATAT		64	
Sbjct	29	TTTTTCACCCAGACGAATTGTACGTGGGCAGACCGCAGAGAGTTTGGCTGTGCATAATAT		88	
Query	65	AACAGTTTGTGAACAAAAAATCTCAGAATGGGGAAAAATAAAGGAATGCCCAATCCCTCA		124	
Sbjct	89	AACAGTTTGTGAACAAAAAATCTCAGAATGGGGAAAAATAAAGGAATGCCCAATCCCTCA		148	
Query	125	GTTTGCTGGAAACCCCTCCTATGGTATGTACAATTCAITGTTGTTATTACAGTTTCATTAC		184	
Sbjct	149	GTTTGCTGGAAACCCCTCCTATGGTATGTACAATTCAITGTTGTTATTACAGTTTCATTAC		208	
Query	185	TGACAA 190			
Sbjct	209	TGACAA 214			

Alignment of exon 10:

Homo sapiens cytochrome b-245 beta polypeptide (CYBB) gene, exon 10

Sequence ID: [gb|AF469766.1|F469757S10](#) Length: 258 Number of Matches: 1

Range 1: 48 to 249		GenBank	Graphics	Next Match	Previous Match
Score	Expect	Identities	Gaps	Strand	
374 bits(202)	4e-100	202/202(100%)	0/202(0%)	Plus/Plus	
Query	9	CTTCAGGATAGCGGTTGATGGGCCCTTTGGCACTGCCAGTGAAGATGTGTTTCAGCTATGA		68	
Sbjct	48	CTTCAGGATAGCGGTTGATGGGCCCTTTGGCACTGCCAGTGAAGATGTGTTTCAGCTATGA		107	
Query	69	GGTGGTGAATGTTAGTGGGAGCAGGGATTGGGGTCACACCCCTTCGCATCCATTCTCAAGTC		128	
Sbjct	108	GGTGGTGAATGTTAGTGGGAGCAGGGATTGGGGTCACACCCCTTCGCATCCATTCTCAAGTC		167	
Query	129	AGTCTGGTACAAATATTGCAATAACGCCACCAATCTGAAGCTCAAAAAGGTAAGTCCTTT		188	
Sbjct	168	AGTCTGGTACAAATATTGCAATAACGCCACCAATCTGAAGCTCAAAAAGGTAAGTCCTTT		227	
Query	189	CATTTATCGGAGGGCCTTAGAG 210			
Sbjct	228	CATTTATCGGAGGGCCTTAGAG 249			

Patient 9:

Alignment of exon 2:

Homo sapiens cytochrome b-245 beta polypeptide (CYBB) gene, exon 2

Sequence ID: [gb|AF469758.1|F469757S02](#) Length: 230 Number of Matches: 1

Range 1: 82 to 226		GenBank	Graphics	Next Match	Previous Match
Score	Expect	Identities	Gaps	Strand	
268 bits(145)	1e-68	145/145(100%)	0/145(0%)	Plus/Plus	
Query	9	TTTCTGTTTGTGCAGCTGGTTTGGCTGGGGTTGAACGCTCTTCCTCTTTGTCTGGTATTAC		68	
Sbjct	82	TTTCTGTTTGTGCAGCTGGTTTGGCTGGGGTTGAACGCTCTTCCTCTTTGTCTGGTATTAC		141	
Query	69	CGGGTTTATGATAATCCACCTAAGTTCTTTTACACAAGAAAACTTCTGGGGTAAGTATA		128	
Sbjct	142	CGGGTTTATGATAATCCACCTAAGTTCTTTTACACAAGAAAACTTCTGGGGTAAGTATA		201	
Query	129	AATCCATCCCAATGCAATATTGGCT	153		
Sbjct	202	AATCCATCCCAATGCAATATTGGCT	226		

Alignment of exon 3:

Homo sapiens cytochrome b-245 beta polypeptide (CYBB) gene, exon 3

Sequence ID: [gb|AF469759.1|F469757S03](#) Length: 256 Number of Matches: 1

Range 1: 75 to 250		GenBank	Graphics	Next Match	Previous Match
Score	Expect	Identities	Gaps	Strand	
313 bits(169)	7e-82	174/176(99%)	2/176(1%)	Plus/Plus	
Query	7	GCT-CCTTT-CCGCCTCTTCTAGTCAGCACTGGCACTGGCCAGGGCCCTGCAGCCTGCC		64	
Sbjct	75	GCTCCCTTTCCCGCCTCTTCTAGTCAGCACTGGCACTGGCCAGGGCCCTGCAGCCTGCC		134	
Query	65	TGAATTTCAACTGCATGCTGATTCTCTTGCCAGTCTGTGAAATCTGCTGTCCTTCTCA		124	
Sbjct	135	TGAATTTCAACTGCATGCTGATTCTCTTGCCAGTCTGTGAAATCTGCTGTCCTTCTCA		194	
Query	125	GGGGTTCCAGTGCGGTAAGAGAAAATGTTTTACTAAGTTCCTCTAATTTTCAAAGG	180		
Sbjct	195	GGGGTTCCAGTGCGGTAAGAGAAAATGTTTTACTAAGTTCCTCTAATTTTCAAAGG	250		

Alignment of exon 5:

Homo sapiens cytochrome b-245 beta polypeptide (CYBB) gene, exon 5

Sequence ID: [gb|AF469761.1|F469757S05](#) Length: 311 Number of Matches: 1

Range 1: 69 to 277		GenBank	Graphics	Next Match	Previous Match
Score	Expect	Identities	Gaps	Strand	
381 bits(206)	3e-102	208/209(99%)	0/209(0%)	Plus/Plus	
Query	8	CCTTTTAGCGATTACACCATTCACATCTAATTAATGTGGAATGGTGTGTAATGCC		67	
Sbjct	69	CCTTTTAGCGATTACACCATTCACATCTAATTAATGTGGAATGGTGTGTAATGCC		128	
Query	68	GAGTCAATAAATCTGATCCTTATTCAGTAGCACTCTCTGAACITGGAGACAGGCAAAATG		127	
Sbjct	129	GAGTCAATAAATCTGATCCTTATTCAGTAGCACTCTCTGAACITGGAGACAGGCAAAATG		188	
Query	128	AAAGTTATCTCAATTTTGTCTCGAAAGAGAATAAAGGTAAGCCTCTCATTATCTGACTTAG		187	
Sbjct	189	AAAGTTATCTCAATTTTGTCTCGAAAGAGAATAAAGGTAAGCCTCTCATTATCTGACTTAG		248	
Query	188	ATATTCTTAGGCCATTACAATTGAGGAC	216		
Sbjct	249	ATATTCTTAGGCCATTACAATTGAGGAC	277		

Alignment of exon 7:

Homo sapiens cytochrome b-245 beta polypeptide (CYBB) gene, exon 7

Sequence ID: [gb|AF469763.1|F469757S07](#) Length: 244 Number of Matches: 1

Range 1: 29 to 214		GenBank	Graphics	Next Match	Previous Match
Score	Expect	Identities	Gaps	Strand	
322 bits(174)	1e-84	183/187(98%)	2/187(1%)	Plus/Plus	
Query	4	ttttttACCAAGGACG-ATTGTACGTGGGCAGACCGCAGAGAGTTTGGCTGTGCATAATA		62	
Sbjct	29	TTTTTCACCCA-GACGAATTGTACGTGGGCAGACCGCAGAGAGTTTGGCTGTGCATAATA		87	
Query	63	TAACAGTTTGTGAACAAAAAATCTCAGAATGGGGAAAAATAAAGGAATGCCCAATCCCTC		122	
Sbjct	88	TAACAGTTTGTGAACAAAAAATCTCAGAATGGGGAAAAATAAAGGAATGCCCAATCCCTC		147	
Query	123	AGTTTGCTGGAAACCCCTCCTATGGTATGTACAATTCATTGTTGTTATTACAGTTTCATTA		182	
Sbjct	148	AGTTTGCTGGAAACCCCTCCTATGGTATGTACAATTCATTGTTGTTATTACAGTTTCATTA		207	
Query	183	CTGACAA	189		
Sbjct	208	CTGACAA	214		

Alignment of exon 10:

Homo sapiens cytochrome b-245 beta polypeptide (CYBB) gene, exon 10

Sequence ID: [gb|AF469766.1|F469757S10](#) Length: 258 Number of Matches: 1

Range 1: 52 to 249		GenBank	Graphics	Next Match	Previous Match
Score	Expect	Identities	Gaps	Strand	
366 bits(198)	7e-98	198/198(100%)	0/198(0%)	Plus/Plus	
Query	13	AGGATAGCGGTTGATGGGCCCTTTGGCACTGCCAGTGAAGATGTGTTTCAGCTATGAGGTG		72	
Sbjct	52	AGGATAGCGGTTGATGGGCCCTTTGGCACTGCCAGTGAAGATGTGTTTCAGCTATGAGGTG		111	
Query	73	GTGATGTTAGTGGGAGCAGGGATTGGGGTCACACCCCTTCGCATCCATTCTCAAGTCAGTC		132	
Sbjct	112	GTGATGTTAGTGGGAGCAGGGATTGGGGTCACACCCCTTCGCATCCATTCTCAAGTCAGTC		171	
Query	133	TGGTACAAATATTGCAATAACGCCACCAATCTGAAGCTCAAAAAGGTAAGTCCTTTCATT		192	
Sbjct	172	TGGTACAAATATTGCAATAACGCCACCAATCTGAAGCTCAAAAAGGTAAGTCCTTTCATT		231	
Query	193	TATCGGAGGGCCTTAGAG	210		
Sbjct	232	TATCGGAGGGCCTTAGAG	249		

Patient 12:

Alignment of exon 2:

Homo sapiens cytochrome b-245 beta polypeptide (CYBB) gene, exon 2

Sequence ID: [gb|AF469758.1|F469757S02](#) Length: 230 Number of Matches: 1

Range 1: 78 to 225		GenBank	Graphics	Next Match	Previous Match
Score	Expect	Identities	Gaps	Strand	
268 bits(145)	1e-68	147/148(99%)	0/148(0%)	Plus/Plus	
Query 2	ATTTTTCTGTTTGTGCAGCTGGTTGGCTGGGGTTGAACGCTTCCTCTTTGTCTGGTA			61	
Sbjct 78	ATTATTTCTGTTTGTGCAGCTGGTTGGCTGGGGTTGAACGCTTCCTCTTTGTCTGGTA			137	
Query 62	TTACCGGGTTTATGATATTCACCTAAGTTCTTTTACACAAGAAAACCTCTTGGGGTAAAG			121	
Sbjct 138	TTACCGGGTTTATGATATTCACCTAAGTTCTTTTACACAAGAAAACCTCTTGGGGTAAAG			197	
Query 122	TATAAATTCATCCCATGCAATATTGGC	149			
Sbjct 198	TATAAATTCATCCCATGCAATATTGGC	225			

Alignment of exon 3:

Homo sapiens cytochrome b-245 beta polypeptide (CYBB) gene, exon 3

Sequence ID: [gb|AF469759.1|F469757S03](#) Length: 256 Number of Matches: 1

Range 1: 81 to 250		GenBank	Graphics	Next Match	Previous Match
Score	Expect	Identities	Gaps	Strand	
307 bits(166)	3e-80	169/170(99%)	1/170(0%)	Plus/Plus	
Query 10	TTT-CCGCCTCTTCTAGTCAGCACTGGCACTGGCCAGGGCCCTGCAGCCTGCCTGAATT	68			
Sbjct 81	TTTCCGCCTCTTCTAGTCAGCACTGGCACTGGCCAGGGCCCTGCAGCCTGCCTGAATT	140			
Query 69	TCAACTGCATGCTGATTCTTGGCCAGTCTGTCGAAATCTGCTGTCCTTCCTCAGGGGT	128			
Sbjct 141	TCAACTGCATGCTGATTCTTGGCCAGTCTGTCGAAATCTGCTGTCCTTCCTCAGGGGT	200			
Query 129	CCAGTGCGGTAAGAGAAAATGTTTACTAAGTTCCTCTAATTTTCAAAGG	178			
Sbjct 201	CCAGTGCGGTAAGAGAAAATGTTTACTAAGTTCCTCTAATTTTCAAAGG	250			

Alignment of exon 5:

Homo sapiens cytochrome b-245 beta polypeptide (CYBB) gene, exon 5

Sequence ID: [gb|AF469761.1|F469757S05](#) Length: 311 Number of Matches: 1

Range 1: 70 to 277		GenBank	Graphics	Next Match	Previous Match
Score	Expect	Identities	Gaps	Strand	
372 bits(201)	1e-99	206/208(99%)	2/208(0%)	Plus/Plus	
Query 5	CTTTT-AGCGATT-CACCATTGCACATCTATTTAATGTGGAATGGTGTGTGAATGCCCG	62			
Sbjct 70	CTTTTCAGCGATTACACCATTGCACATCTATTTAATGTGGAATGGTGTGTGAATGCCCG	129			
Query 63	AGTCAATAATTCTGATCCTTATTTCAGTAGCACTCTCTGAACCTGGAGACAGGCAAAATGA	122			
Sbjct 130	AGTCAATAAATTCTGATCCTTATTTCAGTAGCACTCTCTGAACCTGGAGACAGGCAAAATGA	189			
Query 123	AAGTTATCTCAATTTTGCTCGAAAGAGAATAAAGGTAAGCCTCTCATTATCTGACTTAGA	182			
Sbjct 190	AAGTTATCTCAATTTTGCTCGAAAGAGAATAAAGGTAAGCCTCTCATTATCTGACTTAGA	249			
Query 183	TATTCTTAGGCCATTACAATTGAGGAC	210			
Sbjct 250	TATTCTTAGGCCATTACAATTGAGGAC	277			

Alignment of exon 7:

Homo sapiens cytochrome b-245 beta polypeptide (CYBB) gene, exon 7

Sequence ID: [gb|AF469763.1|F469757S07](#) Length: 244 Number of Matches: 1

Range 1: 29 to 214		GenBank	Graphics	Next Match	Previous Match
Score	Expect	Identities	Gaps	Strand	
324 bits(175)	4e-85	185/189(98%)	3/189(1%)	Plus/Plus	
Query	4	tttttCCCCCAGGAACGAATTGTACGTGGGCAGACCGCAGAGAGTTGGCTGTGCATAA			63
Sbjct	29	TTTTT-CACCCA-G-ACGAATTGTACGTGGGCAGACCGCAGAGAGTTGGCTGTGCATAA			85
Query	64	TATAACAGTTTGTGAACAAAAATCTCAGAATGGGGAAAAATAAAGGAATGCCCAATCCC			123
Sbjct	86	TATAACAGTTTGTGAACAAAAATCTCAGAATGGGGAAAAATAAAGGAATGCCCAATCCC			145
Query	124	TCAGTTTGCTGGAAACCCCTCCTATGGTATGTACAATTCATTGTTGTTATTACAGTTTCAT			183
Sbjct	146	TCAGTTTGCTGGAAACCCCTCCTATGGTATGTACAATTCATTGTTGTTATTACAGTTTCAT			205
Query	184	TACTGACAA			192
Sbjct	206	TACTGACAA			214

Alignment of exon 10:

Homo sapiens cytochrome b-245 beta polypeptide (CYBB) gene, exon 10

Sequence ID: [gb|AF469766.1|F469757S10](#) Length: 258 Number of Matches: 1

Range 1: 43 to 249		GenBank	Graphics	Next Match	Previous Match
Score	Expect	Identities	Gaps	Strand	
377 bits(204)	3e-101	206/207(99%)	0/207(0%)	Plus/Plus	
Query	5	TTTCCATTCAGGATAGCGGTTGATGGGCCCTTTGGCACTGCCAGTGAAGATGTGTTCAGC			64
Sbjct	43	TTTCCCTTCAGGATAGCGGTTGATGGGCCCTTTGGCACTGCCAGTGAAGATGTGTTCAGC			102
Query	65	TATGAGGTGGTGTGTTAGTGGGAGCAGGGATTGGGGTCACACCCTTCGCATCCATTCTC			124
Sbjct	103	TATGAGGTGGTGTGTTAGTGGGAGCAGGGATTGGGGTCACACCCTTCGCATCCATTCTC			162
Query	125	AAGTCAGTCTGGTACAAATATTGCAATAACGCCACCAATCTGAAGCTCAAAAAGGTAAGT			184
Sbjct	163	AAGTCAGTCTGGTACAAATATTGCAATAACGCCACCAATCTGAAGCTCAAAAAGGTAAGT			222
Query	185	CCTTTCATTTATCGGAGGGCCTTAGAG			211
Sbjct	223	CCTTTCATTTATCGGAGGGCCTTAGAG			249

Patient 13:

Alignment of exon 2:

Homo sapiens cytochrome b-245 beta polypeptide (CYBB) gene, exon 2

Sequence ID: [gb|AF469758.1|F469757S02](#) Length: 230 Number of Matches: 1

Range 1: 83 to 227		GenBank	Graphics	Next Match	Previous Match
Score	Expect	Identities	Gaps	Strand	
268 bits(145)	1e-68	145/145(100%)	0/145(0%)	Plus/Plus	
Query	8	TTCTGTTTGTGCAGCTGGTTTGGCTGGGGTTGAACGCTTCCTCTTTGCTGGTATTACC	67		
Sbjct	83	TTCTGTTTGTGCAGCTGGTTTGGCTGGGGTTGAACGCTTCCTCTTTGCTGGTATTACC	142		
Query	68	GGGTTTATGATAITCCACCTAAGTTCTTTTACACAAGAAAATTCTTGGGGTAAGTATAA	127		
Sbjct	143	GGGTTTATGATAITCCACCTAAGTTCTTTTACACAAGAAAATTCTTGGGGTAAGTATAA	202		
Query	128	ATCCATCCCATGCAATATTGGCTG	152		
Sbjct	203	ATCCATCCCATGCAATATTGGCTG	227		

Alignment of exon 3:

Homo sapiens cytochrome b-245 beta polypeptide (CYBB) gene, exon 3

Sequence ID: [gb|AF469759.1|F469757S03](#) Length: 256 Number of Matches: 1

Range 1: 75 to 251		GenBank	Graphics	Next Match	Previous Match
Score	Expect	Identities	Gaps	Strand	
315 bits(170)	2e-82	175/177(99%)	2/177(1%)	Plus/Plus	
Query	8	GCT-CCTTT-CCGCCTCTTCTAGTCAGCACTGGCACIGGCCAGGGCCCTGCAGCCTGCC	65		
Sbjct	75	GCTCCCTTTCCCGCCTCTTCTAGTCAGCACTGGCACIGGCCAGGGCCCTGCAGCCTGCC	134		
Query	66	TGAATTTCAACTGCATGCTGATTCTCTTGCCAGTCTGTGCGAAATCTGCTGTCCTTCTCA	125		
Sbjct	135	TGAATTTCAACTGCATGCTGATTCTCTTGCCAGTCTGTGCGAAATCTGCTGTCCTTCTCA	194		
Query	126	GGGGTTCAGTGGGTAAGAGAAAATGTTTTACTAAGTTCCTCTAATTTTCAAAGGC	182		
Sbjct	195	GGGGTTCAGTGGGTAAGAGAAAATGTTTTACTAAGTTCCTCTAATTTTCAAAGGC	251		

Alignment of exon 5:

Homo sapiens cytochrome b-245 beta polypeptide (CYBB) gene, exon 5

Sequence ID: [gb|AF469761.1|F469757S05](#) Length: 311 Number of Matches: 1

Range 1: 70 to 277		GenBank	Graphics	Next Match	Previous Match
Score	Expect	Identities	Gaps	Strand	
377 bits(204)	3e-101	207/208(99%)	1/208(0%)	Plus/Plus	
Query	7	CTTTTC-GCGATTACACCATTGCACATCTATTTAATGTGGAATGGTGTGTGAATGCCCG	65		
Sbjct	70	CTTTTCAGCGATTACACCATTGCACATCTATTTAATGTGGAATGGTGTGTGAATGCCCG	129		
Query	66	AGTCAATAATTCTGATCCTTATTCAGTAGCACTCTCTGAACTGGAGACAGGCAAAATGA	125		
Sbjct	130	AGTCAATAATTCTGATCCTTATTCAGTAGCACTCTCTGAACTGGAGACAGGCAAAATGA	189		
Query	126	AAGTTATCTCAATTTTGCTCGAAAGAGAATAAAGGTAAGCCTCTCATTATCTGACTTAGA	185		
Sbjct	190	AAGTTATCTCAATTTTGCTCGAAAGAGAATAAAGGTAAGCCTCTCATTATCTGACTTAGA	249		
Query	186	TATTCTTAGGCCATTACAATTGAGGAC	213		
Sbjct	250	TATTCTTAGGCCATTACAATTGAGGAC	277		

Alignment of exon 7:

Homo sapiens cytochrome b-245 beta polypeptide (CYBB) gene, exon 7

Sequence ID: [gb|AF469763.1|F469757S07](#) Length: 244 Number of Matches: 1

Range 1: 29 to 214		GenBank	Graphics	Next Match	Previous Match
Score	Expect	Identities	Gaps	Strand	
320 bits(173)	5e-84	185/190(97%)	4/190(2%)	Plus/Plus	
Query	5	tttttAACCCAAGAACGAAATTTGTACGTGGGCAGACCGCAGAGAGTTTGGCTGTGCATA		64	
Sbjct	29	TTTTTCACCC-AG-ACG-AA-TTGTACGTGGGCAGACCGCAGAGAGTTTGGCTGTGCATA		84	
Query	65	ATATAACAGTTTGTGAACAAAAAATCTCAGAATGGGGAAAAATAAAGGAATGCCCAATCC		124	
Sbjct	85	ATATAACAGTTTGTGAACAAAAAATCTCAGAATGGGGAAAAATAAAGGAATGCCCAATCC		144	
Query	125	CTCAGTTTGCTGGAAACCCTCCTATGGTATGTACAATTCATTGTTGTTATTACAGTTTCA		184	
Sbjct	145	CTCAGTTTGCTGGAAACCCTCCTATGGTATGTACAATTCATTGTTGTTATTACAGTTTCA		204	
Query	185	TTACTGACAA	194		
Sbjct	205	TTACTGACAA	214		

Alignment of exon 10:

Homo sapiens cytochrome b-245 beta polypeptide (CYBB) gene, exon 10

Sequence ID: [gb|AF469766.1|F469757S10](#) Length: 258 Number of Matches: 1

Range 1: 55 to 249		GenBank	Graphics	Next Match	Previous Match
Score	Expect	Identities	Gaps	Strand	
361 bits(195)	3e-96	195/195(100%)	0/195(0%)	Plus/Plus	
Query	21	ATAGCGGTTGATGGGCCCTTTGGCACTGCCAGTGAAGATGTGTTTCAGCTATGAGGTGGTG		80	
Sbjct	55	ATAGCGGTTGATGGGCCCTTTGGCACTGCCAGTGAAGATGTGTTTCAGCTATGAGGTGGTG		114	
Query	81	ATGTTAGTGGGAGCAGGGATTGGGGTCACACCCTTCGCATCCATTCTCAAGTCAGTCTGG		140	
Sbjct	115	ATGTTAGTGGGAGCAGGGATTGGGGTCACACCCTTCGCATCCATTCTCAAGTCAGTCTGG		174	
Query	141	TACAAATATTGCAATAACGCCACCAATCTGAAGCTCAAAAAGGTAAGTCCITTCATTTAT		200	
Sbjct	175	TACAAATATTGCAATAACGCCACCAATCTGAAGCTCAAAAAGGTAAGTCCITTCATTTAT		234	
Query	201	CGGAGGGCCTTAGAG	215		
Sbjct	235	CGGAGGGCCTTAGAG	249		

Blast alignment of patient's DNA sequence (CYBB Gene) with control sample:

Patient 1:

Alignment of exon 2:

Sequence ID: lcl|Query_107911 Length: 152 Number of Matches: 1

Range 1: 5 to 152 [Graphics](#) ▼ Next Match ▲ Previous Match

Score	Expect	Identities	Gaps	Strand
274 bits(148)	5e-79	148/148(100%)	0/148(0%)	Plus/Plus
Query 5	AAAAATCTGTTTGTGCAGCTGGTTTGGCTGGGGTTGAACGTCCTCCTTTGTCTGGTAT	64		
Sbjct 5	AAAAATCTGTTTGTGCAGCTGGTTTGGCTGGGGTTGAACGTCCTCCTTTGTCTGGTAT	64		
Query 65	TACCGGGTTTATGATATCCACCTAAGTTCTTTTACACAAGAAAACCTTCTGGGGTAAGT	124		
Sbjct 65	TACCGGGTTTATGATATCCACCTAAGTTCTTTTACACAAGAAAACCTTCTGGGGTAAGT	124		
Query 125	ATAAATCCATCCCATGCAATATTGGCT	152		
Sbjct 125	ATAAATCCATCCCATGCAATATTGGCT	152		

Alignment of exon 3:

Sequence ID: lcl|Query_136813 Length: 183 Number of Matches: 1

Range 1: 13 to 182 [Graphics](#) ▼ Next Match ▲ Previous Match

Score	Expect	Identities	Gaps	Strand
315 bits(170)	4e-91	170/170(100%)	0/170(0%)	Plus/Plus
Query 11	CTTTCGCCTCTTCTAGTCAGCACTGGCACTGGCCAGGGCCCTGCAGCCTGCCTGAATT	70		
Sbjct 13	CTTTCGCCTCTTCTAGTCAGCACTGGCACTGGCCAGGGCCCTGCAGCCTGCCTGAATT	72		
Query 71	TCAACTGCATGCTGATTCTCTTGGCAGTCTGTGCAAACTGTCTGTCCCTCAGGGGT	130		
Sbjct 73	TCAACTGCATGCTGATTCTCTTGGCAGTCTGTGCAAACTGTCTGTCCCTCAGGGGT	132		
Query 131	CCAGTGCAGTAAGAGAAAATGTTTTACTAAGTTCCTCTAATTTCAAAGG	180		
Sbjct 133	CCAGTGCAGTAAGAGAAAATGTTTTACTAAGTTCCTCTAATTTCAAAGG	182		

Alignment of exon 5:

Sequence ID: lcl|Query_149671 Length: 217 Number of Matches: 1

Range 1: 6 to 215 [Graphics](#) ▼ Next Match ▲ Previous Match

Score	Expect	Identities	Gaps	Strand
377 bits(204)	8e-110	208/210(99%)	0/210(0%)	Plus/Plus
Query 6	TTCATTTTAGCGATTACACCAATGCACATCTATTTAATGTGGAATGGTGTGTAATGCC	65		
Sbjct 6	TTCGTTTTTCGCGATTACACCAATGCACATCTATTTAATGTGGAATGGTGTGTAATGCC	65		
Query 66	CGAGTCAATAAATCTGATCCTTATTAGTAGCACTCTCTGAACTTGGAGACAGGCAAAAT	125		
Sbjct 66	CGAGTCAATAAATCTGATCCTTATTAGTAGCACTCTCTGAACTTGGAGACAGGCAAAAT	125		
Query 126	GAAAGTTATCTCAATTTTGGCTCGAAAGAGAATAAAGGTAAGCCTCTCATTATCTGACTTA	185		
Sbjct 126	GAAAGTTATCTCAATTTTGGCTCGAAAGAGAATAAAGGTAAGCCTCTCATTATCTGACTTA	185		
Query 186	GATATTCTTAGGCCATTACAATTGAGGAC	215		
Sbjct 186	GATATTCTTAGGCCATTACAATTGAGGAC	215		

Alignment of exon 7:

Sequence ID: lcl|Query_80561 Length: 193 Number of Matches: 1

Range 1: 18 to 193 [Graphics](#) ▼ Next Match ▲ Previous Match

Score	Expect	Identities	Gaps	Strand
318 bits(172)	4e-92	175/176(99%)	1/176(0%)	Plus/Plus
Query 13	ACG-ATTGTACGTGGGCAGACCGCAGAGAGTTTGGCTGTGCATAATATAACAGTTTGTGA	71		
Sbjct 18	ACGAATTGTACGTGGGCAGACCGCAGAGAGTTTGGCTGTGCATAATATAACAGTTTGTGA	77		
Query 72	ACAAAAAATCTCAGAATGGGGAAAAATAAAGGAATGCCCAATCCCTCAGTTTGTCTGGAAA	131		
Sbjct 78	ACAAAAAATCTCAGAATGGGGAAAAATAAAGGAATGCCCAATCCCTCAGTTTGTCTGGAAA	137		
Query 132	CCCTCCTATGGTATGTACAATTCATTGTTGTTATTACAGTTTCATTACTGACAAA	187		
Sbjct 138	CCCTCCTATGGTATGTACAATTCATTGTTGTTATTACAGTTTCATTACTGACAAA	193		

Alignment of exon 10:

Sequence ID: lcl|Query_94893 Length: 210 Number of Matches: 1

Range 1: 6 to 210 [Graphics](#) ▼ Next Match ▲ Previous Match

Score	Expect	Identities	Gaps	Strand
368 bits(199)	4e-107	204/206(99%)	1/206(0%)	Plus/Plus
Query 5	TTCGTTCCGATAGCGGTTGATGGGCCCTTTGGCACTGCCAGTGAAGATGTGTTCCAGCTAT	64		
Sbjct 6	TTCCTTCGGATAGCGGTTGATGGGCCCTTTGGCACTGCCAGTGAAGATGTGTTCCAGCTAT	65		
Query 65	GAGGTGGTGTGTTAGTGGGAGCAGGGATTGGGGTCACACCCTTCGCATCCATTCTCAAG	124		
Sbjct 66	GAGGTGGTGTGTTAGTGGGAGCAGGGATTGGGGTCACACCCTTCGCATCCATTCTCAAG	125		
Query 125	TCAGTCTGGTACAAATATTGCAATAACGCCACCAATCTGAAGCTCAAAAAGGTAAGTCCT	184		
Sbjct 126	TCAGTCTGGTACAAATATTGCAATAACGCCACCAATCTGAAGCTCAAAAAGGTAAGTCCT	185		
Query 185	TTCATTTAICGGAGGGCCCTTAGAGA	210		
Sbjct 186	TTCATTTAICGGAGGG-CCTTAGAGA	210		

Patient2:

Alignment of exon 2

Sequence ID: lcl|Query_144173 Length: 152 Number of Matches: 1

Range 1: 10 to 152		Graphics			Next Match	Previous Match
Score	Expect	Identities	Gaps	Strand		
265 bits(143)	3e-76	143/143(100%)	0/143(0%)	Plus/Plus		
Query	9	TCTGTTTGIGCAGCTGGTTGGCTGGGGTTGAACGCTTCCTCTTTGICTGGTATTACCG			68	
Sbjct	10	TCTGTTTGIGCAGCTGGTTGGCTGGGGTTGAACGCTTCCTCTTTGICTGGTATTACCG			69	
Query	69	GGTTTATGATATCCACCTAAGTTCTTTTACACAAGAAAACCTCTTGGGGTAAGTATAAA			128	
Sbjct	70	GGTTTATGATATCCACCTAAGTTCTTTTACACAAGAAAACCTCTTGGGGTAAGTATAAA			129	
Query	129	TTCCATCCCATGCAATATTGGCT	151			
Sbjct	130	TTCCATCCCATGCAATATTGGCT	152			

Alignment of exon 3

Sequence ID: lcl|Query_246671 Length: 183 Number of Matches: 1

Range 1: 10 to 182		Graphics			Next Match	Previous Match
Score	Expect	Identities	Gaps	Strand		
320 bits(173)	9e-93	173/173(100%)	0/173(0%)	Plus/Plus		
Query	8	CTCCTTTCCGCCTCTTCTAGTCAGCACTGGCACTGGCCAGGGCCCTGCAGCCTGCCTGA			67	
Sbjct	10	CTCCTTTCCGCCTCTTCTAGTCAGCACTGGCACTGGCCAGGGCCCTGCAGCCTGCCTGA			69	
Query	68	ATTTCAACTGCAIGCTGATTCTCTTGCCAGTCTGTCGAAATCTGCTGTCCTTCCTCAGGG			127	
Sbjct	70	ATTTCAACTGCAIGCTGATTCTCTTGCCAGTCTGTCGAAATCTGCTGTCCTTCCTCAGGG			129	
Query	128	GTTCCAGTGC GGTAAGAGAAAAIGTTTTACTAAGTTCCTCTAATTTTCAAAGG	180			
Sbjct	130	GTTCCAGTGC GGTAAGAGAAAAIGTTTTACTAAGTTCCTCTAATTTTCAAAGG	182			

Alignment of exon 5

Sequence ID: lcl|Query_21315 Length: 217 Number of Matches: 1

Range 1: 10 to 215		Graphics			Next Match	Previous Match
Score	Expect	Identities	Gaps	Strand		
359 bits(194)	3e-104	203/207(98%)	2/207(0%)	Plus/Plus		
Query	8	TTTTCGCGATTTCACCCATTGCACATCTATTTAATAGTGGAAAGGTGTGTGAAAGCCCGA			66	
Sbjct	10	TTTTCGCGATTTCACCCATTGCACATCTATTTAAT-GTGGAAATGGTGTGTGAAAGCCCGA			68	
Query	67	GTCAATAATTCTGATCCTTATTTCAGTAGCACTCTCTGAACTTGGAGACAGGCAAAATGAA			126	
Sbjct	69	GTCAATAATTCTGATCCTTATTTCAGTAGCACTCTCTGAACTTGGAGACAGGCAAAATGAA			128	
Query	127	AGTTATCTCAATTTTGCTCGAAAGAGAAATAAAGGTAAGCCTCTCATTATCTGACTTAGAT			186	
Sbjct	129	AGTTATCTCAATTTTGCTCGAAAGAGAAATAAAGGTAAGCCTCTCATTATCTGACTTAGAT			188	
Query	187	ATTCTTAGGCCATTACAATTGAGGAC	213			
Sbjct	189	ATTCTTAGGCCATTACAATTGAGGAC	215			

Alignment of exon 7

Sequence ID: lcl|Query_44591 Length: 193 Number of Matches: 1

Range 1: 3 to 191 [Graphics](#) ▼ Next Match ▲ Previous Match

Score	Expect	Identities	Gaps	Strand
318 bits(172)	4e-92	184/189(97%)	3/189(1%)	Plus/Plus
Query 2	tttttttACCC-A-GACG-ATTGTACGTGGGCAGACCCGAGAGAGTTTGGCTGTGCATAA	58		
Sbjct 3	TTTTTTTCCCAACAACGAATTGTACGTGGGCAGACCCGAGAGAGTTTGGCTGTGCATAA	62		
Query 59	TATAACAGTTTGTGAACAAAAAATCTCAGAATGGGGAAAAATAAAGGAATGCCCAATCCC	118		
Sbjct 63	TATAACAGTTTGTGAACAAAAAATCTCAGAATGGGGAAAAATAAAGGAATGCCCAATCCC	122		
Query 119	TCAGTTTGTCTGGAAACCCTCCTATGGTATGTACAATTCATTGTTGTTATTACAGTTTCAT	178		
Sbjct 123	TCAGTTTGTCTGGAAACCCTCCTATGGTATGTACAATTCATTGTTGTTATTACAGTTTCAT	182		
Query 179	TACTGACAA 187			
Sbjct 183	TACTGACAA 191			

Alignment of exon 10

Sequence ID: lcl|Query_73369 Length: 210 Number of Matches: 1

Range 1: 10 to 210 [Graphics](#) Next Match Previous Match

Score	Expect	Identities	Gaps	Strand
366 bits(198)	2e-106	201/202(99%)	1/202(0%)	Plus/Plus
Query 9	TTCGGATAGCGGTTGATGGGCCCTTTGGCACTGCCAGTGAAGATGTGTTTCAGCTATGAGG	68		
Sbjct 10	TTCGGATAGCGGTTGATGGGCCCTTTGGCACTGCCAGTGAAGATGTGTTTCAGCTATGAGG	69		
Query 69	TGGTGAIGTTAGTGGGAGCAGGGATTGGGGTCACACCCCTTCGCATCCATTCTCAAGTCAG	128		
Sbjct 70	TGGTGAIGTTAGTGGGAGCAGGGATTGGGGTCACACCCCTTCGCATCCATTCTCAAGTCAG	129		
Query 129	TCGGTACAAATATTGCAATAACGCCACCAATCTGAAGCTCAAAAAGGTAAGTCCTTTCA	188		
Sbjct 130	TCGGTACAAATATTGCAATAACGCCACCAATCTGAAGCTCAAAAAGGTAAGTCCTTTCA	189		
Query 189	TTTATCGGAGGGCCTTAGAGA 210			
Sbjct 190	TTTATCGGAGGG-CCTTAGAGA 210			

Patient 3:

Alignment of exon 2

Sequence ID: lcl|Query_97923 Length: 152 Number of Matches: 1

Range 1: 10 to 152		Graphics			Next Match	Previous Match
Score	Expect	Identities	Gaps	Strand		
265 bits(143)	3e-76	143/143(100%)	0/143(0%)	Plus/Plus		
Query	9	TCIGTTTGTGCAGCTGGTTTGGCTGGGGTTGAACGCTCTCCCTCTTGTCTGGTATTACCG			68	
Sbjct	10	TCIGTTTGTGCAGCTGGTTTGGCTGGGGTTGAACGCTCTCCCTCTTGTCTGGTATTACCG			69	
Query	69	GGTTTATGATATCCACCTAAGTTCTTTTACACAAGAAAACCTCTTGGGGTAAGTATAAA			128	
Sbjct	70	GGTTTATGATATCCACCTAAGTTCTTTTACACAAGAAAACCTCTTGGGGTAAGTATAAA			129	
Query	129	TTCCATCCCATGCAATATTGGCT	151			
Sbjct	130	TTCCATCCCATGCAATATTGGCT	152			

Alignment of exon 3

Sequence ID: lcl|Query_10689 Length: 183 Number of Matches: 1

Range 1: 13 to 182		Graphics			Next Match	Previous Match
Score	Expect	Identities	Gaps	Strand		
315 bits(170)	4e-91	170/170(100%)	0/170(0%)	Plus/Plus		
Query	10	CTTTCGCCCTCTTCTAGTCAGCACTGGCACTGGCCAGGGCCCTGCAGCCTGCCTGAATT			69	
Sbjct	13	CTTTCGCCCTCTTCTAGTCAGCACTGGCACTGGCCAGGGCCCTGCAGCCTGCCTGAATT			72	
Query	70	TCAACTGCATGCTGATTCTCTTCCAGTCTGTGCGAAATCTGCTGTCCTTCTCAGGGGT			129	
Sbjct	73	TCAACTGCATGCTGATTCTCTTCCAGTCTGTGCGAAATCTGCTGTCCTTCTCAGGGGT			132	
Query	130	CCAGTCCGGTAAGAGAAAATGTTTTACTAAGTTCCCTAATTTTCAAAGG	179			
Sbjct	133	CCAGTCCGGTAAGAGAAAATGTTTTACTAAGTTCCCTAATTTTCAAAGG	182			

Alignment of exon 5

Sequence ID: lcl|Query_50637 Length: 217 Number of Matches: 2

Range 1: 10 to 215		Graphics			Next Match	Previous Match
Score	Expect	Identities	Gaps	Strand		
375 bits(203)	6e-109	205/206(99%)	0/206(0%)	Plus/Plus		
Query	6	TTTTAGCGATTACACCATTGCACATCTATTTAATGIGGAATGGTGTGTGAATGCCCGAG			65	
Sbjct	10	TTTTAGCGATTACACCATTGCACATCTATTTAATGIGGAATGGTGTGTGAATGCCCGAG			69	
Query	66	TCAATAATCTGATCCTTATTTCAGTAGCACTCTGAACTTGGAGACAGGCAAAATGAAA			125	
Sbjct	70	TCAATAATCTGATCCTTATTTCAGTAGCACTCTGAACTTGGAGACAGGCAAAATGAAA			129	
Query	126	GTTATCTCAATTTTGTCTGAAAGAGAATAAAGGTAAGCCTCTCATTATCTGACTTAGATA			185	
Sbjct	130	GTTATCTCAATTTTGTCTGAAAGAGAATAAAGGTAAGCCTCTCATTATCTGACTTAGATA			189	
Query	186	TTCTAGGCCATTACAATTGAGGAC	211			
Sbjct	190	TTCTAGGCCATTACAATTGAGGAC	215			

Alignment of exon 7

Sequence ID: lcl|Query_23743 Length: 193 Number of Matches: 1

Range 1: 18 to 191					Next Match	Previous Match
Score	Expect	Identities	Gaps	Strand		
315 bits(170)	5e-91	173/174(99%)	1/174(0%)	Plus/Plus		
Query	12	ACG-ATTGTACGTGGGCAGACCGCAGAGAGTTTGGCTGTGCATAATATAACAGTTTGTGA			70	
Sbjct	18	ACGAATTGTACGTGGGCAGACCGCAGAGAGTTTGGCTGTGCATAATATAACAGTTTGTGA			77	
Query	71	ACAAAAATCTCAGAATGGGGAAAAATAAAGGAATGCCCAATCCCTCAGTTTGTCTGGAAA			130	
Sbjct	78	ACAAAAATCTCAGAATGGGGAAAAATAAAGGAATGCCCAATCCCTCAGTTTGTCTGGAAA			137	
Query	131	CCCTCCTATGGTATGTACAATTCATTGTTGTTATTACAGTTTCATTACTGACAA			184	
Sbjct	138	CCCTCCTATGGTATGTACAATTCATTGTTGTTATTACAGTTTCATTACTGACAA			191	

Alignment of exon 10

Sequence ID: lcl|Query_21787 Length: 210 Number of Matches: 1

Range 1: 6 to 210					Next Match	Previous Match
Score	Expect	Identities	Gaps	Strand		
363 bits(196)	2e-105	203/206(99%)	1/206(0%)	Plus/Plus		
Query	5	TTCATTAGGATAGCGGTTGATGGGCCCTTTGGCACTGCCAGTGAAGATGTGTTTCAGCTAT			64	
Sbjct	6	TTCCTTCGGATAGCGGTTGATGGGCCCTTTGGCACTGCCAGTGAAGATGTGTTTCAGCTAT			65	
Query	65	GAGGTGGTGTATGTTAGTGGGAGCAGGGATTGGGGTCACACCCTTCGCATCCATTCTCAAG			124	
Sbjct	66	GAGGTGGTGTATGTTAGTGGGAGCAGGGATTGGGGTCACACCCTTCGCATCCATTCTCAAG			125	
Query	125	TCAGTCTGGTACAAATATTGCAATAACGCCACCAATCTGAAGCTCAAAAAGGTAAGTCCT			184	
Sbjct	126	TCAGTCTGGTACAAATATTGCAATAACGCCACCAATCTGAAGCTCAAAAAGGTAAGTCCT			185	
Query	185	TTCATTTATCGGAGGGGCCCTTAGAGA	210			
Sbjct	186	TTCATTTATCGGAGGG-CCTTAGAGA	210			

Patient 6:

Alignment of exon 2

Sequence ID: lcl|Query_46957 Length: 152 Number of Matches: 1

Range 1: 6 to 152 Graphics					Next Match	Previous Match
Score	Expect	Identities	Gaps	Strand		
272 bits(147)	2e-78	147/147(100%)	0/147(0%)	Plus/Plus		
Query 5	AAATTCGTGTTGTGCAGCTGGTTTGGCTGGGGITGAACGTCCTCCTTTGCTGGTATT				64	
Sbjct 6	AAATTCGTGTTGTGCAGCTGGTTTGGCTGGGGITGAACGTCCTCCTTTGCTGGTATT				65	
Query 65	ACCGGGTTTATGATATCCACCTAAGTCTTTTACACAAGAAAATCTTGGGGTAAGTA				124	
Sbjct 66	ACCGGGTTTATGATATCCACCTAAGTCTTTTACACAAGAAAATCTTGGGGTAAGTA				125	
Query 125	TAAATCCATCCCATGCAATATTGGCT	151				
Sbjct 126	TAAATCCATCCCATGCAATATTGGCT	152				

Alignment of exon 3

Sequence ID: lcl|Query_9835 Length: 183 Number of Matches: 1

Range 1: 11 to 183 Graphics					Next Match	Previous Match
Score	Expect	Identities	Gaps	Strand		
320 bits(173)	9e-93	173/173(100%)	0/173(0%)	Plus/Plus		
Query 9	TCCTTCCGCCCTCTTCTAGTCAGCACTGGCACTGGCCAGGGCCCCTGCAGCCTGCCTGAA				68	
Sbjct 11	TCCTTCCGCCCTCTTCTAGTCAGCACTGGCACTGGCCAGGGCCCCTGCAGCCTGCCTGAA				70	
Query 69	TTTCAACTGCAIGCTGATTCTCTTGCCAGTCTGTGCGAAATCTGCTGTCCTTCCTCAGGGG				128	
Sbjct 71	TTTCAACTGCAIGCTGATTCTCTTGCCAGTCTGTGCGAAATCTGCTGTCCTTCCTCAGGGG				130	
Query 129	TTCCAGTGCGGTAAGAGAAAATGTTTTACTAAGTTCCTCTAATTTCAAAGGC	181				
Sbjct 131	TTCCAGTGCGGTAAGAGAAAATGTTTTACTAAGTTCCTCTAATTTCAAAGGC	183				

Alignment of exon 5

Sequence ID: lcl|Query_11095 Length: 217 Number of Matches: 1

Range 1: 4 to 215 Graphics					Next Match	Previous Match
Score	Expect	Identities	Gaps	Strand		
381 bits(206)	6e-111	210/212(99%)	0/212(0%)	Plus/Plus		
Query 3	CTTTCCTTTTAGCGATTACACCAATTGCACATCTATTTAATGTGGAATGGTGTGAATG				62	
Sbjct 4	CTTTCGTTTTCGCGATTACACCAATTGCACATCTATTTAATGTGGAATGGTGTGAATG				63	
Query 63	CCCGAGTCAATAATTCTGATCCTTATTAGTAGCACCTCTGAACTGGAGACAGGCAAA				122	
Sbjct 64	CCCGAGTCAATAATTCTGATCCTTATTAGTAGCACCTCTGAACTGGAGACAGGCAAA				123	
Query 123	ATGAAAGTTATCTCAATTTTGCTCGAAAGAGAATAAAGGTAAGCCTCTCATTATCTGACT				182	
Sbjct 124	ATGAAAGTTATCTCAATTTTGCTCGAAAGAGAATAAAGGTAAGCCTCTCATTATCTGACT				183	
Query 183	TAGATATTCTTAGGCCATTACAATTGAGGAC	214				
Sbjct 184	TAGATATTCTTAGGCCATTACAATTGAGGAC	215				

Alignment of exon 7

Sequence ID: Icl|Query_144819 Length: 193 Number of Matches: 1

Range 1: 2 to 193		Graphics			Next Match	Previous Match
Score	Expect	Identities	Gaps	Strand		
329 bits(178)	2e-95	190/195(97%)	4/195(2%)	Plus/Plus		
Query	2	ttttttttCACCCCAA-GACGAAATGTACGTGGGCAGACCGCAGAGAGTTGGCTGTGC			60	
Sbjct	2	TTTTTTTT--CCCAACAACG-AATGTACGTGGGCAGACCGCAGAGAGTTGGCTGTGC			58	
Query	61	ATAATATAACAGTTTGTGAACAAAAAATCTCAGAATGGGGAAAAATAAAGGAATGCCCAA			120	
Sbjct	59	ATAATATAACAGTTTGTGAACAAAAAATCTCAGAATGGGGAAAAATAAAGGAATGCCCAA			118	
Query	121	TCCCTCAGTTTGTCTGGAAACCCTCCTATGGTATGTACAATTCATTGTTGTTATTACAGTT			180	
Sbjct	119	TCCCTCAGTTTGTCTGGAAACCCTCCTATGGTATGTACAATTCATTGTTGTTATTACAGTT			178	
Query	181	TCATTACTGACAAAA	195			
Sbjct	179	TCATTACTGACAAAA	193			

Alignment of exon 10

Sequence ID: Icl|Query_107781 Length: 210 Number of Matches: 1

Range 1: 3 to 210		Graphics			Next Match	Previous Match
Score	Expect	Identities	Gaps	Strand		
375 bits(203)	3e-109	208/210(99%)	2/210(0%)	Plus/Plus		
Query	2	TTTTTCCTTTTCGGATAGCGGTTGATGGGCCCTTTGGCACTGCCAGTGAAGATGTGTTCA			61	
Sbjct	3	TTTTTC--TTCGGATAGCGGTTGATGGGCCCTTTGGCACTGCCAGTGAAGATGTGTTCA			60	
Query	62	GCTATGAGGTGGTGAIGTTAGTGGGAGCAGGGATTGGGGTCACACCCTTCGCATCCATT			121	
Sbjct	61	GCTATGAGGTGGTGAIGTTAGTGGGAGCAGGGATTGGGGTCACACCCTTCGCATCCATT			120	
Query	122	TCAAGTCAGTCTGGTACAAATATTGCAATAACGCCACCAATCTGAAGCTCAAAAAGGTAA			181	
Sbjct	121	TCAAGTCAGTCTGGTACAAATATTGCAATAACGCCACCAATCTGAAGCTCAAAAAGGTAA			180	
Query	182	GTCCTTTCATTATCGGAGGGCCTTAGAGA	211			
Sbjct	181	GTCCTTTCATTATCGGAGGGCCTTAGAGA	210			

Patient 7:

Alignment of exon 2

Sequence ID: lcl|Query_18249 Length: 152 Number of Matches: 1

Range 1: 6 to 152 Graphics					Next Match	Previous Match
Score	Expect	Identities	Gaps	Strand		
265 bits(143)	3e-76	146/147(99%)	1/147(0%)	Plus/Plus		
Query	6	AAA-TCTGTTTGTGTCAGCTGGTTTGGCTGGGGTTGAACGTCTTCCTCTTTGTCTGGTATT			64	
Sbjct	6	AAATTCGTGTTGTGTCAGCTGGTTTGGCTGGGGTTGAACGTCTTCCTCTTTGTCTGGTATT			65	
Query	65	ACCGGGTTTATGATATTCACCTAAGTTCTTTTACACAAGAAAACCTTCTGGGGTAAGTA			124	
Sbjct	66	ACCGGGTTTATGATATTCACCTAAGTTCTTTTACACAAGAAAACCTTCTGGGGTAAGTA			125	
Query	125	TAAATTCATCCCATGCAATATTGGCT	151			
Sbjct	126	TAAATTCATCCCATGCAATATTGGCT	152			

Alignment of exon 3

Sequence ID: lcl|Query_57167 Length: 183 Number of Matches: 1

Range 1: 10 to 183 Graphics					Next Match	Previous Match
Score	Expect	Identities	Gaps	Strand		
322 bits(174)	3e-93	174/174(100%)	0/174(0%)	Plus/Plus		
Query	8	CTCCTTTCGGCCTCTTCTAGTCAGCACTGGCACTGGCCAGGGCCCTGCAGCCTGCCTGA			67	
Sbjct	10	CTCCTTTCGGCCTCTTCTAGTCAGCACTGGCACTGGCCAGGGCCCTGCAGCCTGCCTGA			69	
Query	68	ATTTCAACTGCATGCTGATTCTCTTGCCAGTCTGTCGAAATCTGCTGTCCTTCTCAGGG			127	
Sbjct	70	ATTTCAACTGCATGCTGATTCTCTTGCCAGTCTGTCGAAATCTGCTGTCCTTCTCAGGG			129	
Query	128	GTTCCAGTGGCGTAAGAGAAAATGTTTTACTAAGTTCCTCTAATTTTCAAAGGC	181			
Sbjct	130	GTTCCAGTGGCGTAAGAGAAAATGTTTTACTAAGTTCCTCTAATTTTCAAAGGC	183			

Alignment of exon 5

Sequence ID: lcl|Query_50817 Length: 217 Number of Matches: 1

Range 1: 10 to 215 Graphics					Next Match	Previous Match
Score	Expect	Identities	Gaps	Strand		
368 bits(199)	5e-107	204/206(99%)	1/206(0%)	Plus/Plus		
Query	11	TTTTCGCGATTTCACACCATTCACATCTATTTAATGTGGAATGGTGTGTAATGCCCGAG			69	
Sbjct	10	TTTTCGCGATTTCACACCATTCACATCTATTTAATGTGGAATGGTGTGTAATGCCCGAG			69	
Query	70	TCAATAATTCTGATCCTTATTTCAGTAGCACTCTCTGAACTTGGAGACAGGCAAAATGAAA			129	
Sbjct	70	TCAATAATTCTGATCCTTATTTCAGTAGCACTCTCTGAACTTGGAGACAGGCAAAATGAAA			129	
Query	130	GTTATCTCAATTTGTCGAAAAGAGAAATAAAGGTAAGCCTCTCATTATCTGACTTAGATA			189	
Sbjct	130	GTTATCTCAATTTGTCGAAAAGAGAAATAAAGGTAAGCCTCTCATTATCTGACTTAGATA			189	
Query	190	TTCTTAGGCCATTACAATTGAGGAC	215			
Sbjct	190	TTCTTAGGCCATTACAATTGAGGAC	215			

Alignment of exon 7

Sequence ID: Icl|Query_179351 Length: 193 Number of Matches: 1

Range 1: 2 to 193 Graphics		Next Match	Previous Match	
Score	Expect	Identities	Gaps	Strand
337 bits(182)	1e-97	190/193(98%)	3/193(1%)	Plus/Plus
Query 2	ttttttttCCCC--CAGACGAATGTACGTGGGCAGACCGCAGAGAGTTTGGCTGTGCA	59		
Sbjct 2	TTTTTTTCCCCAACA-ACGAATGTACGTGGGCAGACCGCAGAGAGTTTGGCTGTGCA	60		
Query 60	AATATAACAGTTTGTGAACAAAAATCTCAGAATGGGGAAAAATAAAGGAATGCCCAATC	119		
Sbjct 61	AATATAACAGTTTGTGAACAAAAATCTCAGAATGGGGAAAAATAAAGGAATGCCCAATC	120		
Query 120	CCTCAGTTTGTCTGGAAACCCTCCTATGGTATGTACAATTCATTGTTGTTATTACAGTTTC	179		
Sbjct 121	CCTCAGTTTGTCTGGAAACCCTCCTATGGTATGTACAATTCATTGTTGTTATTACAGTTTC	180		
Query 180	ATTACTGACAAA 192			
Sbjct 181	ATTACTGACAAA 193			

Alignment of exon 10

Sequence ID: Icl|Query_236551 Length: 210 Number of Matches: 1

Range 1: 3 to 210 Graphics		Next Match	Previous Match	
Score	Expect	Identities	Gaps	Strand
374 bits(202)	1e-108	207/209(99%)	1/209(0%)	Plus/Plus
Query 3	TTTTTCTTCAGGATAGCGGTTGATGGGCCCTTTGGCACTGCCAGTGAAGATGTGTTTCAG	62		
Sbjct 3	TTTTTCCTTC-GGATAGCGGTTGATGGGCCCTTTGGCACTGCCAGTGAAGATGTGTTTCAG	61		
Query 63	CTATGAGGTGGTGTGATGTTAGTGGGAGCAGGGATTGGGGTCACACCCTTCGCATCCATTCT	122		
Sbjct 62	CTATGAGGTGGTGTGATGTTAGTGGGAGCAGGGATTGGGGTCACACCCTTCGCATCCATTCT	121		
Query 123	CAAGTCAGTCTGGTACAAATATTGCAATAACGCCACCAATCTGAAGCTCAAAAAGGTAAG	182		
Sbjct 122	CAAGTCAGTCTGGTACAAATATTGCAATAACGCCACCAATCTGAAGCTCAAAAAGGTAAG	181		
Query 183	TCCTTTCATTTATCGGAGGGCCTTAGAGA 211			
Sbjct 182	TCCTTTCATTTATCGGAGGGCCTTAGAGA 210			

Patient 9:

Alignment of exon 2

Sequence ID: lcl|Query_4971 Length: 152 Number of Matches: 1

Range 1: 9 to 152 Graphics					Next Match	Previous Match
Score	Expect	Identities	Gaps	Strand		
267 bits(144)	9e-77	144/144(100%)	0/144(0%)	Plus/Plus		
Query	10	TTCTGTTTGTGCAGCTGGTTTGGCTGGGGTTGAACGCTTCCTCTTTGTCTGGTATTACC		69		
Sbjct	9	TTCTGTTTGTGCAGCTGGTTTGGCTGGGGTTGAACGCTTCCTCTTTGTCTGGTATTACC		68		
Query	70	GGGTTTATGATATTCCACCTAAGTTCTTTTACACAAGAAAACCTCTTGGGGTAAGTATAA		129		
Sbjct	69	GGGTTTATGATATTCCACCTAAGTTCTTTTACACAAGAAAACCTCTTGGGGTAAGTATAA		128		
Query	130	AITCCATCCCATGCAATATTGGCT	153			
Sbjct	129	AITCCATCCCATGCAATATTGGCT	152			

Alignment of exon 3

Sequence ID: lcl|Query_139153 Length: 183 Number of Matches: 1

Range 1: 10 to 182 Graphics					Next Match	Previous Match
Score	Expect	Identities	Gaps	Strand		
320 bits(173)	9e-93	173/173(100%)	0/173(0%)	Plus/Plus		
Query	8	CTCCTTTCCGCCCTTCTAGTCAGCACTGGCACTGGCCAGGGCCCTGCAGCCTGCCTGA		67		
Sbjct	10	CTCCTTTCCGCCCTTCTAGTCAGCACTGGCACTGGCCAGGGCCCTGCAGCCTGCCTGA		69		
Query	68	ATTTCAACTGCAIGCTGATTCTCTTGCCAGTCTGTGAAATCTGCTGTCCTTCCTCAGGG		127		
Sbjct	70	ATTTCAACTGCAIGCTGATTCTCTTGCCAGTCTGTGAAATCTGCTGTCCTTCCTCAGGG		129		
Query	128	GTTCAGTGGGTAAGAGAAAATGTTTTACTAAGTTCCTCTAATTTTCAAAGG	180			
Sbjct	130	GTTCAGTGGGTAAGAGAAAATGTTTTACTAAGTTCCTCTAATTTTCAAAGG	182			

Alignment of exon 5

Sequence ID: lcl|Query_62697 Length: 217 Number of Matches: 1

Range 1: 10 to 215 Graphics					Next Match	Previous Match
Score	Expect	Identities	Gaps	Strand		
375 bits(203)	3e-109	205/206(99%)	0/206(0%)	Plus/Plus		
Query	11	TTTTAGCGATTACACCAATTGCACATCTATTTAATGTGGAATGGTGTGTAATGCCCGAG		70		
Sbjct	10	TTTTAGCGATTACACCAATTGCACATCTATTTAATGTGGAATGGTGTGTAATGCCCGAG		69		
Query	71	TCAATAATTCTGATCCTTATTTCAGTAGCACTCTGAACTTGGAGACAGGCAAAAATGAAA		130		
Sbjct	70	TCAATAATTCTGATCCTTATTTCAGTAGCACTCTGAACTTGGAGACAGGCAAAAATGAAA		129		
Query	131	GTTATCTCAATTTTGTCTGAAAGAGAATAAAGGTAAGCCTCTCATTATCTGACTTAGATA		190		
Sbjct	130	GTTATCTCAATTTTGTCTGAAAGAGAATAAAGGTAAGCCTCTCATTATCTGACTTAGATA		189		
Query	191	TTCTTAGGCCATTACAATTGAGGAC	216			
Sbjct	190	TTCTTAGGCCATTACAATTGAGGAC	215			

Alignment of exon 7

Sequence ID: lcl|Query_41981 Length: 152 Number of Matches: 1

Range 1: 9 to 152 Graphics		Next Match	Previous Match	
Score	Expect	Identities	Gaps	Strand
267 bits(144)	9e-77	144/144(100%)	0/144(0%)	Plus/Plus
Query 10	TTCIGTTTGTGCAGCTGGTTTGGCTGGGGTTGAACGCTTCCTCTTTGTCTGGTATTACC	69		
Sbjct 9	TTCIGTTTGTGCAGCTGGTTTGGCTGGGGTTGAACGCTTCCTCTTTGTCTGGTATTACC	68		
Query 70	GGGTTTATGATATTCCACCTAAGTTCTTTTACACAAGAAAACCTTCTGGGGTAAGTATAA	129		
Sbjct 69	GGGTTTATGATATTCCACCTAAGTTCTTTTACACAAGAAAACCTTCTGGGGTAAGTATAA	128		
Query 130	ATTCCATCCCATGCAATATTGGCT	153		
Sbjct 129	ATTCCATCCCATGCAATATTGGCT	152		

Alignment of exon 10

Sequence ID: lcl|Query_220137 Length: 210 Number of Matches: 1

Range 1: 4 to 210 Graphics		Next Match	Previous Match	
Score	Expect	Identities	Gaps	Strand
372 bits(201)	3e-108	205/207(99%)	0/207(0%)	Plus/Plus
Query 5	TTTTCAITAGGATAGCGGTTGATGGGCCCTTTGGCACTGCCAGTGAAGATGTGTTTCAGCT	64		
Sbjct 4	TTTTCTTCGGATAGCGGTTGATGGGCCCTTTGGCACTGCCAGTGAAGATGTGTTTCAGCT	63		
Query 65	ATGAGGTGGTGAATGTTAGTGGGAGCAGGGATTGGGGTCACACCCTTCGCATCCATTCTCA	124		
Sbjct 64	ATGAGGTGGTGAATGTTAGTGGGAGCAGGGATTGGGGTCACACCCTTCGCATCCATTCTCA	123		
Query 125	AGTCAGTCTGGTACAAATATTGCAATAACGCCACCAATCTGAAGCTCAAAAAGGTAAGTC	184		
Sbjct 124	AGTCAGTCTGGTACAAATATTGCAATAACGCCACCAATCTGAAGCTCAAAAAGGTAAGTC	183		
Query 185	CTTTCATTTATCGGAGGGCCTTAGAGA	211		
Sbjct 184	CTTTCATTTATCGGAGGGCCTTAGAGA	210		

Patient 12:

Alignment of exon 2

Sequence ID: Icl|Query_19627 Length: 152 Number of Matches: 1

Range 1: 9 to 151 Graphics		Next Match	Previous Match	
Score	Expect	Identities	Gaps	Strand
265 bits(143)	3e-76	143/143(100%)	0/143(0%)	Plus/Plus
Query 7	TTCTGTTTGTGCAGCTGGTTTGGCTGGGGTTGAACGCTTCCTCTTTGTCTGGTATTACC	66		
Sbjct 9	TTCTGTTTGTGCAGCTGGTTTGGCTGGGGTTGAACGCTTCCTCTTTGTCTGGTATTACC	68		
Query 67	GGGTTTATGATATTCCACCTAAGTTCTTTTACACAAGAAAACCTCTTGGGGTAAGTATAA	126		
Sbjct 69	GGGTTTATGATATTCCACCTAAGTTCTTTTACACAAGAAAACCTCTTGGGGTAAGTATAA	128		
Query 127	ATTCCATCCCATGCAATATTGGC	149		
Sbjct 129	ATTCCATCCCATGCAATATTGGC	151		

Alignment of exon 3

Sequence ID: Icl|Query_215485 Length: 183 Number of Matches: 1

Range 1: 14 to 182 Graphics		Next Match	Previous Match	
Score	Expect	Identities	Gaps	Strand
313 bits(169)	2e-90	169/169(100%)	0/169(0%)	Plus/Plus
Query 10	TTTCCGCCTCTTCTAGTCAGCACTGGCACTGGCCAGGGCCCTGCAGCCTGCCTGAATTT	69		
Sbjct 14	TTTCCGCCTCTTCTAGTCAGCACTGGCACTGGCCAGGGCCCTGCAGCCTGCCTGAATTT	73		
Query 70	CAACTGCATGCTGATTCTCTTGCCAGICTGTCGAAAICTGCTGTCTTCTCAGGGGTTT	129		
Sbjct 74	CAACTGCATGCTGATTCTCTTGCCAGICTGTCGAAAICTGCTGTCTTCTCAGGGGTTT	133		
Query 130	CAGTGCGGTAAGAGAAAATGTTTTACTAAGTTCCTCTAATTTCAAAGG	178		
Sbjct 134	CAGTGCGGTAAGAGAAAATGTTTTACTAAGTTCCTCTAATTTCAAAGG	182		

Alignment of exon 5

Sequence ID: Icl|Query_20127 Length: 217 Number of Matches: 1

Range 1: 10 to 215 Graphics		Next Match	Previous Match	
Score	Expect	Identities	Gaps	Strand
368 bits(199)	5e-107	204/206(99%)	1/206(0%)	Plus/Plus
Query 6	TTTTCGCGATTTCACACCATTTGACATCTATTTAATGTGGAATGGTGTGTGAATGCCCGAG	64		
Sbjct 10	TTTTCGCGATTTCACACCATTTGACATCTATTTAATGTGGAATGGTGTGTGAATGCCCGAG	69		
Query 65	TCAATAATTCTGATCCTTATTTCAGTAGCACTCTCTGAACTTGGAGACAGGCAAAAATGAAA	124		
Sbjct 70	TCAATAATTCTGATCCTTATTTCAGTAGCACTCTCTGAACTTGGAGACAGGCAAAAATGAAA	129		
Query 125	GTTATCTCAATTTTGCTCGAAAAGAGAATAAAGGTAAGCCTCTCATTATCTGACTTAGATA	184		
Sbjct 130	GTTATCTCAATTTTGCTCGAAAAGAGAATAAAGGTAAGCCTCTCATTATCTGACTTAGATA	189		
Query 185	TTCTCTAGGCCATTACAATTGAGGAC	210		
Sbjct 190	TTCTCTAGGCCATTACAATTGAGGAC	215		

Alignment of exon 7

Sequence ID: Icl|Query_8281 Length: 193 Number of Matches: 1

Range 1: 1 to 193 Graphics		Next Match	Previous Match	
Score	Expect	Identities	Gaps	Strand
335 bits(181)	4e-97	190/194(98%)	1/194(0%)	Plus/Plus
Query 1	AtttttttCCCCCAGGAACGAATTGTACGTGGGCAGACCGCAGAGAGTTTGGCTGTGCA			60
Sbjct 1	ATTTTTTT-ICCCCAACAACGAATTGTACGTGGGCAGACCGCAGAGAGTTTGGCTGTGCA			59
Query 61	TAATATAACAGTTTGTGAACAAAAATCTCAGAATGGGGAAAAATAAAGGAATGCCCAAT			120
Sbjct 60	TAATATAACAGTTTGTGAACAAAAATCTCAGAATGGGGAAAAATAAAGGAATGCCCAAT			119
Query 121	CCCTCAGTTTGTCTGGAAACCCCTCCTATGGTAIGTACAATTCATTGTTGTTATTACAGTTT			180
Sbjct 120	CCCTCAGTTTGTCTGGAAACCCCTCCTATGGTAIGTACAATTCATTGTTGTTATTACAGTTT			179
Query 181	CATTACTGACAAAA	194		
Sbjct 180	CATTACTGACAAAA	193		

Alignment of exon 10

Sequence ID: Icl|Query_19479 Length: 210 Number of Matches: 1

Range 1: 3 to 210 Graphics		Next Match	Previous Match	
Score	Expect	Identities	Gaps	Strand
375 bits(203)	3e-109	208/210(99%)	2/210(0%)	Plus/Plus
Query 3	TTTTTCCATT CAGGATAGCGGTTGATGGGCCCTTTGGCAC TGCCAGTGAAGATGTGTTCA			62
Sbjct 3	TTTTTCC-TTC-GGATAGCGGTTGATGGGCCCTTTGGCAC TGCCAGTGAAGATGTGTTCA			60
Query 63	GCTATGAGGTGGTGAIGTTAGTGGGAGCAGGGATTGGGGTCACACCCTTCGCATCCATT			122
Sbjct 61	GCTATGAGGTGGTGAIGTTAGTGGGAGCAGGGATTGGGGTCACACCCTTCGCATCCATT			120
Query 123	TCAAGTCAGTCTGGTACAAATATTGCAATAACGCCACCAATCTGAAGCTCAAAAAGGTAA			182
Sbjct 121	TCAAGTCAGTCTGGTACAAATATTGCAATAACGCCACCAATCTGAAGCTCAAAAAGGTAA			180
Query 183	GTCCTTTCATTATCGGAGGGCCTTAGAGA	212		
Sbjct 181	GTCCTTTCATTATCGGAGGGCCTTAGAGA	210		

Patient 13:

Alignment of exon 2

Sequence ID: lcl|Query_92405 Length: 152 Number of Matches: 1

Range 1: 3 to 152		Graphics			Next Match	Previous Match
Score	Expect	Identities	Gaps	Strand		
272 bits(147)	2e-78	150/151(99%)	1/151(0%)	Plus/Plus		
Query	1	ATAAATAATTCGTGTTTGTGCAGCTGGTTTGGCTGGGGTTGAACGCTTCCTCTTTGCTGG			60	
Sbjct	3	ATAAA-AITCTGTTTGTGCAGCTGGTTTGGCTGGGGTTGAACGCTTCCTCTTTGCTGG			61	
Query	61	TATTACCGGGTTTATGATATCCACCTAAGTCTTTTACACAAGAAAACCTCTTGGGGTA			120	
Sbjct	62	TATTACCGGGTTTATGATATCCACCTAAGTCTTTTACACAAGAAAACCTCTTGGGGTA			121	
Query	121	AGTATAAATCCATCCCATGCAATATTGGCT	151			
Sbjct	122	AGTATAAATCCATCCCATGCAATATTGGCT	152			

Alignment of exon 3

Sequence ID: lcl|Query_208189 Length: 183 Number of Matches: 1

Range 1: 10 to 183		Graphics			Next Match	Previous Match
Score	Expect	Identities	Gaps	Strand		
322 bits(174)	3e-93	174/174(100%)	0/174(0%)	Plus/Plus		
Query	9	CTCCTTTCGGCCTCTTCTAGTCAGCACTGGCACTGGCCAGGGCCCTGCAGCCTGCCTGA			68	
Sbjct	10	CTCCTTTCGGCCTCTTCTAGTCAGCACTGGCACTGGCCAGGGCCCTGCAGCCTGCCTGA			69	
Query	69	ATTCAACTGCAIGCTGATTCTCTTGCCAGTCTGTGAAATCTGCTGTCCTTCTCAGGG			128	
Sbjct	70	ATTCAACTGCAIGCTGATTCTCTTGCCAGTCTGTGAAATCTGCTGTCCTTCTCAGGG			129	
Query	129	GTTCCAGTGCGGTAAGAGAAAATGTTTTACTAAGTTCCTCTAATTTTCAAAGGC	182			
Sbjct	130	GTTCCAGTGCGGTAAGAGAAAATGTTTTACTAAGTTCCTCTAATTTTCAAAGGC	183			

Alignment of exon 5

Sequence ID: lcl|Query_5029 Length: 217 Number of Matches: 1

Range 1: 3 to 215		Graphics			Next Match	Previous Match
Score	Expect	Identities	Gaps	Strand		
381 bits(206)	6e-111	211/213(99%)	1/213(0%)	Plus/Plus		
Query	2	CCTGTC-ITTTTCGCGATTACACCATTGCACATCTATTTAATGTGGAATGGTGTGTAAT			60	
Sbjct	3	CCTTTCGTTTTCGCGATTACACCATTGCACATCTATTTAATGTGGAATGGTGTGTAAT			62	
Query	61	GCCCGAGTCAATAAATTCTGATCCTTATTAGTACACTCTCTGAACTGGAGACAGGCAA			120	
Sbjct	63	GCCCGAGTCAATAAATTCTGATCCTTATTAGTACACTCTCTGAACTGGAGACAGGCAA			122	
Query	121	AAITGAAAGTTATCTCAATTTTGTCTCGAAGAGAATAAAGGTAAGCCCTCTCATTATCTGAC			180	
Sbjct	123	AAITGAAAGTTATCTCAATTTTGTCTCGAAGAGAATAAAGGTAAGCCCTCTCATTATCTGAC			182	
Query	181	TTAGATATTCTCTAGGCCATTACAATTGAGGAC	213			
Sbjct	183	TTAGATATTCTCTAGGCCATTACAATTGAGGAC	215			

Alignment of exon 7

Sequence ID: lcl|Query_48923 Length: 193 Number of Matches: 1

Range 1: 2 to 193		Graphics			Next Match	Previous Match
Score	Expect	Identities	Gaps	Strand		
329 bits(178)	2e-95	190/195(97%)	3/195(1%)	Plus/Plus		
Query	2	ttttttttAACCCAAGAACGAAATTTGTACGTGGGCAGACCGCAGAGAGTTTGGCTGTGC			61	
Sbjct	2	TTTTTTTT-CCCCAACACG-AA-TTGTACGTGGGCAGACCGCAGAGAGTTTGGCTGTGC			58	
Query	62	ATAATATAACAGTTTGTGAACAAAAATCTCAGAATGGGGAAAAATAAAGGAATGCCCAA			121	
Sbjct	59	ATAATATAACAGTTTGTGAACAAAAATCTCAGAATGGGGAAAAATAAAGGAATGCCCAA			118	
Query	122	TCCCTCAGTTTGTCTGGAAACCTCCTATGGTATGTACAATTCATTGTTGTTATTACAGTT			181	
Sbjct	119	TCCCTCAGTTTGTCTGGAAACCTCCTATGGTATGTACAATTCATTGTTGTTATTACAGTT			178	
Query	182	TCATTACTGACAAAA			196	
Sbjct	179	TCATTACTGACAAAA			193	

Alignment of exon 10

Sequence ID: lcl|Query_47107 Length: 210 Number of Matches: 1

Range 1: 15 to 210		Graphics			Next Match	Previous Match
Score	Expect	Identities	Gaps	Strand		
363 bits(196)	2e-105	196/196(100%)	0/196(0%)	Plus/Plus		
Query	21	ATAGCGGTTGATGGGCCCTTTGGCACTGCCAGTGAAGATGTGTTTCAGCTATGAGGTGGTG			80	
Sbjct	15	ATAGCGGTTGATGGGCCCTTTGGCACTGCCAGTGAAGATGTGTTTCAGCTATGAGGTGGTG			74	
Query	81	ATGTTAGTGGGAGCAGGGATTGGGGTCACACCCTTCGCATCCATTCTCAAGTCAGTCTGG			140	
Sbjct	75	ATGTTAGTGGGAGCAGGGATTGGGGTCACACCCTTCGCATCCATTCTCAAGTCAGTCTGG			134	
Query	141	TACAAATATTGCAATAACGCCACCAATCTGAAGCTCAAAAAGGTAAGTCCTTTCATTAT			200	
Sbjct	135	TACAAATATTGCAATAACGCCACCAATCTGAAGCTCAAAAAGGTAAGTCCTTTCATTAT			194	
Query	201	CGGAGGGCCTTAGAGA			216	
Sbjct	195	CGGAGGGCCTTAGAGA			210	

4. Discussion

CGD was first described in 1957 independently by (Berendes et al., 1957) and by Landing and Shirkey (Landing et al., 1957) as a lethal disease in males associated with increased susceptibility to infection and pigment containing macrophages in the visceral organs (Baehner & Nathan, 1968; Epling et al., 1992). CGD results from the inability of neutrophils to complete the first step of the respiratory burst pathway, generation of superoxide, with the downstream consequence of impaired microbe killing. CGD leads to recurrent and potentially lethal infections. Pneumonia is the most common infection before diagnosis (47%) (Martire et al., 2008) and occurs in the majority (79%) of patients within four years of diagnosis (Winkelstein et al., 2000) Lymphadenitis is the second most common infection before diagnosis (45%) (Martire et al., 2008) and subcutaneous abscess is the second most common infection that occurs within 4 years of diagnosis (43%) Other presenting infections include osteomyelitis, liver and perirectal abscesses, enteritis, and septicemia (Martire et al., 2008), CGD can, in very rare circumstances, present with ascites (Castro et al., 1992).

In Libya CGD is characterized by severe symptoms, where by reticuloendothelial, cutaneous and respiratory manifestations are the most prevalent symptoms (Matoug et al., 2014)

Despite all of this, there is no Libyan study that represents chronic granulomatous disease from molecular genetics view.

The first component in the care of the CGD patient is early diagnosis. CGD should be suspected in patients with recurrent or unusually severe infections, such as liver abscess caused by *S. aureus*. In addition, specific opportunistic infections should prompt an evaluation for CGD; these include invasive mould diseases (e.g., aspergillosis), and infections by *B. cepacia*, *S. marcescens*, and *Nocardia* species in the absence of a known immunodeficiency. Inflammatory disorders such as inflammatory bowel disease at an early age and granulomatous cystitis can be manifestations of CGD. A family history of males with severe or unusual infections can be a clue to the diagnosis of X-linked CGD, while consanguineous parents increase the risk for autosomal recessive disorders (Segal et al., 2011).

Differential diagnosis of CGD from other disorders associated with granuloma formation and hyperinflammation such as cystic fibrosis, hyper IgE syndrome, Crohn's disease, allergic bronchopulmonary aspergillosis, and glucose 6-phosphate dehydrogenase deficiency (www. Prevention Genetics.com) is based on respiratory burst measurement manifested in oxygen consumption, superoxide (O_2^-) generation in the nitro blue tetrazolium test (NBT), or hydrogen peroxide production (Jurkowska et al., 2004, A).

In the 1960s and 1970s, defective NADPH oxidase was found to be the cause of CGD, leading to the development of the nitro blue tetrazolium (NBT) test for its diagnosis (Baehner & Nathan, 1968; Epling et al., 1992)., a few decades later, the (DHR) was developed as a more quantitative measure of oxidative burst and it is now the preferred test for CGD (Epling et al., 1992). In addition genetic testing can aid in the differential diagnosis of CGD ([http://: www.Prevention Genetics. com](http://www.PreventionGenetics.com)).

Treatment should be started immediately after CGD has been definitely diagnosed, or even before. This involves determination of the exact complicating infections and selection of

the most appropriate antibiotic or anti-fungal therapy. Surgical drainage of infected lymph nodes and abscesses involving the liver, skin, rectum, kidney and brain is often necessary for healing, particularly for the visceral abscesses. Daily prophylaxis with Bactrim and/or Itraconazole is recommended during infection-free periods (Roos & Boer, 2014).

In the present study we included fourteen (14) patients who were admitted to the immunology unit at the Pediatric Hospital of Benghazi. Their ages range from 2 months to 13 years, and for most of them the symptoms started in the first 3 months of age. Nine (9) out of the fourteen (14) patients had positive **NBT** test and hence, confirmed as CGD patients, while the rest were diagnosed clinically as suspected CGD. Ten (10) out of the fourteen (14) patients came from consanguineous marriage (their parents were relatives), and seven (7) out of the fourteen (14) had positive CGD family history.

The results of the laboratory investigations showed that, all patients were anemic; their mean **Hb** was 9.9 g/dl and they had high **ESR** and **CRP** values, their means were 37mm/hr. and 41.2 mg/l respectively and this indicated the presence of infection and inflammation. Five out of seven of patients had **WBC** values $> 10 \times 10^3/\mu\text{l}$ and two of the rest of the patients had normal values, and 2 of another 5 patients had **RBC** values $> 5.2 \times 10^6/\mu\text{l}$, whereas 2 of another 6 patients had **PLT** values $> 400 \times 10^3/\mu\text{l}$. In addition 4 of another 6 patients had **ESR** values $> 8\text{mm/hr}$, and 3 of 4 patients had **Neutrophile** values $> 7.5 \times 10^9/\text{L}$. While most patients had **Albumin** value within the normal range 6 patients had **Globulin** values higher than normal, and 5 patients had **Lymphocyte** values $> 3.5 \times 10^9/\text{L}$, and 2 patients had **T. Lymphocyte** > 2540 , (Tables: 3.1; 3.2).

For the different types of immunoglobulins 2 out of 4 patients had **IgA** values $> 100 \text{ mg/dl}$; one patient had **IgA** value $< 20 \text{ mg/dl}$ and another had normal value; 4 patients had **IgE** value $< 295 \text{ KIU/L}$, and 3 out of 4 patients had **IgG** value $> 1411 \text{ mg/dl}$, whereas one patient had **IgG** value $< 700 \text{ mg/dl}$. Three out of 5 patients had **IgM** values $> 200 \text{ mg/dl}$ (Tables: 3.3).

The estimated total protein (TP) showed that 1 out of 7 patients had **T.P** value $> 8.3 \text{ g/dl}$, whereas 7 out of 11 of patients had **AST** values $> 38 \text{ U/L}$, and 5 out of 11 patients had **ALT** values $> 41 \text{ U/L}$, and 4 patients had **Alkaline Phosphatase** value $> 129 \text{ U/L}$, and most patients had normal **Urea** and **Creatinine** values (Tables: 3.4).

The aim of our study was to obtain DNA samples from CGD patients that were extracted for high purity and concentration. The DNA purity was measured by two methods the first one was by measuring the absorbance of sample by **spectrophotometer** and obtaining the A260/A280 ratio of all samples, which was greater than 1.8 (Table: 3.5). The second method was by separating the DNA samples using **agarose gel (gel electrophoresis)** and comparing the bands with the running marker (Figure: 3.1). Both methods indicated that the DNA samples had good purity and concentration.

Following DNA extraction the samples were subjected to polymerase chain reaction (**PCR gradient thermal cycler TC-5000**) for amplification of the desired exons for the genes of interest (**NCF1, CYBB**). After amplification of exon 2 in **NCF1** gene by using the primers (F: 2LB2 and R: 2RB2) and (F: il-3'f and R: 2RB2) where the 2LB2 primer covered the GTGT sequence at the start of exon 2, and il-3' F primer started at intron 2. The samples were loaded on the agarose gel (Figures: 3.2; 3.3) to ensure the size of the amplified fragment was as desired by comparing the amplified fragment of samples to loaded marker

with known size. The sizes of fragments were about 200bp and 300bp, respectively to primers used.

The PCR samples were purified using **QIAquick PCR Purification Kit** for elimination of the extra primers, nucleotides, polymerases, and salts from the DNA samples. The samples were loaded again on the agarose gel and compared with a marker to ensure the size of samples (Figures: 3.4; 3.5).

For the *CYBB* gene the samples were subjected to sequencing (exons 2, 3, 5, 7, 10) by **3130 Genetic analyzer using the Big dye sequencing kit (Applied Biosystems, USA)** to detect any mutations as a result no mutations were detected using the fore mentioned sequencing primer.

To ensure that, there were no mutations on five exons of the *CYBB* gene we had used the **Blast Alignment tool**, which is a search tool that uploads the query sequence and allows retrieving a DNA query after searching the relevant DNA databases for levels of identity. We had compared the DNA samples with the DNA of control sample and with the database DNA at Gene Bank. The alignment result proved that there were no mutations detected in the five exons of the *CYBB* gene.

Mutations in exon 2 that was known to carry the most common mutation a Δ GT deletion in *NCF1* gene was analyzed by **RT-PCR using the High-resolution melting analysis** that is based on analysis of DNA melting. The curves of patients' samples were compared with the control recruits' samples. (Figure: 3.6) shows the primer **il-3' F** that starts at intron 2, and (Figure: 3.7) shows the forward primers (**2LB2**) and the primer covering the **GTGT** sequence at the start of exon 2, and the reverse primer (**2RB2**), which was the same in both reactions. Using these primers no mutations were detected where the samples of patients and controls had the same melting curves.

Cases of CGD have been associated with defects in genes encoding 4 of the 6 NADPH oxidase subunits, named with reference to their molecular mass (kd) and "phox" for phagocyte oxidase. Flavocytochrome **b558**, the redox center of NADPH oxidase is composed of **gp91phox** and **p22phox**. Defects in the X-linked gene encoding gp91 (*CYBB*) account for about 70% of known mutations causing CGD, whereas autosomal recessive p22phox mutations (*CYBA* gene on chromosome 16) account for an additional 5%, P47-phox (*NCF1* gene on chromosome 7) and p67phox (*NCF2* gene on chromosome) are both regulatory proteins that have been associated with autosomal recessive defects of about 20% and 5% of cases, respectively) (Martire et al., 2008; Winkelstein et al., 2000; Casimir et al., 1992; Morel et al., 2007).

A mutation in any of these genes can cause CGD. If the mutation leaves some residual NADPH oxidase activity intact, the clinical expression of the disease is less serious (Köker et al., 2013) and the chance of survival of the patient is higher than in the case of total oxidase deficiency (Kuhns et al., 2010). This depends upon the mutated gene, the type of mutation and the position of the mutation within the gene. In general, mutations in *NCF1* lead to a milder form of CGD (later presentation, milder clinical expression, better chance of survival) than mutations in any of the other genes. For genetic counseling and prenatal diagnosis, mutation analysis of the CGD genes is mandatory (Roos & Boer, 2014).

To screen the gene in question for mutations in a systematic way we reviewed the published work that recorded specific mutations in certain areas or countries. The site of mutation varied and hence we designed our primers to screen hot gene spots for mutations. For instance, **Martin de Boer, et al. (1992)** studied the molecular defect in four patients with X-linked CGD in the US, and in the fifth they studied the family to find that the mother of the patient had an X-linked CGD mutation who had died before their investigation. Complimentary-DNA and the coding region was amplified by PCR into three fragments. Sequence analysis showed the absence of exon 7, 5, 3, and 2 sequences in patients 1, 2, 3, and 4, respectively. In carrier 5, they found both normal cDNA and cDNA that lacked 57 –nucleotides at the 3'-end of exon 6. They analyzed the splice sites of the flanking introns of the missing exons. In patients 1, 2, and 3 they found single nucleotide substitution within the first five positions of the downstream 5'-end donor splice sites. In patient 4, similar substitution was found at position -1 of the 3'-end acceptor splice site of intron 1. In carrier 5, a single substitution was observed in exon 6 (C → A at nucleotide 633) that created a new donor splice site; mRNA splicing occurs at this newly created splice site. They concluded that the absence of the exon sequences in gp91-phox mRNA of these patients were due to splicing errors. Other research teams such as **Rae et al. (1998)** identified the mutations in the *CYBB* gene responsible for X-linked CGD in 131 consecutive independent kindred. They used SSCP analysis for screening and identified mutations in 124 of the kindred. Through sequencing of all exons and intron boundary regions they revealed the other seven mutations. They were able to detect 103 different specific mutations; no single mutation appeared in more than seven independent kindred. The types of mutations included large and small deletions (11%), frameshifts (24%), nonsense mutations (23%), missense mutations (23%), splice-region mutations (17%), and regulatory-region mutations (2%). The distribution of mutations within the *CYBB* gene exhibited great heterogeneity with no apparent mutational hot spots. Evaluation of 87 available mothers revealed X-linked carrier status in all but 10 cases. They concluded that the heterogeneity of mutations and the lack of any predominant genotype indicate that the disease represents many different mutational events, without a founder effect as is expected for a disorder with a previously lethal phenotype.

In a study conducted in Latin American (Agudelo-Flo'rez et al., 2006), which included 14 patients selected on basis of case history of recurrent severe infections, impaired respiratory burst. They demonstrated an underlying mutation by single strand conformation polymorphism (SSCP) or RT-PCR analysis, followed by genomic DNA or cDNA sequencing. Seven unrelated patients were found to have the X-linked form of CGD (X-CGD). Heterogeneous mutations affected the *CYBB* gene (two insertions, one substitution, and four splice site defects). Seven patients presented with one of the autosomal recessive forms of CGD (A47-CGD); all had the most common mutation, a Δ GT deletion in exon 2 of the *NCF1* gene. They Concluded that X-CGD patients from Latin America showed a high degree of molecular heterogeneity, including two novel mutations (an insertion C.1267- 1268 ins A in exon 10 leading to a frameshift mutation and 1164 –2 A > G substitution in intron 9). Their clinical characteristics included early onset of infections (before age of 2 years) and eventual obstructive granulomas. A47-CGD represented 50% of the reported cases, a higher prevalence than reported in other reports.

In a molecular genetics analysis by **Noack et al. (2001)** carried on 50 patients with confirmed (or suspected) A470 CGD revealed that most patients (44) were homozygous

for the GT deletion at the beginning of exon 2 and exhibited only the pseudogene sequence. The remaining 6 patients showed normal sequence and pseudogene sequence at this position, indicating that they differed from the prevalent genotype.

In Iran, Rezvani et al. (2005) reported a mutation in *CYBB* gene in a patient with X-CGD diagnosed on the base of family history, NBT test, DHR 123 assay. This mutation in the *CYBB* gene was detected using SSCP analysis (single-strand conformation polymorphism) followed by sequencing. They observed an 880 C→ T in exon 8 of *CYBB* gene. This mutation resulted in 290 Arginine to Stop codon TGA. They also observed a change (270 C → A) in the promoter region.

In a Tunisian study, El kares et al. (2006) carried a genetic investigation revealing defects underlying CGD in 15 Tunisian patients from 14 unrelated families. Haplotype analyses and homozygosity mapping with microsatellite markers around known CGD genes assigned the genetic defect to *NCF1* in four patients, to *NCF2* in four patients and to *CYBA* in two patients. However, in one family they were unable to link two CGD patients' genetic defect to any known AR-CGD genes. Mutation screening identified two novel mutations in *NCF2* (an A > T single nucleotide substitution occurring at nucleotide 78 of exon 14, which resulted in an amino acid change from asparagines to isoleucine at codon 419), and *CYBA* (a 7-bp deletion (295-301delGTGCCCG) in exon 5 of *CYBA* that resulted in a shift of the reading frame to premature termination). In addition to the recurrent mutation, ΔGT, in *NCF1* and a splice site mutation reported in North African patients.

Vilaiphan et al. (2007) analyzed samples from two unrelated Thai boys, presented with severe persistent pulmonary infections at the age of two months. Their abnormal dihydrorhodamine (DHR) flow cytometry assays supported the diagnosis of X-CGD. Mutation analysis was performed by PCR, and amplification and sequencing of the entire coding regions of *CYBB*. Mutations identified were confirmed by restriction enzyme analyses. PCR-sequencing of the entire coding regions of *CYBB* identified nonsense mutations, 271C>T in exon 4 and 456T> A in exon 5, in probands of each family. Both of the patients' mothers were found to be carriers.

Voraphani et al. (2009) investigated the clinical and molecular characteristics of two unrelated Thai patients with AR-CGD. The patients' DHR assays revealed abnormalities in both patients, but normal results in their mothers, consistent with the diagnosis of AR-CGD. PCR-sequencing of the entire coding regions of *NCF1*, *NCF2*, and *CYBA* was performed and showed a homozygous (delGT) mutation at the beginning of exon 2 of *NCF1* in both patients. This mutation resulted in a frameshift with premature termination of p47-phox at codon 51. They concluded that the homozygous GT deletion in *NCF1* may be a common mutation in Thai patients with AR-CGD.

European experience publication by van den Berg et al. (2009) in which the clinical data were collected and analyzed from 429 patients showed that 351 patients were males and 78 were females. X-linked (XL) CGD (gp91phox deficient) accounted for 67% of these cases, whereas autosomal recessive (AR) inheritance accounted for 33%. AR-CGD was diagnosed later in life, and the mean survival time was significantly better in AR patients

(49.6 years) than in XL CGD (37.8 years), suggesting a milder disease course in AR patients.

In a study carried by (Hill et al., 2010) high-resolution melting q-PCR analysis was applied to X-linked chronic granulomatous disease, melting curves of the 13 PCR products bracketing *CYBB* exons were predicted by Poland's algorithm and compared with observed curves from 96 normal individuals. Small point mutations or insertions/deletions were detected by mixing the hemizygous male DNA with normal male DNA to produce artificial heterozygotes, whereas detection of gross deletions was performed on unmixed samples. Eighteen validation samples and 22 clinical kindreds were analyzed for *CYBB* mutations. All blinded validation samples were correctly identified. Nineteen different mutations were found, including seven near intron-exon boundaries predicting splicing defects, five substitutions within exons, three small deletions predicting premature termination, and four gross deletions of multiple exons. Ten novel mutations were found, including two missense (730T>A, 134T>G), one nonsense (90C>A), four splice site defects (45-1G>T, 674-4A>G, 1461-2delT, and 1462-2A>C), two small deletions (636delT, 1661-1662delCT), and one gross deletion of exons 6 to 8.

In Turkey, (Koker et al., 2013) studied the correlation between clinical, functional, and genetic data from patients with CGD. They reported the data analysis of 89 patients with CGD from 73 Turkish families in a multicenter study. Most of the families (55%) had an AR genotype, and 38% had an X-linked genotype. Patients from 5 families with a suspected AR genotype (7%) were not fully characterized. They compared patients with CGD according to the severity of NADPH oxidase deficiency of neutrophils. Patients with A22⁰, A67⁰ or X91⁰ phenotypes with a stimulation index of 1.5 or less had early clinical presentation and younger age at diagnosis (mean, 3.2 years). However, in p47phox-deficient cases and in 5 other AR cases with high residual oxidase activity (stimulation index > 3) later and less severe clinical presentation and older age at diagnosis (mean, 7.1 years) were found. Pulmonary involvement was the most common clinical feature, followed by lymphadenitis and abscesses. They concluded that later and less severe clinical presentation and older age at diagnosis are related to the residual NADPH oxidase activity of neutrophils and not to the mode of inheritance. CGD caused by A22⁰ and A67⁰ subtypes were manifested as severe as the X910 subtype.

In Egyptian study, (Meshaal et al., 2015) included twenty male and nine female patients with different presentation. The consanguinity rate was 76% (19/25). The most common manifestations were abscesses in 79.3%, followed by pneumonia in 75.8% and gastrointestinal symptoms in 27.5%. Fatal but rare complications were reported among patients as one patient developed haemophagocytic lymphohistocytosis (HLH) syndrome. Although X linked-CGD universally constitutes the most common pattern of inheritance; only 6 of our patients 6/25 (24%) belonged to this group, and confirmed by carrier pattern of their mothers. Mothers were not available for testing in four male children. Nineteen patients (76%) had autosomal recessive patterns.

In Libya, (Matoug et al., 2014) included in his local study 35 patients (23 males, 12 females). All cases were diagnosed to have CGD between 2007 and 2013. Their diagnosis was based on clinical suspicion and confirmed by NBT. Where 94% of them had onset of the disease before the first year of life, 63% had positive family history and 60% of their

parents were relatives. Reticuloendothelial system was the most commonly involved system (94%) followed by skin (91.4%) and respiratory (83%). 91% had hepatosplenomegaly, 80% suffered from suppurative lymphadenitis, whereas liver abscess and spleen abscess were seen in 17% and 5.7% respectively. Skin abscesses were seen in three quarters, perianal abscesses and fistulas in one third, BCGitis (20%), granuloma (14%), tineacorporis (5.7%) and erythroderma in one patient. Pneumonia was the main respiratory problem (83%), aspergillosis was seen in 22.8%, bronchiectasis (14%) and pulmonary abscess in 5.7%. Anemia was the major hematological abnormality seen in Libyan CGD patients (83%) followed by hypergammaglobulinemia (62.8%), thrombocytosis (51.4%) and leukocytosis (45.7%). Gastrointestine problems were involved in 68.6% and oral findings were present in 48.6%. Osteomyelitis had occurred in 28.6%, meningitis in 5.7%, and sepsis in 45.7%. Forty two percent had failure to thrive. Despite aggressive antimicrobial therapy, 43% of our CGD patients died. Four patients underwent bone marrow transplantation, 3 were successful whereas one died due to chronic graft versus host rejection and died.

Another Libyan study by (Al-Bousafy et al., 2006): They presented a boy from Libya who had chronic lung disease following multiple severe pneumonia attacks. He also had recurrent episodes of fever, and later developed persistent cervical lymphadenitis and failure to gain weight. The final diagnosis by University Children's Hospital of Bonn and Charite Children's Hospital of Berlin (Germany) of chronic granulomatous disease a (NBT and DHR assay) was confirmed by molecular analysis, which revealed a defect in the p22-phox component of the CYBA gene.

The identification of the genetic defects in patients with CGD as for other genetic diseases is invaluable, and one can think of many justifications for that. Therefore, the disease-causing mutation should be determined in every CGD patient. This is necessary for undisputable proof of which gene is affected, and as such would help build the basis for genetic counseling. Carriers of the disease without clinical symptoms can only be diagnosed reliably by mutation analysis. In addition, in case of prenatal diagnosis or for gene therapy as treatment option in the family, this information must be available. For instance, when patients are transplanted with stem cells from a family member, it is imperative to know that this donor is not carrying the mutation (Roos & Boer et al., 2014). Some reports suggest that gene therapy may eventually be successful both in X-linked and autosomal CGD (Ott et al., 2006; Malech et al., 1997).

Gene therapy in combination with bone marrow conditioning can be successfully used to treat inherited diseases affecting the myeloid compartment such as in CGD (Ott et al., 2006).

In conclusion, in our study, based on the family pedigree (consanguinity of patients' parents) the mode of inheritance is most likely to be autosomal recessive in nature.

It is worthy to note that in our study the *CYBB* and *NCF1* genes that have the highest incidence worldwide showed no abnormalities in the sequenced hot spot of our patients' DNA, hence no mutations were detected in neither of them.

Depending on the results in this study and the report obtained from the **Metropolitan Hospital, Athens Greece, 2013**. The result of DHR in combination with the assessment of

the expression of the gp91 unit was negative in the child and normal in his mother, and the study of the oxidative capacity of the parental neutrophilic population presented low intensity in both parents without the presence of two distinct populations in the mother sample, excluded the possibility of X- linked CGD. In addition, in another report obtained from **Charite Hospiatl of Berlin (2003)** concerning another Libyan patient he was diagnosed as AR-CGD case carrying the p22 defect. Based on this information and our results we suspect that, the *CYBA* gene is the defected gene, (where gp22 is associated with gp91 in the cell membrane, which may reflect the severe symptoms on patients). Once we are able to continue our molecular analysis, we will study the *CYBA* gene using melting analysis and sequencing to proof our suspicion.

This study is the first one in Benghazi and Libya to study the molecular basis of chronic granulomatous disease to consider the genetic aspect. Furthermore, identifying the causative mutations of this disease should be a continued process that will go on beyond a master degree project, hence, and in collaborative manner we will continue the project until all occurring mutations are identified.

5. Conclusion:

- We designed this study to elucidate the basis of the molecular genetic defects of the chronic granulomatous disease (CGD) in Libyan patients in Benghazi. In addition to its early onset, his genetic disease has severe symptoms and terrible consequences if not diagnosed and managed.
- Previously, no genetic study was conducted on Libyan patients to find the type(s) of mutations responsible for the disease, therefore this is a first step to study and locate these mutations starting with the *CYBB* and *NCF1* genes, which constitute about 60% and 30% of cases wide world, respectively.
- Our results have indicated that no mutations were found in the studied exons (2, 3, 5, 7, 10 exons) of *CYBB* gene and exon 2 of *NCF1* gene.
- Depending on the family history and consanguinity of patients' parent we expect that the CGD found in Libyan patients is mostly caused by an autosomal recessive trait defect.
- Based on the DHR assay of patient No. 3, we recommend as a second step to screen the *CYBA* gene to detect the mutations in the CGD Libyan patients.
- Both p22^{phox} (encoded by *CYBA* gene) and gp91^{phox} (encoded by *CYBB* gene) represent the flavocytochrom b558, the redox center of NADPH oxidase. This may indicate the cause of the severe symptoms in our patients.
- As our study is the first study in Libya to uncover the genetic basis of this rare but important disease, we are hoping to introduce genetic screening and counseling for chronic granulomatous disease in Libya.

6. Reference:

- Agudelo-Flórez P, Prando-Andrade CC, López JA, et al. (2006), Chronic granulomatous disease in Latin American patients: clinical spectrum and molecular genetics. *Pediatr Blood Cancer*, 2006 Feb; 46(2):243-52.
- Al-Bousafy A., Al-Tubuly A., Dawi E., et al. (2006); Libyan Boy with Autosomal Recessive Trait (P22-phox Defect) of Chronic Granulomatous Disease. *Libyan J Med*. 1(2): 162–171.
- Ameratunga R., Woon ST., Vyas J., et al. (2010), Fulminant mulch pneumonitis in undiagnosed chronic granulomatous disease: a medical emergency. *Clin Pediatr (Phila)* 49:1143-6.
- Ammons MC, Siemsen DW, Nelson-Overton LK, et al. (2007), Binding of pleomorphic adenoma gene-like 2 to the tumor necrosis factor (TNF)-alpha-responsive region of the NCF2 promoter regulates p67(phox) expression and NADPH oxidase activity. *J Biol Chem* 282:17941–17952
- Antonell A, de Luis O, Domingo-Roura X, et al., (2005), Evolutionary mechanisms shaping the genomic structure of the Williams–Beuren syndrome chromosomal region at human 7q11.23. *Genome Res* 9:1179–1188
- Antonell A., De Luis O., Domingo-Roura X., et al., (2006), Evolutionary mechanisms shaping the genomic structure of the Williams–Beuren syndrome chromosomal region at human 7q11.23, *Genome Res*. 15, 1179–1188.
- Arroyo A., Modriansky M., Serinkan FB., et al., (2002), NADPH oxidase-dependent oxidation and externalization of phosphatidylserine during apoptosis in Me2SO-differentiated HL-60 cells. Role in phagocytic clearance, *J Biol Chem*. 277:49965-75.
- Babior B.M., (1999) NADPH oxidase: an update. *Blood* 93, 1464–1476.
- Babior B.M., (1984), Oxidants from phagocytes: agents of defense and destruction. *Blood*.64, 959–966.
- Babior B.M., (2004), NADPHoxidase. *Current OpinioninImmunology* 16:42–47.
- Babior, B.M., Kipnes, R. S., & Curnutte, J. T., (1973), Biological defense mechanisms., The production by leukocytes of superoxide, a potential bactericidal agent. *J Clin Invest* 52, 741–744.
- Baehner RL and Nathan DG., (1968), Quantitative nitro blue tetrazolium test in chronic granulomatous disease, *The New England Journal of Medicine*, vol. 278, no. 18, pp. 971–976.

- Bakri F, Martel C, El-Khateeb MS, et al., (2008), First report of chronic granulomatous disease in ten Jordanian families. *Eur J Clin Invest* 38(Suppl. 1):71
- Barese C.N., Goebel WS., Dinauer MC., (2004), Gene therapy for chronic granulomatous disease. *Expert Opin Biol Ther.*, 4:1423-1434.
- Baum C., von Kalle C., Staal FJ. et al., (2004), Chance or necessity Insertional mutagenesis in gene therapy and its consequences. *Mol Ther.* 9:5-13.
- Beckman JS., Beckman TW., Chen J., et al., (1990), Apparent hydroxyl radical production by peroxynitrite: implications for endothelial injury from nitric oxide and superoxide. *Proceedings of the National Academy of Science of USA* 87:1620–1624.
- Berendes H., Bridges R A., and Good R A. (1957), A fatal granulomatosis of childhood: the clinical study of a new syndrome, *Minnesota Medicine*, vol. 40, no. 5, pp. 309–312.
- Bhattacharya A., Slatter M., Curtis A. et al., (2003), Successful umbilical cord blood stem cell transplantation for chronic granulomatous disease. *Bone Marrow Transplant*, 31: 403-5.
- Biberstine-Kinkade KJ., DeLeo FR., Epstein RI., et al., (2001), Heme-ligating histidines in flavocytochrome b 558, *J. Biol. Chem.* 276, 31105–31112.
- Borgato L, Bonizzato A, Lunardi C, et al., (2001), A 1.1-kb duplication in the p67-phox gene causes chronic granulomatous disease. *Hum Genet* 108:504 – 510
- Brechar S. & Tschirhart EJ., (2008), Regulation of superoxide production in neutrophils: role of calcium influx. *J Leukoc Biol*, 84:1223-37.
- Brown KL., Bylund J., MacDonald KL., et al., (2008), ROS-deficient monocytes have aberrant gene expression that correlates with inflammatory disorders of chronic granulomatous disease. *Clin Immunol.*129:90-102.
- Carson MJ., Chadwick DL., Brubaker CA., et al., (1965), Thirteen boys with progressive septic granulomatous. *Pediatrics*, 35:405-12.
- Casimir C., Chetty M., Bohler MC. et al., (1992), Identification of the defective NADPH-oxidase component in chronic granulomatous disease: a study of 57 European families, *European Journal of Clinical Investigation*, vol. 22, no. 6, pp. 403–406.
- Casimir CM., Bu-Ghanin HN., Rodaway ARF., et al., (1991), Autosomal recessive chronic granulomatous disease caused by deletion at a dinucleotide repeat, *Proc. Natl. Acad. Sci. U. S. A.* 88, 2753–2757.
- Castro M., Balducci L., Ciuffetti C., et al., (1992), Ascites as an unusual manifestation of chronic granulomatous disease in childhood, *Pediatrica Medica e Chirurgica*, vol. 14, no. 3, pp. 317–319.

- Chanock SJ., El Benna J., Smith RM. et al., (1994), The respiratory burst oxidase. *J Biol. Chem.* 269, 24519–24522.
- Chanock SJ., Roesler J., Zhan S., et al., (2000), Genomic structure of the human p47-phox (NCF1) gene, *Blood Cells Mol. Dis.* 26, 37–46
- Chen Q., Powell DW., Rane MJ., et al., (2003), Akt phosphorylates p47phox and mediates respiratory burst activity in human neutrophils. *J. Immunol.* 170, 5302–5308
- Clancy RM., Leszczynska-Piziak J. and Abramson SB., (1992), Nitric oxide, an endothelial cell relaxation factor, inhibits neutrophil superoxide anion production via a direct action on the NADPH oxidase. *J. Clin. Invest.*, 90, 1116–11121.
- Cooper DN, Krawczak M., (1991), Mechanisms of insertional mutagenesis in human genes causing genetic disease. *Hum Genet* 87:409–415
- Cowen EW., Nguyen JC., Miller DD., et al., (2010), Chronic phototoxicity and aggressive squamous cell carcinoma of the skin in children and adults during treatment with voriconazole. *J Am Acad Dermatol*, 62: 31-7.
- Cross AR, Noack D, Rae J, et al., (2000, A) Hematologically Important Mutations: X-Linked Chronic Granulomatous Disease. *Blood Cells Mol Dis*; 26(5):561-5.
- Cross AR, Noack D, Rae J, Curnutte JT, Heyworth PG., (2000, B), Hematologically important mutations: the autosomal recessive forms of chronic granulomatous disease (first update). *Blood Cells Mol Dis* 26:561–565
- Cross AR., Jones OTG., Garcia R., et al., (1982), the association of FAD with the cytochrome b-245 of human neutrophils, *Biochem. J.* 208. 759 – 763.
- Cross AR., Segal AW., (2004), The NADPH oxidase of professional phagocytes-prototype of the NOX electron transport chain systems, *Biochim. Biophys. Acta.* 1657. 1 – 22.
- Dang PM., Fontayne A., Hakim J., et al., (2001), Protein kinase C ζ phosphorylates a subset of selective sites of the NADPH oxidase component p47phox and participates in formyl peptide-mediated neutrophil respiratory burst. *J. Immunol.* 166, 1206–1213
- De Boer M., Bolscher B.G., Dinauer M.C., et al., (1992), Splice Site Mutations Are a Common Cause of X-Linked Chronic Granulomatous Disease. *Blood journal* 80: 1553-1558.
- De Boer M, Singh V, Dekker J, et al., (2002), Prenatal diagnosis in two families with autosomal, p47 (phox)-deficient chronic granulomatous disease due to a novel point mutation in NCF1. *Prenat Diagn* 22:235–240
- De Mendez I., Homayounpour N. and Leto TL. (1997), Specificity of p47phox SH3 domain interactions in NADPH oxidase assembly and activation. *Mol. Cell. Biol.* 17, 2177–2185

- De Ravin SS., Naumann N., Cowen EW., et al., (2008), Chronic granulomatous disease as a risk factor for autoimmune disease. *J Allergy Clin Immunol* 122:1097-103.
- DeLeo FR., Nauseef WM., Jesaitis AJ., et al., (1995, A), A domain of p47phox that interacts with human neutrophil flavocytochrome b 558. *J. Biol. Chem.* 270, 26246–26251
- DeLeo FR., Yu L., Burritt JB., et al., (1995, B), Mapping sites of interaction of p47-phox and flavocytochrome b with random-sequence peptide phage display libraries. *Proc. Natl. Acad. Sci. U.S.A.* 92, 7110–7114
- Diatchuk V., Lotan O., Koshkin V., et al., (1997), Inhibition of NADPH oxidase activation by 4-(2- -aminoethyl)-benzenesulfonyl fluoride and related compounds. *J. Biol. Chem.*, 272, 13292–13301
- Dinauer M., (2003), The phagocyte system and disorders of granulopoiesis and granulocyte function. In: Nathan D, Orkin S, Ginsburg D, Look A, eds. Nathan and Oski's Hematology of Infancy and Childhood. Vol. 1 (ed 6th). Philadelphia: W.B. Saunders Company, 923-1010.
- Dinauer M., Gifford M., Pech N., et al., (2001), Variable correction of host defense following gene transfer and bone marrow transplantation in murine X-linked chronic granulomatous disease. *Blood.* 97:3738-3745.
- Dinauer MC, Pierce EA, Bruns GA, et al., (1990), Human neutrophil cytochrome b light chain (p22-phox). Gene structure, chromosomal location, and mutations in cytochrome- negative autosomal recessive chronic granulomatous disease. *J Clin Invest* 86:1729–1737
- Dinauer MC, Pierce EA, Erickson RW, et al., (1991), Point mutation in the cytoplasmic domain of the neutrophil p22-phox cytochrome b subunit is associated with a nonfunctional NADPH oxidase and chronic granulomatous disease. *Proc Natl Acad Sci USA* 88:11231–11235
- Dusi S. and Rossi F., (1993), Activation of NADPH oxidase of human neutrophils involves the phosphorylation and the translocation of cytosolic p67phox. *Biochem. J.* 296, 367–371.
- Dusi S., Donini M., and Rossi F., (1996) Mechanisms of NADPH oxidase activation: translocation of p40phox, Rac1 and Rac2 from the cytosol to the membranes in human neutrophils lacking p47phox or p67phox. *Biochem. J.* 314, 409–412
- Eklund EA, Kakar R., (1999), Recruitment of CREB-binding protein by PU.1, IFN-regulatory factor-1, and the IFN consensus sequence-binding protein is necessary for IFN-gamma-induced p67phox and gp91phox expression. *J Immunol* 163:6095–6105
- El Benna J., Faust LP. and Babior BM., (1994), The phosphorylation of the respiratory burst oxidase component p47phox during neutrophil activation: phosphorylation of

- sites recognized by protein kinase C and by proline-directed kinases. *J. Biol. Chem.* 269, 23431–23436
- El Kares R, Barbouche MR, Elloumi-Zghal H, et al., (2006), Genetic and mutational heterogeneity of autosomal recessive chronic granulomatous disease in Tunisia. *Hum Genet* 51:887–895
- Elbim C., Reglier H., Fay M., et al., (2001), Intracellular pool of IL-10 receptors in specific granules of human neutrophils: differential mobilization by proinflammatory mediators. *J. Immunol.*, 166, 5201–5207.
- Elloumi HZ, Holland SM., (2007), Diagnostic assays for chronic granulomatous disease and other neutrophil disorders. *Methods Mol Biol* 412:505–523
- Epling CL., Stites D P., McHugh T M., et al, (1992), Neutrophil function screening in patients with chronic granulomatous disease by a flowcytometric method, *Cytometry*, vol. 13,no. 6, pp. 615–620.
- Fadok VA., Bratton DL., Guthrie L., et al. (2001), Differential effects of apoptotic versus lysed cells on macrophage production of cytokines: role of proteases. *J Immunol.* 166:6847-54.
- Faust LR., el Benna J., Babior BM. Et al., (1995), the phosphorylation targets of p47phox, a subunit of the respiratory burst oxidase: functions of the individual target serines as evaluated by site-directed mutagenesis. *J. Clin. Invest.* 96, 1499–1505
- Fernandez-Boyanapalli R., McPhillips KA., Frasch SC., Janssen WJ., Dinauer MC., Riches DW, et al., (2010), Impaired phagocytosis of apoptotic cells by macrophages in chronic granulomatous disease is reversed by IFN-gamma in a nitric oxidedependent manner. *J Immunol.* 185:4030-41.
- Fernandez-Boyanapalli RF., Frasch SC., McPhillips K., Vandivier RW., Harry BL., Riches DW, et al., (2009), Impaired apoptotic cell clearance in CGD due to altered macrophage programming is reversed by phosphatidylserine-dependent production of IL-4. *Blood.* 113:2047-55.
- Foster C., Lehrnbecher T., Mol F., et al., (1998), Host defense molecule polymorphisms influence the risk for immune-mediated complications in chronic granulomatous disease. *J Clin Invest.* 102:2146-2155.
- Fujii H., Ichimori K., Hoshiai K. et al., (1997), Nitric oxide inactivates NADPH oxidase in pig neutrophils by inhibiting its assembling process. *J. Biol. Chem.*, 272, 32773–32778.
- Gallin JI., Alling DW., Malech HL., et al., (2003), Itraconazole to prevent fungal infections in chronic granulomatous disease. *N Engl J Med.*, 348:2416-2422.

- Gallin J I., and Zarembek K., (2007); Lessons About the Pathogenesis and Management of *Aspergillosis* from Studies in Chronic Granulomatous Disease. *Am Clin Climatol Assoc.* 118: 175–185.
- Gallin JI., Buescher ES. (1983), Abnormal regulation of inflammatory skin responses in male patients with chronic granulomatous disease. *Inflammation*, 7: 227-32.
- Gillibert M., Dehry Z., Terrier M., et al., (2005), Another biological effect of N-alpha-tosyl phenylalanine chloromethyl ketone: it prevents p47phox phosphorylation and translocation upon neutrophil stimulation. *Biochem. J.*, 386, 549–556.
- Goebel W., Mark L., Billings S. et al., (2005), Gene correction reduces cutaneous inflammation and granuloma formation in murine X-linked chronic granulomatous disease. *J Invest Dermatol.* 125(4):705-10.
- Goldblatt D. & Thrasher AJ., (2000). Chronic granulomatous disease, *Clin Exp Immunol.*; 122(1): 1–9.
- Goldblatt D., Butcher J., Thrasher AJ., et al., (1999), Chorioretinal lesions in patients and carriers of chronic granulomatous disease. *J Pediatr*, 134:780-83.
- Görlach A., Lee P., Roesler J., et al., (1997), A p47-phox pseudogene carries the most common mutation causing p47-phox deficient chronic granulomatous disease, *J. Clin. Invest.* 100, 1907–1918.
- Goussetis E., Konialis CP., Peristeri I., et al., (2010), Successful hematopoietic stem cell transplantation in 2 children with X-linked chronic granulomatous disease from their unaffected HLA-identical siblings selected using preimplantation genetic diagnosis combined with HLA typing. *Biol Blood Marrow Transplant*, 16:344-9.
- Grant SS., Kauffman BB., Chand NS., et al, (2012), Eradication of bacterial persisters with antibiotic-generated hydroxyl radicals. *Proceedings of the National Academy of Science of USA* 109:12147–12152.
- Greenberg DE., Ding L., Zelazny AM., et al., (2006), A novel bacterium associated with lymphadenitis in a patient with chronic granulomatous disease. *PLoS Pathog*, 2:e28.
- Grez M., Ott M., Stein S, et al., (2005), Correction of chronic granulomatous disease by gene therapy. *Mol Ther.* 11:S130- 131.
- Groemping Y. and Rittinger K., (2005), Activation and assembly of the NADPH oxidase: a structural perspective. *Biochem. J.* 386, 401–416
- Gungor T., Halter J., Klink A., et al., (2005), Successful low toxicity hematopoietic stem cell transplantation for high-risk adult chronic granulomatous disease patients. *Transplantation*, 79:1596-606.

- Halliwell B. and Gutteridge JMC., (2007), *Free Radicals in Biology and Medicine*, 4th ed. Oxford: Oxford University Press 79-185.
- Hancock JT. and Jones O. T., (1987), The inhibition by diphenyleneiodonium and its analogues of superoxide generation by macrophages. *Biochem. J.*, 242, 103–107.
- Hayrapetyan A, Dencher PC, Leeuwen K, et al., (2013), Different unequal cross-over events between NCF1 and its pseudogenes in autosomal p47^{phox} deficient chronic granulomatous disease, The Netherlands. *Biochimica et Biophysica Acta* 1832: 1662–1672
- Heyworth PG, Curnutte JT, Rae J, et al., (2001), Hematologically important mutations: X-linked chronic granulomatous disease (second update). *Blood Cells Mol Dis* 27:16–26
- Heyworth PG, Noack D, Cross AR., (2002), Identification of a novel NCF-1 (p47-phox) pseudogene not containing the signature GT deletion: significance for A47 degree chronic granulomatous disease carrier detection. *Blood* 100:1845–1851
- Hill HR., Augustine NH., Pryor RJ., et al. (2010), Rapid Genetic Analysis of X-Linked Chronic Granulomatous Disease by High-Resolution Melting, *Journal of Molecular Diagnostics*, Vol. 12, No. 3.
- Hiraoka W., Vazquez N., Nieves-Neira W., et al., (1998), Role of oxygen radicals generated by NADPH oxidase in apoptosis induced in human leukemia cells. *J of Clinical Investigation*, 102:1961-1968.
- Holland SM., (2010), Chronic Granulomatous Disease, *Clinic Rev Allerg Immunol*, 38:3–10.
- Horwitz ME., Barrett AJ., Brown MR., et al., (2001), Treatment of chronic granulomatous disease with nonmyeloablative conditioning and a T-cell-depleted hematopoietic allograft. *N Engl J Med*, 344:881-8.
- [http://: www. PreventionGenetics.com](http://www.PreventionGenetics.com). chronic granulomatous disease via the CYBA gene.
- Inanami O., Johnson JL., McAdara JK., et al., (1998), Activation of the leukocyte NADPH oxidase by phorbol ester requires the phosphorylation of p47PHOX on serine 303 or 304. *J. Biol. Chem.* 273, 9539 –9543.
- Ishibashi F, Nunoi H, Endo F, et al., (2000), Statistical and mutational analysis of chronic granulomatous disease in Japan with special reference to gp91-phox and p22-phox deficiency. *Hum Genet* 106:473–481.
- Iwata M., Nunoi H., Yamzaki H., (1994), Homologous dinucleotide (GT or TG) deletion in Japanese patients with chronic granulomatous disease with p47-phox deficiency, *Biochem. Biophys. Res. Commun.* 199, 1372–1377.

- Jackson SH., Gallin JL., Holland SM. (1995), The p47phox mouse knock-out model of chronic granulomatous disease. *J Exp Med.* 182:751-8.
- Jaing TH., Lee WI., Cheng PJ., et al., (2010), Successful unrelated donor cord blood transplantation for chronic granulomatous disease. *Int J Hematol.*91:670-2.
- Janeway CA, Craig J, Davidson M, et al., (1954), Hyper gammaglobulinemia associated with severe, recurrent and chronic non-specific infection. *Am J Dis Child* 88:388–392
- Johnson JL., Park JW., Benna JE., et al., (1998), Activation of p47PHOX, a cytosolic subunit of the leukocyte NADPH oxidase: phosphorylation of ser-359 or ser-370 precedes phosphorylation at other sites and is required for activity. *J. Biol. Chem.* 273, 35147–35152
- Jones LB, McGrogan P, Flood TJ, et al. (2008); Special article: chronic granulomatous disease in the United Kingdom and Ireland: a comprehensive national patient-based registry. *Clin Exp Immunol*; 152:211.
- Jurkowska L M., Bernatowska E. and Ball J., (2004, A), Genetic and biochemical background of chronic granulomatous disease. *Arch Immunol Ther Exp*, 52, 113–120
- Jurkowska M, Kurenko-Deptuch M, Bal J, et al., (2004, B), The search for a genetic defect in Polish patients with chronic granulomatous disease. *Arch Immunol Ther Exp (Warsz)* 52:441– 46
- Kalyanarman B., (2013), Teaching the basics of redox biology to medical and graduate students: Oxidants, antioxidants and disease mechanisms. *Redox Biology*: 1. 244-257.
- Kang EM, Marciano BE., DeRavin S, et al., (2011). Chronic granulomatous disease: Overview and hematopoietic stem cell transplantation. *J Allergy Clin Immunol.*; 127 (6): 1319-26:
- Kikuta A., Ito M., Mochizuki K., et al., (2006), Nonmyeloablative stem cell transplantation for nonmalignant diseases in children with severe organ dysfunction. *Bone Marrow Transplant*, 38:665-669.
- Kim SJ., Gon Kim J., Yu US., (2003), Chorioretinal lesions in patients with chronic granulomatous disease. *Retina*, 23:360-65.
- Kleinberg ME, Malech HL, Rotrosen D., (1990), The phagocyte 47-kiloDalton cytosolic oxidase protein is an early reactant in activation of the respiratory burst. *J Biol Chem* 265:15577– 15583
- Kobayashi SD., Voyich JM., Braughton KR., et al., (2004), Gene expression profiling provides insight into the pathophysiology of chronic granulomatous disease. *J. Immunol.* 2004; 172: 636 -643.

- Köker MY., Camcıoğlu Y., Van Leeuwen K. et al., (2013), Clinical, functional and genetic characterization of eighty-nine patients in Turkey with chronic granulomatous disease. *J. Allergy Clin Immunol.* 132:1156–1163.
- Krawczak M, Cooper DN., (1991), Gene deletions causing human genetic disease: mechanisms of mutagenesis and the role of the local DNA sequence environment. *Hum Genet* 86:425–441
- Krawczak M, Thomas NS, Hundrieser B, et al., (2007), Single base-pair substitutions in exon-intron junctions of human genes: nature, distribution, and consequences for mRNA splicing. *Hum Mutat* 28:150–158
- Kuhns DB., Alvord WG., Heller T., et al., (2010) Residual NADPH oxidase and survival in chronic granulomatous disease. *New England Journal of Medicine* 363:2600–2610.
- Kustikova O., Fehse B., Modlich U, et al., (2005), Clonal dominance of hematopoietic stem cells triggered by retroviral gene marking. *Science*, 308: 1171-1174
- Landing BH. and Shirkey HS., (1957), A syndrome of recurrent infection and infiltration of viscera by pigmented lipid histiocytes, *Pediatrics*, vol. 20, no. 3, pp. 431–438.
- Laufs U., Adam O., Strehlow K., et al., (2003), Down-regulation of Rac-1 GTPase by Estrogen. *J. Biol. Chem.*, 278, 5956–5962.
- Le Cabec V. and Maridonneau-Parini I., (1995), Complete and reversible inhibition of NADPH oxidase in human neutrophils by phenylarsine oxide at a step distal to membrane translocation of the enzyme subunits, *J. Biol. Chem.*, 270, 2067–2073.
- Lekstrom-Himes JA., Kuhns DB., Alvord WG., et al., (2005), Inhibition of human neutrophil IL-8 production by hydrogen peroxide and dysregulation in chronic granulomatous disease, *J. Immunol.* 174:411-7.
- Leto TL., Adams AG. and de Mendez I., (1994), Assembly of the phagocyte NADPH oxidase: binding of Src homology 3 domains to proline-rich targets. *Proc. Natl. Acad. Sci. U.S.A.* 91, 10650–10654
- Leusen JH, Bolscher BG, Hilarius PM, et al., (1994, A), 156Pro→Gln substitution in the light chain of cytochrome b558 of the human NADPH oxidase (p22-phox) leads to defective translocation of the cytosolic proteins p47-phox and p67-phox. *J Exp Med* 180:2329–2334
- Leusen JH., de Boer M., Bolscher BG., et al., (1994, B), A point mutation in gp91-phox of cytochrome b 558 of the human NADPH oxidase leading to defective translocation of the cytosolic proteins p47-phox and p67-phox . *J. Clin. Invest.* **93**, 2120–2126
- Lindsey S, Huang W, Wang H, et al., (2007), Activation of SHP2 protein-tyrosine phosphatase increases HoxA10-induced repression of the genes encoding gp91(PHOX) and p67(PHOX). *J Biol Chem* 282:2237–2249

- Lublin M., Bartlett DL., Danforth DN., et al., (2002), Hepatic abscess in patients with chronic granulomatous disease. *Ann Surg*, 235:383-91.
- Luzzatto L, Battistuzzi G., (1985), Glucose-6-phosphate dehydrogenase, *Adv Hum Genet*, 14: 217 –329.
- Lynch RE., Fridovich I., (1978), Permeation of the erythrocyte stroma by superoxide radical, *J. Biol. Chem.* 253, 4697–4699.
- Malech H., Maples P., Whiting-Theobald N. et al., (1997), Prolonged production of NADPH oxidase-corrected granulocytes after gene therapy of chronic granulomatous disease. *Proc Natl Acad Sci.* 94:12133-12138.
- Malech HL. (1999), Progress in gene therapy for chronic granulomatous disease. *J Infect Dis.*; 179:S318–325.
- Marciano BE., Rosenzweig SD., Kleiner DE. et al., (2004, A). Gastrointestinal involvement in chronic granulomatous disease. *Pediatrics*, 114: 462-8.
- Marciano BE., Wesley R., De Carlo ES., et al., (2004, B) Long-term interferon-gamma therapy for patients with chronic granulomatous disease. *Clin Infect Dis.* 39:692-699.
- Martire B., Rondelli R., Soresina A., et al., (2008), Clinical features, long-term follow-up and outcome of a large cohort of patients with Chronic Granulomatous Disease: an Italian multicenter study. *Clin Immunol*, 126:155-64.
- Martyn LJ., Lischner HW., Pilegi AJ., et al., (1971), Chorioretinal lesions in familial chronic granulomatous disease of childhood. *Trans Am Ophthalmol Soc*, 69:84-112.
- Matoug I., Elfaituri S., Elsalheen H., et al., (2014), Chronic granulomatous disease in Libya: clinical and laboratory, 23 EADV Congress. [http://: www. eadv amsterdam, 2014-m.poken.com](http://www.eadv.amsterdam,2014-m.poken.com).
- Matute JD, Arias AA, Wright NA, et al., (2009), A new genetic subgroup of chronic granulomatous disease with autosomal recessive mutations in p40 phox and selective defects in neutrophil NADPH oxidase activity. *Blood*; 114:3309-15.
- Meshaal S, El Hawary R, Abd Elaziz D, et al., (2015). Chronic granulomatous disease: Review of a cohort of Egyptian patients. *Allergol Immunopathol (Madr)*; 43(3):279-85.
- Messina CG., Reeves EP., Roes J., et al., (2002), Catalase negative *Staphylococcus aureus* retain virulence in mouse model of chronic granulomatous disease. *FEBS Lett*, 518:107-10.
- Miller DD., Cowen EW., Nguyen JC., et al., (2010), Melanoma associated with long-term voriconazole therapy: a new manifestation of chronic photosensitivity. *Arch Dermatol*, 146:300-4.

- Morel F. (2007), Molecular aspects of chronic granulomatous disease. The NADPH oxidase complex. *Bulletin de l'Academie Nationale de Medecine*, vol. 191, no. 2, pp. 377–392.
- Moreno MU, San José G, Orbe J, et al., (2003), Preliminary characterisation of the promoter of the human p22(phox) gene: identification of a new polymorphism associated with hypertension. *FEBS Lett* 542:27–31
- Morgenstern D., Gifford M., Li L., et al., (1997), Absence of respiratory burst in x-linked chronic granulomatous disease mice leads to abnormalities in both host defense and inflammatory response to *Aspergillus fumigatus*. *J Exp Med.*185:207-218.
- Mouy R., Seger R., Bourquin JP., et al., (1991), Interferon gamma for chronic granulomatous disease. *N Engl J Med.* 325:1516-7.
- Mouy R., Veber F., Blanche S., et al., (1994), Long-term itraconazole prophylaxis against *Aspergillus* infections in thirty-two patients with chronic granulomatous disease. *J Pediatr* 125:998-1003.
- Muhlebach TJ, Robinson W, Seger RA, et al., (1990), A second NsiI RFLP at the CYBB locus. *Nucl Acids Res* 1990; 18:4966. Kenney RT, Leto TLA. HindIII polymorphism in the human NCF2 gene. *Nucl Acids Res* 1990; 18:7193.
- Nakamura M, Imajoh-Ohmi S, Kanegasaki S et al., (1990), Prenatal diagnosis of cytochrome-deficient chronic granulomatous disease. *Lancet* 1990; 336:118±9
- Nakano T., Boku E., Yoshioka A., Fukimara Y., (1999), A case of McLeod phenotype chronic granulomatous disease who received unrelated cord blood transplantation. *J Pediatr Hematol* 12:264.
- Nauseef WM., (2008), Biological roles for the NOX family NADPH oxidases. *J Biol Chem*; 283:16961–5.
- Nauseef WM., (2014), Detection of superoxide anion and hydrogen peroxide production by cellular NADPH oxidases. *Biochimica et Biophysica Acta* 1840 - 757–767
- Noack D, Rae J, Cross AR, et al., (2001), Autosomal recessive chronic granulomatous disease caused by defects in NCF-1, the gene encoding the phagocyte p47-phox: mutations not arising in the NCF-1 pseudogenes. *Blood* 97:305–311
- O'Dowd Y M., El-Benna J., Perianin A. et al., (2004), Inhibition of formyl-methionyl-leucyl-phenylalanine-stimulated respiratory burst in human neutrophils by adrenaline: inhibition of phospholipase A2 activity but not p47phox phosphorylation and translocation. *Biochem. Pharmacol.*, 67, 183–190.
- Ott MG., Schmidt M., Schwarzwälder K., et al. (2006), Correction of X-linked chronic granulomatous disease by gene therapy, augmented by insertional activation of MDS1-EVI1, PRDM16 or SETBP1. *Nat Med.* 12: 401–409.

- Paclet MH., Coleman AW., Vergnaud S. et al., (2000), P67-phox –mediated NADPH oxidase assembly: imaging of cytochrome b 558 liposomes by atomic force microscopy. *Biochemistry* 39, 9302–9310
- Palestine AG., Meyers SM., Fanci AS., et al., (1983), Ocular findings in patients with neutrophils dysfunction. *AmJ Ophthalmol* 1983; 95:598 - 604.
- Perticarari S, Presani G, Banfi E., (1994), A new flow cytometric assay for the evaluation of phagocytosis and the oxidative burst in whole blood. *J Immunol Methods* 1994; 170:117±24.
- Piirilä H, Väliäho J, VihinenM., (2006), Immunodeficiency mutation databases (IDbases). *Hum Mutat* 27:1200–1208
- Rae J, Newburger PE, Dinauer MC, et al., (1998), X-linked chronic granulomatous disease: mutations in the CYBB gene encoding the gp91-phox component of respiratory-burst oxidase. *Am J Hum Genet* 62:1320–1331
- Rae J, Noack D, Heyworth PG, et al., (2000), Molecular analysis of 9 new families with chronic granulomatous disease caused by mutations in CYBA, the gene encoding p22-phox. *Blood* 96:1106–1112
- Reichenbach J., Lopatin U., Mahlaoui N., et al., (2009), Actinomyces in chronic granulomatous disease: an emerging and unanticipated pathogen. *Clin Infect Dis.* 49:1703-10.
- Reichenbach J., Van de Velde H., De Rycke M., et al., (2008), First successful bone marrow transplantation for X-linked chronic granulomatous disease by using preimplantation female gender typing and HLA matching. *Pediatrics* 122: e778-82.
- Repine JE, Rasmussen B, White JG., (1979) An improved nitro blue tetrazolium test using phorbol myristate acetate-coated coverslips. *Am J Clin Pathol.*, 71:582±5.
- Rezvani Z., Zadeh IM., Pourpak Z., et al., (2005), CYBB Gene Mutation Detection in an Iranian Patient with Chronic Granulomatous Disease. *J Allergy Asthma Immunol.* 4(2): 103-6
- Rodrigues MM., Palestine AG., Macher AM., et al., (1983), Histopathology of ocular changes in chronic granulomatous disease. *Am J Ophthalmol*, 96:810- 11.
- Roesler J., Curnutte JT., Rae J., et al., (2000), Recombination events between the p47-phoxgene and its highly homologous pseudogenes are the main cause of autosomal recessive chronic granulomatous disease, *Blood* 95, 2150–2156.
- Roos D, de Boer M, Kuribayashi F, et al, Ahlin A, Nemet K, Hossle JP, Bernatowska-Matuszkiewicz E, Middleton-Price H., (1996), Mutations in the X-linked and autosomal recessive forms of chronic granulomatous disease. *Blood* 87:1663–1681

- Roos D, Kuhns DB, Maddalena A, et al., (2010), Hematologically important mutations: the autosomal recessive forms of chronic granulomatous disease (second update). *Blood Cells Mol Dis*; 44:291-9.
- Roos D, Kuijpers TW, Curnutte JT., (2007), chronic granulomatous disease. In: Ochs HD, Smith CIE, Puck J M, editors, Primary immunodeficiency diseases. 2nd ed. New York: Oxford University Press; p. 525-49.
- Roos D, van Bruggen R, Meischl C., (2003), Oxidative killing of microbes by neutrophils. *Microbes Infect* 5:1307–1315
- Roos D, van Zwieten R, Wijnen JT et al., (1999), Molecular basis and enzymatic properties of glucose 6-phosphate dehydrogenase volendam, leading to chronic non spherocytic anemia, granulocyte dysfunction, and increased susceptibility to infections. *Blood*, 94:2955–62.
- Roos D. and Boer M. (2014), Molecular diagnosis of chronic granulomatous disease. *Clin Exp Immunol*. 175(2): 139–149
- Roos D., Eckmann CM., Yazdanbakhsh M , et al., (1984), Excretion of superoxide by phagocytes measured with cytochrome c entrapped in resealed erythrocyte ghosts, *J. Biol. Chem*. 259, 1770–1775.
- Sanchez-Ortega I, Patino B., Arnan M., Peralta T., Parody R., Gudiol C., et al., (2010), Clinical efficacy and safety of primary antifungal prophylaxis with posaconazole vs itraconazole in allogeneic blood and marrow transplantation. *Bone Marrow Transplant* 46(5):733-9.
- Schmidt M, Schwarzwaelder K, Ott M, et al., (2005), Stable polyclonal hematopoietic repopulation after successful clinical gene therapy of chronic granulomatous disease (CGD). *Mol Ther*.11:S415.
- Schuetz C., Hoenig M., Gatz S., et al., (2009), Hematopoietic stem cell transplantation from matched unrelated donors in chronic granulomatous disease. *Immunol Res.*, 44: 35-41.
- Segal BH, DeCarlo ES, Kwon-Chung KJ, et al., (1998), Aspergillus nidulans infection in chronic granulomatous disease. *Medicine*; 77:345-54.
- Segal BH, Leto TL, Gallin JI, et al., (2000), Genetic, biochemical, and clinical features of chronic granulomatous disease, *Medicine*; 79(3):170- 200.
- Segal BH., Han W., Bushey JJ., et al., (2010), NADPH oxidase limits innate immune responses in the lungs in mice. *PLoS One*, 16; 5 (3):e9631.
- Segal BH., Kuhns DB., Ding L., et al. (2002), Thioglycollate peritonitis in mice lacking C5, 5-lipoxygenase, or p47(phox): complement, leukotrienes, and reactive oxidants in acute inflammation. *J Leukoc Biol*. 71:410-6.

- Segal BH., Veys P., Malech H., et al. (2011), Chronic Granulomatous Disease: Lessons from a Rare Disorder. *Biol Blood Marrow Transplant*, (1 Suppl): S123–S131.
- Seger RA., Gungor T., Belohradsky BH., et al., (2002), Treatment of chronic granulomatous disease with myeloablative conditioning and an unmodified hemopoietic allograft: a survey of the European experience, 1985-2000. *Blood* 100: 4344-50.
- Shiose A. and Sumimoto H., (2000), Arachidonic acid and phosphorylation synergistically induce a conformational change of p47phox to activate the phagocyte NADPH oxidase. *J. Biol. Chem.* 275, 13793–13801
- Siddiqui S., Anderson VL., Hilligoss DM., et al., (2007), Fulminant mulch pneumonitis: an emergency presentation of chronic granulomatous disease. *Clin Infect Dis.* 45:673-81.
- Soler-Palacín P, Margareto C, Llobet P, et al. (2007); Chronic granulomatous disease in pediatric patients: 25 years of experience. *Allergol Immunopathol (Madr)*; 35:83.
- Someya A., Nuno H., Hasebe T., et al., (1999), Phosphorylation of p40 phox during activation of neutrophil NADPH oxidase. *J. Leukocyte Biol.* 66, 851–857
- Soncini E., Slatter M., Jones L., et al., (2008), Haematopoietic stem cell transplantation for chronic granulomatous disease—a single-centre experience. *Bone Marrow Transplantation*, 41(suppl):S28.
- Stasia MJ & Li XJ., (2008), Genetics and immunopathology of chronic granulomatous disease. *Semin Immunopathol* 30:209–235
- Stasia MJ, Bordigoni P, Martel C, et al., (2002), A novel and unusual case of chronic granulomatous disease in a child with a homozygous 36-bp deletion in the CYBA gene A220 leading to the activation of a cryptic splice site in intron 4. *Hum Genet* 110:444–450
- Stasia MJ, Brion JP, Boutonnat J, et al., (2003), Severe clinical forms of cytochrome b-negative chronic granulomatous disease (X91-) in 3 brothers with a point mutation in the promoter region of CYBB. *J Infect Dis* 188:1593–1604
- Stenson PD, Ball EV, Mort M, et al., (2003), Human gene mutation database (HGMD): *Hum Mutat* 21:577–581
- Stolk J., Hiltermann TJ., Dijkman JH., et al., (1994), Characteristics of the inhibition of NADPH oxidase activation in neutrophils by apocynin, a methoxy-substituted catechol. *Am. J. Respir. Cell. Mol. Biol.*, 11, 95–102.
- Suliaman F, Amra N, Sheikh S, et al. (2009); Epidemiology of chronic granulomatous disease of childhood in Eastern Province, Saudi Arabia. *Pediatr Asthma Allergy Immunol*; 22:21.

- Sumimoto H, Hata K, Mizuki K, et al., (1996), Assembly and activation of the phagocyte NADPH oxidase. Specific interaction of the N-terminal Src homology 3 domain of p47phox with p22phox is required for activation of the NADPH oxidase. *J Biol Chem* 271:22152–22158
- Sumimoto H., Kage Y., Nuno H., et al., (1994), Role of Src homology 3 domains in assembly and activation of the phagocyte NADPH oxidase. *Proc. Natl. Acad. Sci. U.S.A.* **91**, 5345–5349
- Suzuki N., Hatakeyama N., Yamamoto M., et al., (2007); Treatment of McLeod phenotype chronic granulomatous disease with reduced intensity conditioning and unrelated-donor umbilical cord blood transplantation. *Int J Hematol.* 85:70-2.
- Taga K, Seki H, Miyawaki T et al., (1985), Flow cytometric assessment of neutrophil oxidative metabolism in chronic granulomatous disease on small quantities of whole blood: heterogeneity in female patients. *Hiroshima J Med Sci*; 34:53±60.
- Tanugi-Cholley LC, Issartel JP, Lunardi J, et al., (1995), A mutation located at the 5' splice junction sequence of intron 3 in the p67phox gene causes the lack of p67phox mRNA in a patient with chronic granulomatous disease. *Blood* 85:242–249
- The International Chronic Granulomatous Disease Cooperative Study Group, (1991), A controlled trial of interferon gamma to prevent infection in chronic granulomatous disease. *N Engl J Med*, 324:509-16
- Tsunawaki S, Yoshikawa K., (2002), Relationships of p40 (phox) with p67 (phox) in the activation and expression of the human respiratory burst NADPH oxidase. *J Biochem* 128:777–783
- Uzel G., Orange JS., Poliak N., et al. (2010), Complications of tumor necrosis factor-alpha blockade in chronic granulomatous disease-related colitis. *Clin Infect Dis.* 51:1429-34.
- Van den Berg JM, van Koppen E, Ahlin A, et al., (2009), Chronic granulomatous disease: the European experience. *PLoS One*; 4 (4): e 5234.
- Vázquez N., Lehrnbecher T., Chen R., et al., (2001), Mutational analysis of patients with p47-phox-deficient chronic granulomatous disease: the significance of recombination events between the p47-phox gene (NCF1) and its highly homologous pseudogenes, *Exp. Hematol.* 29, 234–243.
- Vergnaud S, Pacllet MH, El Benna J, et al., (2000), Complementation of NADPH oxidase in p67-phox-deficient CGD patients p67-phox/p40-phox interaction. *Eur J. Biochem* 267:1059–1067
- Vilaiphan P., Chatchatee P., Ngamphaiboon J., et al. (2007), Nonsense Mutations of the *CYBB* Gene in Two Thai Families with X-linked Chronic Granulomatous Disease. *Asian pacific journal of allergy and immunology* 25: 245-249

- Vinh DC., Shea YR., Jones PA., et al., (2009, A) Chronic invasive aspergillosis caused by *Aspergillus viridinutans*. *Emerg Infect Dis.*, 15: 1292-4.
- Vinh DC., Shea YR., Sugui JA., et al., (2009, B) Invasive aspergillosis due to *Neosartorya udagawae*. *Clin Infect Dis* 2009; 49:102-11.
- Voraphania N., Chatchatea P., Ngamphaiboona J., et al. (2009), Clinical and molecular characteristics of Thai families with autosomal recessive chronic granulomatous disease. *Asian Biomedicine* Vol. 3 No. 6; 603-609
- Weiss SJ., (1989), Tissue destruction by neutrophils. *New England Journal of Medicine* 320: 365 – 376.
- Winkelstein JA., Marino MC., Johnston RB., et al., (2000), Chronic granulomatous disease, report on a national registry of 368 patients, *Medicine*; 79(3):155-69.
- Yamamoto A., Taniuchi S., Tsuji S., et al., (2002), Role of reactive oxygen species in neutrophil apoptosis following ingestion of heat-killed *Staphylococcus aureus*. *Clin Exp Immunol.* 129:479-84.
- Yamazaki-Nakashimada MA., Stiehm ER., Pietropaolo-Cienfuegos D., et al., (2006), Corticosteroid therapy for refractory infections in chronic granulomatous disease: case reports and review of the literature. *Ann Allergy Asthma Immunol*; 97: 257-61.
- Yu L., Quinn MT., Cross AR., et al., (1998), Gp91 phox is the heme binding subunit of the superoxide-generating NADPH oxidase, *Proc. Natl. Acad. Sci. U. S. A.* 95, 7993 – 7998.
- Zhou Y., Lin G. and Murtaugh MP., (1995), Interleukin-4 suppresses the expression of macrophage NADPH oxidase heavy chain subunit (gp91-phox). *Biochim. Biophys. Acta*, 1265, 40–48.



الوراثة الجزيئية للمرض الحبيبي المزمن في المرضى الليبيين
في بنغازي

رسالة مقدمة من
منى حامد عثمان الرملى

المشرف
الدكتور أحمد زايد

المشرف المساعد
الدكتور إدريس معتوق

قسم الكيمياء الحيوية – كلية الطب – جامعة بنغازي

2015

الوراثة الجزيئية للمرض الحبيبي المزمن في المرضى الليبيين في بنغازي

المقدمة:

المرض الحبيبي المزمن هو مرض وراثي نادر وهو احد امراض نقص المناعة و نسبة انتشاره حول العالم تقدر بحوالي 1 لكل 250.000 شخص، وهو يحدث بسبب طفرة في الجينات التي تشفر مكونات انزيم الاكسيداز (NADPH oxidase) حيث ان هذا الانزيم هو المسؤول عن انتاج مشتقات الاكسجين مثل: فوق الاكسيد (O_2^-) و الجذور الحرة (Free Radicals). هذه الطفرات الجينية تؤدي الي نقص او انعدام قدرة الخلايا البلعمية (Phagocytic Cells) علي اباده الميكروبات كالبكتيريا والفطريات مما يؤدي الي حدوث نوبات متكررة من الالتهابات البكتيرية والفطرية خلال فترات زمنية متقاربة.

المرض الحبيبي المزمن يورث بواسطة نمطين: النمط الأول متعلق بالكروموزوم (X(X- Liked Pattern) وهو يحدث بسبب طفرة في الجين (CYBB) الذي يشفر الجلايكوبروتين ($gp91^{phox}$) و يسبب حوالي 60% من الحالات المرضية.

اما النمط الصبغي الجسدي المتنحي (Autosomal Recessive Pattern) فهو يحدث بسبب طفرات في احدي الجينات التالية: الجين NCF1 الذي يشفر البروتين $p47^{phox}$, والجين NCF2 الذي يشفر البروتين p67 والجين CYBB الذي يشفر البروتين $p22^{phox}$ والتي تسبب حوالي 30% , 5% , 5% علي التوالي من الحالات المرضية.

المرضي وطرق الفحص:

في الدراسة الحالية بحثنا عن الخلل الجيني في الجينين (NCF1, CYBB) الذين لديهما نسبة حدوث عالية في مناطق مختلفة حول العالم، فقد قمنا بفحص أربعة عشر حالة مرضية ادخلوا الي قسم المناعة بمستشفى الاطفال ببنغازي، حيث ان بعض المرضى شخصوا سريريا كمرضي للداء الحبيبي المزمن والبعض الآخر تم تأكيد تشخيص حالاتهم بواسطة اختبار NBT .

تحليل الطفرات الجينية قد انجز بواسطة تضخيم خمسة اكرونات (2, 3, 5, 7, 10) للجين CYBB بواسطة تفاعل البوليميريز التسلسلي (Polymerase Chain Reaction, PCR) متبوعا بعملية الترتيب التسلسلي للحمض النووي (sequencing)، بينما جين NCF1 تم فحصه بواسطة Real Time PCR . كل النتائج تم تأكيدها بواسطة استخدام أداة الاصطاف Blast Alignment Tool من الموقع الالكتروني NCBI .

النتائج:

اعتمادا علي صلة القرابة بين آباء المرضى والتاريخ العائلي للمرضي تبين ان اغلب المرضى الليبيين لديهم المرض الحبيبي المزمن من النوع الصبغي الجسدي المتنحي.

بعد فحص الجين CYBB بواسطة تضخيم الحمض النووي (DNA amplification)، وعملية الترتيب التسلسلي للحمض النووي (sequencing)، واداة الاصطاف (Blast Alignment) وفحص الجين NCF1 بواسطة Real Time PCR اتضح انه لا يوجد خلل في كلا الجينين، بالإضافة الي ذلك اعتمادا علي اختبار DHR للعينة رقم (3) لوحظ وجود خلل في البروتين $p22^{phox}$ الذي يشفر بواسطة الجين CYBA الذي من المحتمل ان يكون سبب الطفرة الجينية عند المرضى الليبيين.

الخاتمة والتوصية:

الكشف عن الخلل الجيني للمرض الحبيبي المزمن هو مهمة صعبة وبما ان الخلل الجيني للمرضي الليبيين غير معروف ادي ذلك الي زيادة صعوبة المهمة، لاستكمال هذه الدراسة يتطلب الأمر استخدام تحاليل اخري مثال علي ذلك تحليل CGH و MLPA، بالإضافة الي ذلك نحن نوصي بدراسة الجين CYBA الذي قد يكون الخلل فيه سبب لهذا المرض، بما ان هذه الدراسة هي الأولى من نوعها في بنغازي وليبيا عموما نحن نسعي ان تكون هذه الدراسة قاعدة اساسية لدراسة المرض الحبيبي المزمن من الناحية الجينية.